WUSCHEL dynamically regulates auxin biosynthesis to promote stemness and progenitor cell differentiation in the shoot apical meristem of Arabidopsis

Shalini Yadav

Thesis submitted for the partial fulfillment of the degree of

DOCTOR OF PHILOSOPHY

Department of Biological Sciences
Indian Institute of Science Education and Research Mohali
Knowledge city, Sector 81, SAS Nagar, Manauli PO, Mohali
140306, Punjab, India

October, 2020

Dedicated to My Beloved Parents

Declaration

The work presented in this thesis has been carried out by me under the guidance of Dr. Ram Kishore Yadav, at the Indian Institute of Science Education and Research Mohali. This work has not been submitted in part or in full for a degree, a diploma, or a fellowship to any other university or institute. Whenever contributions of others are involved, every effort is made to indicate this clearly, with due acknowledgement of collaborative research and discussions. This thesis is a bona fide record of original work done by me and all sources listed within have been detailed in the bibliography.

Date:
Place: Mohali

Shalini Yadav

In my capacity as the supervisor of the candidate's thesis work, I certify that the above statements by the candidate are true to the best of my knowledge.

Dr. Ram Yadav
(Supervisor)

Table of Contents

Declaration ..... *ii*

Acknowledgements ..... *iv*

List of Publications ..... *vi*

List of abbreviations ..... *vii*

Synopsis ..... *viii*

List of Tables ..... *xiv*

List of Figures ..... *xv*

Chapter 1 ..... *1*

General Introduction *1*

1.1. *Arabidopsis thaliana* as a model system **2**

1.2. Importance of studying plant development **3**

1.3. Shoot apical meristem (SAM) **3**

1.3.1. SAM maintenance by WUSCHEL (WUS)-CLAVATA(CLV) pathway 4

1.3.2. SAM maintenance by *KNOX* family of genes 7

1.3.3. Role of chromatin remodellers in SAM development 8

1.3.4. Meristem maintenance by cytokinin 9

1.3.5. Auxin and its role in plant development 11

1.4. Auxin a central regulator of phyllotaxy and organogenesis **25**

1.5. Thesis Objectives **28**

Chapter 2 ..... *30*

Material and Methods *30*

2.1. Plant work **31**

2.1.1. Plant growth media and conditions 31

2.1.2. Seeds sterilization 31

2.1.3. Plant material 31

2.1.4. Plant transformation 33

2.1.5. Selection of transgenic lines 34

2.2. Molecular biology techniques **35**

2.2.1. Primers 35

2.2.2. Plasmid DNA extraction 39

2.2.3. Total RNA Isolation 39

2.2.4. Genomic DNA extraction 40

2.2.5. Purification of DNA fragment from agarose gel 41

2.2.6. Molecular Clonings 41

2.2.7. Plasmids 47

2.2.8. Site-directed mutagenesis 50

2.2.9. cDNA synthesis and qRT PCRs 50

2.3. Protein biochemistry techniques **52**

2.3.1. WUS protein induction 52

2.3.2. Western blotting 53

2.3.3. Electrophoretic mobility shift assay (EMSA) 53
2.4. Confocal Laser Scanning Microscopy of SAM 54
2.4.1. Confocal imaging of SAMs 54
2.4.2. Confocal imaging of embryos 55
2.4.3. Confocal imaging of seedling shoot apex 55
2.5. SAM size measurement 56
2.6. In-situ hybridization assay 56
2.6.1. Fixation and embedding of tissues 56
2.6.2. Tissue sectioning 58
2.6.3. Composition of stock solutions 58
2.6.4. *In-vitro* transcription 60
2.6.5. In-situs sections pre-treatment 62
2.6.6. Hybridization 63
2.6.7. In-situ post-hybridization 64
2.7. Treatment of plants 66
2.8. Quantification of GFP +ve and GFP -ve cells in the SAM 66
2.9. Quantification of Auxin maxima in SAM 67
2.10. Quantification of data 68
2.11. Statistical analysis 68
Chapter 3 ..... *70*
TAA1 and TAR2 mediated auxin biosynthesis is essential for organogenesis and shoot development *70*
3.1. Introduction 71
3.2. Results 73
3.2.1. *TAA1* expression is restricted to the epidermal cell layer 73
3.2.2. *TAR2* expression coincides with incipient organ primordia in shoot and floral meristem 75
3.2.3. *taa1 tar2* double mutant plants are dwarf and show reduced growth 77
3.2.4. Expression of *TAR2* in the PZ of SAM is sufficient for organogenesis and SAM development 82
3.3. *TAA1/TAR2* mediated auxin biosynthesis is essential to maintain auxin responses in SAM 84
3.3.1. Auxin levels and auxin responses are perturbed in *taa1 tar2* double mutant 84
3.3.2. Auxin biosynthesis and transport inhibitors drugs show less DR5 responses in the shoot apex 87
3.4. Auxin biosynthesis and transport both are required for SAM maintenance and patterning 89
3.4.1. *TAA1/ TAR2* mediated auxin biosynthesis contributes for activation of MP and PIN1 in SAM 89
3.4.3. Auxin biosynthesis in the incipient organ primordia is critical for lateral organ initiation 93
3.4.4. Auxin biosynthesis and transport both are essential for both shoot and root development 97
3.4.5. Auxin signalling control the transition of stem cell progenitors into differentiating cells in PZ 98
3.4.6. Auxin signalling is required for organ boundary formation and shoot growth 101
3.5. Discussion 105

Chapter 4 ..... *107*

WUSCHEL negatively regulates auxin biosynthesis in stem cell niche *107*

4.1. Introduction **108**

4.2. Results **112**

4.2.1. WUS represses auxin biosynthesis gene *TAR2* in the stem cell niche 112

4.2.2. *TAR2* is a direct target of WUS 115

4.2.3. *TAR2* expression is dynamic in SAM and inhibited by WUS in the emerging flower meristem 117

4.2.4. WUS loss of function results in *TAR2* mis-expression in SAM 118

4.2.5. WUS prevents *TAR2* expression in stem cell daughters 121

4.2.6. High dosage of WUS results in a decrease in *TAR2* transcription in PZ 123

4.2.7. High dosages of WUS modulates auxin levels in the SAM 125

4.2.8. Mis-expression of *TAR2* reduces SAM size and plant growth 127

4.2.9. Ectopic expression of *TAR2* is detrimental for stem cells 130

4.3. Discussion **132**

Chapter 5 ..... *135*

Bibliography *135*

ANNEXURE: List of the Chemicals *160*

Acknowledgements

This is the most important phase of my academic career and there have been many supporting figures in this achievement. This is the moment when I can actually thank all friends and family for their love and support.

First and foremost, I offer my utmost gratitude to my guide **Dr. Ram Kishore Yadav**, for his supervision, advice and guidance from the very early stages of my research as well as giving me extraordinary learning experiences throughout the work. Above all and the most needed, he provided me with unflinching encouragement and support in various ways whilst providing me the room to work in my own way. His immense trust in my abilities has always helped me to come out of difficult times during my Ph.D. It was a rewarding experience to work under his supervision and without him this thesis would not have been completed or written. His dedication for science has inspired me to include the same in my work. Thank you sir, for providing me an opportunity to work under your supervision.

I extend my sincere thanks to the past and present thesis committee members, **Dr. Rajesh Ramachandran, Dr. Santosh B. Satbhai**, and **Dr. Kavita Babu** for all the advices and scientific inputs that has helped to shape my project better. I thank all my course Instructors for their enlightening classes during my first year at IISER Mohali.

I am especially thankful to **Dr. Venu Reddy** (University of California Riverside), **Dr. Anna N. Stepnova** (University of North Carolina), **Dr. Teva Vernoux** (Université de Lyon) for sharing valuable resources.. I would like to give my special thanks to **Dr. Utpal Nath** (IISc Bangalore) for giving me the an opportunity to learn EMSA technique in his laboratory.

I would also like to thank all my past and present lab members **Shivani Bhatia, Prince Saini, Sonal Yadav**, **Anshul Kaushik, Sujan Vimal, Asis Kumar, Manisha, Athul, Jayesh, Mahima, Asha, Rimpy, Meghna, Avneet, Anu** for their constant encouragement, support and motivation till and throughout my doctoral studies. Furthermore, I would like to thank **Harish Kumar,** my colleague cum friend for his valuable contributions for my research work and for all his support during all the ups and downs in lab.

It was a pleasure to share my life with wonderful people in beautiful IISER campus. This endeavour would have not been a success without the enduring support and love of my friends. I would like to give my heartiest thanks to my dearest Friends **Abhishek Sharma, Dahlia Bhattacharjee, Simran Kaur, Sonal Yadav, Vikas Singh, Bhupinder Singh, Alok Tiwari, Nupur Tiwari, Divya Jagga**, **Kunal Narad, Sajal Rastogi,** and list goes on. Many thanks to them for their care, concern, help, support and advices.

I would like to acknowledge **DBT, IYBA, IISER Mohali** for financial support for my research work and **UGC** for providing me fellowship throughout my course of Ph.D.

Words are inadequate to thank **Dada ji, Maa** and **Papaji** for their constant support throughout my career. Without their support and love this path of Ph.D. was impossible. I would like to give my sincere thanks to my sister **Ragini Yadav**, my brother **Anmol Yadav** and my brother-in-law cum friend **Divyesh Yadav** for giving me all the love and support. Finally, I would like to acknowledge my other family members, their blessings and unconditional love have given me strength and support throughout my life.

List of Publications

- Yadav, S., Kumar, H., and Yadav, RK. Local auxin biosynthesis promotes stem cell differentiation and organogenesis in Arabidopsis shoot apex. doi: https://doi.org/10.1101/819342

- Bhatia, S., Kumar, H., Sundaram, J., Saini, P., Mahajan, M., **Yadav, S.**, Yadav, S., Sahu,S., and Yadav, RK. Deciphering the regulatory network of epidermal and sub-epidermal enriched transcription factors in the shoot apical meristem of *Arabidopsis* thaliana. (Manuscript under preparation).

List of abbreviations

%	Percent
bp	Base pair
BSA	Bovine Serum Albumin
cm	Centimetre
CTAB	Cetyl Trimethyl Ammonium Bromide
ddH2O	Double distilled water
DNA	Deoxyribonucleic Acid
EtBR	Ethidium bromide
GFP	GFP fluorescent protein
gm	gram
h	Hour
HF	High-Fidelity
IPTG	Isopropyl β- d-1-thiogalactopyranoside
Kb	Kilo base pair
LB	Luria-Bertani
mg	Milligram
µg	Microgram
min	Minute
ml	Milliliter
µl	Microliter
mM	Mirco molar
mm	Micro meter
mM	milli molar
ng	Nano gram
nM	Nano molar
OD	Optical Density
PBS	Phosphate buffer saline
PCR	polymerase chain reaction
qRT-PCR	quatitative reverse transcriptase polymerase chain reaction
RNA	Ribonucleic Acid
rpm	Rotation Per Minute
RT	Room Temperature
SDS-PAGE	Sodium dodecyl sulphate–Polyacrylamide Gel Electrophoresis
Sec	Second
SOB	Super Optimal Broth
UBQ10	Ubiquitin 10
V	Voltage
YFP	Yellow fluorescent protein

Synopsis

Introduction:

Unlike animals, plants have the remarkable ability to form organs post embryonically by virtue of pluripotent stem cells, which are located at the growing tips within the shoot apical meristem (SAM). In the SAM, stem cells are housed in central zone (CZ), the descendants of these cells enters into peripheral zone (PZ) and there they divide actively before differentiating into new organs. A few stem cell descendants get pushed below CZ and specifies the rib meristem (RM), which is important for stem tissue formation. Hence, SAM can be subdivided into three distinct zones based on the distinct cell identities and cell functions they executes (Meyerowitz 1997; Steeves, Taylor A. and Sussex 1989).

Past studies in model plant *Arabidopsis thaliana* have shown the role of *WUSCHEL* (*WUS*), a homeodomain transcription factor, in stem cell maintenance(K. F. Mayer et al. 1998). *WUS* is transcribed in the niche cells, and the protein moves out of these cells as a signal towards the CZ and PZ cell types. In the CZ, WUS binds to *CLAVATA3* (*CLV3*) and activates its transcription (Yadav, Perales, Gruel, Yadav, et al. 2011). *CLV3* encode a peptide, which binds to its cognate receptor CLAVATA1 (CLV1) (Ogawa et al. 2008). CLV3-CLV1 mediated signalling cascade negatively regulates expression of *WUS* in the niche (Schoof, Lenhard, Haecker, Klaus F.X. Mayer, et al. 2000). Thus, *CLV-WUS* pathway acts as a dynamic feedback system that allows the stem cell domain and the underlying organizing centre (OC/niche) to continually adjust to the differing concentration of signals without any noticeable impact on the SAM size.

In the PZ of shoot auxin plays a major role in organ formation. Primordium development and their positioning in the meristem are tightly regulated by auxin (Reinhardt et al. 2003a). Past studies have shown that higher level of auxin in incipient primordium is achieved through PIN1

mediated polar transport (Heisler et al. 2005). Most of the events related to primordium development occurs close to stem cell niche despite that stem cells never succumb to differentiation pathways. This intriguing tight link was uncoupled in a live-imaging study where down regulation of *WUS* by RNAi lead to the enhanced auxin signalling in the PZ of SAM, suggesting that the auxin responses are kept low by WUS mediated regulation in the CZ (Yadav, Tavakkoli, and Reddy 2010). This study also suggested a regulatory mechanism where WUS is not only involved in CZ identity but also actively communicate with PZ cell types.

This thesis, I have organized into five chapters. Chapter 1 is dedicated to introduction while in chapter 2, I have compiled material and methods. I report the importance of local auxin biosynthesis in lateral organ formation and its role in meristem organization in chapter 3. In chapter 4, I report my findings related to WUS mediated regulation of *TAR2*, which is critical for long term fate of stem cells and their timely transition into differentiating cell types. Chapter 5 is reserved for references.

TAA1/TAR2 mediated auxin biosynthesis is required for organogenesis and SAM development

Previous studies mainly focused on PIN1 and implicated its role in primordium development. PIN1 mediated polar auxin transport achieve auxin maxima in the PZ, which specify primordia formation. Repolarization of PIN1 later depletes auxin in the vicinity of newly formed organ primordium (Heisler et al. 2005). This reiterative process is tightly regulated and give rise to robust phyllotactic patterns in the land plants. To achieve a critical threshold of auxin maxima in the shoot plants not only rely on polar auxin transport but also requires auxin biosynthesis. In this study, I have shown the role of local auxin biosynthesis mediated through two closely related *TRYPTOPHAN AMINOTRANSFERASE RELATED* family genes *TAA1/TAR2* in

achieving this critical threshold to form lateral organs. In order to understand, the function of *TAA1* and *TAR2* in organogenesis, I studied the expression patterns of *TAA1* and *TAR2,* and found that both genes are expressed during the plant development. *TAA1* is confined to epidermal cell layer while *TAR2* is mainly expressed in the PZ of SAM. *taa1 tar2* double mutant analysis revealed that the relative size of the shoot is smaller and lateral organs have lost their polarity. To investigate the role of local auxin biosynthesis further, I studied PIN1 polarization, and found that the protein has lost polarity partially in the double mutant compared to *taa1* and *tar2* single mutants. In parallel, I also show that R2D2, an auxin input sensor, and DR5, an auxin output sensor, show opposite response in the *taa1 tar2* double mutant background, suggesting that *TAA1/TAR2* mediated auxin biosynthesis is essential to maintain optimum auxin levels in SAM.

Next, I investigated the role of polar transport in the absence of auxin biosynthesis by using *pin1-5,* a weak allele, and made triple mutant. In this genetic study, I have identified a novel phenotype for *taa1 tar2 pin1-5* triple mutant. Interestingly, *taa1 tar2 pin1* triple mutant plants fail to produce leaves and expression pattern of several key marker genes such as *CLV3, WUS, ARF3, ARF4*, *ARF5* and *CUC1* are perturbed, suggesting that the organization of SAM is tightly linked to auxin signalling.

WUS negatively regulates auxin biosynthesis in stem cell niche

In chapter 4, I report where and when WUS mediated regulation of *TAR2* occurs in the SAM, and why this regulation is biologically relevant for long terms pluripotency of stem cells. How WUS communicates with PZ cell types? To answer these question, I have analysed the previously published microarray dataset generated by Yadav et al., (2013). In this study, *YABBY3, KANADI 1 / 2,* and *ASYMMETRIC LEAVES 2* were identified as direct targets of

WUS. I looked for genes that are responsive to WUS but are involved in auxin biosynthesis or signaling. *ANTHRANILATE SYNTHASE ALPHA SUBUNIT1* (*ASA1*), *TRYPTOPHAN SYNTHASE ALPHA1* (*TSA1*), *TRYPTOPHAN AMINOTRANSFERASE RELATED2* (*TAR2*) and *PHYTOALEXIN DEFICIENT3* (*PAD3*) were identified as WUS responsive genes. *ASA1* and *TSA1* are involved in indole biosynthesis, an essential precursor for L-Tryptophan (L-Trp). *TAR2* and its closest homologue *TAA1* uses L-Trp as a substrate and converts to IPyA. Surprisingly, *TAA1* expresses in the L1 layer of SAM and overlap with WUS, but it did not show any change in its expression in response to WUS in the microarray study. To establish whether the selected genes are direct targets of WUS, plants were treated simultaneously with 10 µM Dex plus 10 µM Cycloheximide (Cyc) and Cyc alone for 4 h. WUS mediated repression of *ASA1* and *TSA1* was found neither in Dex nor in Dex+Cyc treated plants compared with control. However, I found more than a 2-fold decrease in the *TAR2* transcript levels in Dex/Cyc treated plants compared to Cyc alone. In parallel, I quantified the changes in *TAA1* transcript levels by qRT-PCR in response to WUS modulation both in Dex, and Dex/Cyc treated plants and did not find consistent regulation.

In my effort to understand the dynamic regulation of auxin biosynthesis in SAM, I tested the WUS mediated regulation of *TAA1* and *TAR2*. For this, IM of 4 week old *35S::WUS-GR* plants were treated either with 10 µM Dex or ethanol for 24 h and tissue was fixed for *in situ* hybridization. Conversely, in Dex treated *35S::WUS-GR* plants, *TAR2* expression was not detected by in situ studies. I confirmed using EMSA and FAIRE biochemical approaches that WUS binds to the TAAT core containing cis-element (BS1(-897) and BS2(-2094)) in *TAR2* promoter, and promotes transcriptional repression of *TAR2* in stem cell niche. Deletion of BS1, BS2, and BS1 BS2 sites was accomplished using site directed mutagenesis. BS2 deletion (*pTAR2(m2)::H2B-YFP*) reporter shows expression pattern similar to WT (*pTAR2::H2B-YFP*), however, BS1 (*pTAR2(m1)::H2B-YFP*) and BS1BS2 deletion (*pTAR2ΔWUS::H2B-YFP*)

showed broader misexpression compared to WT in the PZ of SAM. Analysis of *pTAR2::H2B-YFP* reporter in *wus-7* and in *clv3-2* mutant show that *TAR2* is responsive to WUS dosages in the SAM.

Functional characterization of cis-regulatory elements was undertaken to understand the role of BS1 and BS2 binding sites. Construct lacking both BS1BS2 (*pTAR2ΔWUS :TAR2*) was introduced in WT and in *pCLV3::mGFP-ER* reporter line. These studies revealed slower growth of the plants and a decrease in the SAM size with fewer stem cells. However, ectopic expression of *TAR2* under 35S promoter or stem cell/niche specific promoters leads to termination of shoot. Taken together these results, I deciphered the regulation of auxin biosynthesis by WUS in stem cell niche. My findings show that the apparent distinction in the auxin signaling output between the CZ and PZ cells is not only due to polar transport of auxin but it is locally produced in the PZ. Thus, WUS not only promote the fate of stem cells in CZ but also required for their timely transition into differentiated cell types.

Summary

In this study, I show that coinciding the disruption of auxin biosynthesis pathway with that of transport leads to a complete block in auxin signaling in SAM. As a result of this, not only organ primordia growth gets arrested, but stem cells also fail to differentiate into PZ and RM cell types. Genetic evidence offered in this study support that locally produced auxin is vital for primordium growth. Our finding also confirms that in the absence of local auxin biosynthesis, optimum auxin response in the PZ are revoked. Double mutant analysis of auxin biosynthesis gene with transport revealed that *TAA1* is critically required for stem tissue growth, whereas *TAR2* is required for lateral organ formation and their growth, which connects with their spatiotemporal expression patterns. Based on the auxin signaling and SAM marker genes analysis in *taa1 tar2 pin1* triple mutant, I determine that shoot stem cells do not require

auxin signaling for their maintenance and self-renewal. However, data presented here show that elevated auxin responses in SAM are detrimental to stem cell maintenance. My data support a model where auxin emanating from PZ cells give positional information to stem cell descendants to differentiate into organ primordia. WUS protein gradient counters the auxin maxima driven signaling gradient from the PZ cells to prevent premature differentiation of stem cell daughters. Thus, underlying feedback mechanisms maintain SAM with distinct functional domains whose boundaries are dynamic.

List of Tables

Chapter 2

Table 2.1. Transgenic lines generated in the present study.....35
Table 2.2. Primers used for clonings.....36
Table 2.3. Primers used for probe synthesis for In-situ hybridization.....37
Table 2.4. Primers used for qRT-PCR.....37
Table 2.5. Primers used for genotyping.....38
Table 2.6. Oligos used for EMSA.....38
Table 2.7. Primers used for site directed mutagenesis.....38

List of Figures

Chapter 1

Figure 1.1. The Structure of the Arabidopsis SAM organized into different Layers L1, L2 and L3 and different Zones CZ, OC and PZ. Courtesy: (Murray et al. 2012).....4
Figure 1.2. Structure of Indole Acetic Acid.....12
Figure 1.3. IAA metabolism in higher plants. (Courtesy: Ljung 2013).....14
Figure 1.4. Schematic showing main auxin signalling pathway. Courtesy:(Leyser 2018).....25

Chapter 2

Figure 2.1. Tools used for quantification of stem cells (GFP +ve) and PZ cells (GFP -ve)...67
Figure 2.2. Tools used for quantification of Auxin maxima and DR5- positive cells in the SAM.....68

Chapter 3

Figure 3.1. TAA1 expression in embryo, vegetative and reproductive phases of plant development.....74
Figure 3.2. *TAR2* expression pattern during embryogenesis, vegetative and reproductive phase of plant development. 76
Figure 3.3. taa1 tar2 double mutant plant shows smaller shoot size.....79
Figure 3.4. Organ patterning defects in *taa1 tar2* double mutant.....80
Figure 3.5. Stem cells (CZ cells) and Peripheral zone (PZ) cells fate in auxin biosynthesis mutants.....81
Figure 3.6. *TAR2* expression pattern in PZ is essential for proper plant growth and shoot development.....83
Figure 3.7. Locally produced auxin required for maintaining auxin input and auxin output in the SAM.....86
Figure 3.8. L-Kyn and NPA treatment lead to lesser DR5 responses in SAM.....88
Figure 3.9. *TAA1/TAR2* mediated auxin biosynthesis is required to maintain *MP* and *PIN1* expression. 91
Figure 3.10. Overlapping expression pattern of *TAR2*, MP and PIN1 in SAM.....93
Figure 3.11. Auxin biosynthesis and transport both contribute to lateral organ formation. ...94
Figure 3.12. *TAA1/TAR2* mediated local auxin biosynthesis and PIN1 mediated auxin transport both are required for organ formation and SAM development. 96

Figure 3.13. Auxin biosynthesis and auxin transport act together for lateral organ formation. 98
Figure 3.14. Inhibition of auxin biosynthesis and transport fail to maintain the functional SAM zonation. 100
Figure 3.15. The expression of Auxin responsive factors (ARFs) get perturbed in auxin biosynthesis mutant. 102
Figure 3.16. Auxin biosynthesis and transport both are essential for maintaining Auxin signalling in the shoot apex. 103
Figure 3.17. Auxin biosynthesis and transport both are required for organ boundary separation 105

Chapter 4

Figure 4.1. WUS represses *TAR2* in the SAM 113
Figure 4.2. WUS represses *TAR2* expression in SAM. 115
Figure 4.3.WUS represses *TAR2* in the SAM. 116
Figure 4.4. *TAR2*, *CLV3* and *WUS* are expressed in complementary domains of SAM. 118
Figure 4.5. WUS regulates *TAR2* expression in SAM. 119
Figure 4.6. Deletion of WUS binding sites in the *TAR2* promoter leads to expansion of *TAR2* expression towards the centre of the meristem. 122
Figure 4.7. *TAR2*, *WUS* and *CLV3* expression in the *clv3-2* mutant. 124
Figure 4.8. *TAR2* is repressed in the *clv3-2* mutant. 125
Figure 4.9. Auxin level (input) in the *clv3-2* mutant. 127
Figure 4.10. WUS binding sites in *TAR2* promoter are essential for SAM size and plant growth. 129
Figure 4.11. Ectopic expression of *TAR2* leads to termination of SAM. 131

Chapter 1
General Introduction

1.1. *Arabidopsis thaliana* as a model system

Humans started tweaking plants long back to domesticate them for food, fodder and fibre. Major modern-day crops have got wild relatives. Despite having a common genetic origin, many crop plants have substantially different plant architecture from their wild relatives. Arabidopsis was adopted as a model plant at the beginning of 1980s by a handful of scientists. This has turned out one of the fortunate choices in the history of plant biology. Because in the last three decades, scientists working across the globe have made remarkable progress in understanding plant growth, plant's response to biotic and abiotic stress at the molecular level. Although, *Arabidopsis thaliana* is native to Eurasia, but the findings are applicable to major crop plants. Arabidopsis, as a model organism, offers several advantages over other plants such as rice and maize. It is very convenient to grow, and its relatively faster growth compared to other model plants makes it an attractive system to study. It can be grown in controlled conditions easily inside the laboratory by creating modest facilities, which is not possible for many other plant species. Depending on the growth conditions, Arabidopsis can develop into a mature plant from seed in the duration of 5-6 weeks. Short life cycle makes Arabidopsis more feasible to use as a model system. In consideration with seed and seedling size, hundreds of plants can be grown on a single petri dish under aseptic conditions. Beyond its growth time and size of the plant, several specific features in the Arabidopsis genome makes it useful for genetic research. The genome of Arabidopsis is small around 132mbp, contains approximately 30000 genes in 5 chromosomes. Arabidopsis model plant contains the typical feature of all seed plants, such as root apical meristem, shoot apical meristem, trichomes, vascular tissues, male gametophyte, female gametophyte and bears the complete set of flower organs including stamen and carpel.

1.2. Importance of studying plant development

According to the World Health Organization (WHO), nearly half of the children die every year because of malnutrition. Lack of proper nutrition puts them on the higher risks of getting infections and diseases and further weakens their growth. In the current scenario, there is no doubt politically, economically and scientifically; these problems have a lot in common. To overcome these difficulties, we cannot deny the fact that understanding the basic mechanism in plant development is necessary, and also has the potential to overcome challenges related to malnutrition faced by children and adults are identical. Therefore, studying the fundamental mechanisms that control the three-dimensional growth of plant body in space and time, including stem cell fate determination in the shoot apex and their differentiation are of immense importance. By unlocking these secrets, we can fine-tune plant architecture and increase the yield of highly nutritious crops with minimal input in the form of water and fertilizers.

1.3. Shoot apical meristem (SAM)

In higher plants, SAMs have a number of basic characteristics in common. It is a multi-layered structure consisting of three distinct cell layers, namely L1/epidermal cell layer, L2/subepidermal cell layer, and L3/ corpus layer, and each layer contains stem cells (Fig.1.1). On this layered organization, a zonal organization can be superimposed. This can be further classified into the central zone (CZ), present at the tip of the SAM, which harbours stem cells, peripheral zone (PZ), where stem cells differentiate into organs primordia, and the rib meristem (RM) (Fig.1.1). RM cells give rise to the internal tissues of stem and vasculature (Carles and Fletcher 2003).

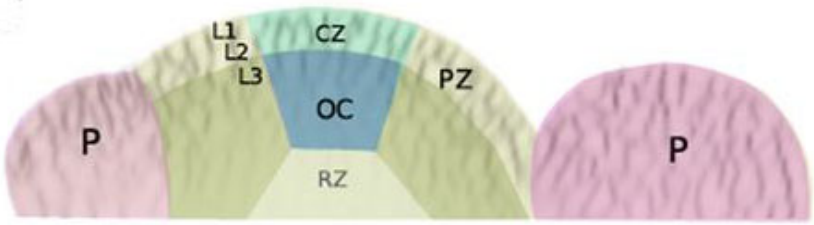

Figure 1.1. The Structure of the Arabidopsis SAM organized into different Layers L1, L2 and L3 and different Zones CZ, OC and PZ. Courtesy: (Murray et al. 2012)

Maintenance of the stem cells is the most important phenomena for plants to generate the organs and reproduce during the whole life cycle. Without the SAM and stem cells, it is impossible for a plant to make the lateral organs. Therefore, to make the lateral organs and complete the life cycle, plants maintains several molecular mechanisms.

1.3.1. SAM maintenance by WUSCHEL (WUS)-CLAVATA(CLV) pathway

WUS-CLV is the central pathway which maintains a constant number of stem cells in the apical meristem of plants. *WUS* is required for maintaining the pluripotency of the stem cells and encodes a homeodomain transcription factor (K. F. X. Mayer et al. 1998). Its transcript is detected first in the four inner cells of a 16 cell stage embryo, and later these cells divide asymmetrically to give rise to OC (K. F. X. Mayer et al. 1998). In the adult SAM, *WUS* mRNA expression is restricted in the niche cells present below the CZ (K. F. X. Mayer et al. 1998). Restriction of *WUS* activity in niche cells is essential to maintain a constant number of stem cells and SAM size. Apart from the stem cells maintenance, *WUS* is also required for anther and female gametophyte development (Deyhle et al. 2007; Lieber et al. 2011). *WUS* knock out plants show termination of SAM because of the consumption of stem cells, while its overexpression leads to enlarged meristem and induction of shoot stem cells in the root meristem (Gallois et al. 2004). *WUS* acts together with *HAIRY MERISTEM (HAM)* family of

genes to control stem cells function and restricts *CLV3* expression exclusively in the outermost layers of the SAM (Zhou et al. 2015, 2018).

The other components of this pathway are *CLAVATA1* (*CLV1*) and *CLAVATA3* (*CLV3*). Both are required to maintain a negative feedback loop in the SAM. *CLV1* encodes an extracellular leucine-rich repeat (LRR) receptor, consists of 21 LRR repeats in the extracellular domain, a transmembrane domain and an intracellular kinase domain (Clark, Williams, and Meyerowitz 1997). *CLV1* mRNA is expressed in shoot and floral meristem. Its expression partially overlap with CZ and RM cell types (Clark et al. 1997). *CLV3* is expressed in the stem cells and encodes a 96 aa long pre-protein, which is processed into 13 aa long mature peptide, and secreted by stem cells in the vicinity (Fletcher et al. 1999; Rojo et al. 2002). Further, CLV3 peptide undergoes posttranslational modification in the form of arabinosylation, which makes it active and facilitate its interaction with CLV1 (Cock and Mccormick 2001; Ohyama, Shinohara, and Ogawa-ohnishi 2009). In parallel to CLV3-CLV1, yet another *CLAVATA* gene *CLV2* encodes a receptor-like protein with extracellular LRRs containing receptor domain, a transmembrane domain and a short cytoplasmic tail with and expressed in many tissues including shoot apices, seedlings, flower meristems, siliques etc (Jeong, Trotochaud, and Clark 1999). Initially, it was believed that CLV3 binds to the CLV1 receptor and CLV2 thought to acts as the co-receptor in this process (Jeong et al. 1999). Later on, another receptor CORYNE was identified in an EMS mutagenesis screen. CORYNE consists of an intracellular transmembrane domain and an inactive pseudokinase domain (Mu and Bleckmann 2008). *CLV2, CORYNE* and *WUS* expression domains overlap with each other in the L3 layer of SAM and expressed throughout the meristem except in the cells of CZ (Mu and Bleckmann 2008). Previous studies suggested that CLV2 and CORYNE can interact with each other through their transmembrane domains (TMDs) to activate CLV3 signalling pathway for stem cells maintenance (Bleckmann et al. 2010; Guo et al. 2011; Mu and Bleckmann 2008).

WUS mRNA is expressed in OC; however, protein can move to the cells of CZ through plasmodesmata and binds to the *CLV3* promoter region to activate its expression (Daum, Medzihradszky, Suzaki, and Jan U Lohmann 2014; Laux et al. 1996; K. F. X. Mayer et al. 1998; Yadav, Perales, Gruel, Yadav, et al. 2011). CLV3 binds to either CLV1 or CLV2/CORYNE heterodimers receptor complex and activates the downstream signalling cascade to represses *WUS* expression in OC (U Brand et al. 2000; Jeong et al. 1999; Schoof, Lenhard, Haecker, Klaus F X Mayer, et al. 2000). *CLV3* and *CLV2* loss of function mutants display enlarged meristems because they fail to restrict *WUS* expression and as a result of stem cells overproliferation, while overexpression of *CLV3* leads to early termination of SAM, due to strong repression of *WUS* (Clark, Running, and Meyerowitz 1993, 1995). Apart from the CLV1/CLV2/CORYNE receptor complex, three other leucine-rich repeat receptor protein kinases (LRR-RPKs) known as *BARELY ANY MERISTEM 1, 2* and *3* (*BAM1, BAM2 and BAM3*) have a redundant function in meristem and stem cell homeostasis (DeYoung et al. 2006). In contrast to *CLV1,* the expression pattern of *BAM1, BAM2,* and *BAM3* are slightly different. In the inflorescence meristem, *BAM1* is expressed in the L1 layer and completely absent from the RM. *BAM3* is not active in SAM and floral organs; rather, its expression is restricted to vasculature tissue (Nimchuk et al. 2015). *BAMs* single mutants do not have any obvious phenotype, but the double mutant *bam1 bam2* have smaller SAM (Deyoung et al. 2006). *bam1 clv1* double mutant show more severe phenotype in comparison to the single mutant of *clv1* (Deyoung et al. 2006). *CLV1* functions in the RM area and it represses the expression of *BAM* genes in RM (Nimchuk et al. 2015). LRR receptor-like kinase Receptor-Like Protein Kinase 2 (RPK2) physically interact with BAM1 protein to maintain stem cell pluripotency through CLV3 signalling pathway (Kinoshita et al. 2010). In response to CLV3, another group of LRR-RLKs, CLAVATA3 INSENSITIVE RECEPTOR KINASES (CIKs) get phosphorylated and function as co-receptors of CLV1 BAM-RPK2 and CLV2-CRN receptors

complexes for cell fate specification and stem cells maintenance (Cui et al. 2018; Hu et al. 2018). Thus, the *CLV-WUS* pathway functions as a dynamically regulated negative feedback loop that allows the stem cell domain and the underlying OC to continually adjust their sizes and maintain SAM homeostasis.

1.3.2. SAM maintenance by *KNOX* family of genes

KNOX family of genes includes *SHOOT-MERISTEMLESS (STM), KNAT1, KNAT2*, and *KNAT6*. They have overlapping and reductant function in the SAM maintenance (Brand et al. 2002; Lenhard, Jürgens, and Laux 2002). *STM* is expressed all over the shoot apex, in the stem cells and in the cells PZ, except in those cells where new organ primordia will arise (Heisler et al. 2005; Jurkuta et al. 2009; Landrein et al. 2015). *STM* is required to prevent stem cells from taking part in the organ formation. Loss of function mutation in *STM* gene shows the defects in the maintenance of meristem in Arabidopsis, and Maize (Barton and Poethig 1993; Kerstetter et al. 1997; Long et al. 1996), however ectopic overexpression of *KNOX* family of gene leads to change the fate of the cells from determinate to indeterminate (Sinha, Williams, and Hake 1993). *STM* activates the expression of *ISOPENTYL TRANSFERASE* (*IPT7),* which is involved in cytokinin biosynthesis in SAM, and thus, upregulates cytokinin responses and cytokinin signalling in the meristem (Yanai et al. 2005). When cytokinin is applied exogenously to the *stm* mutant, it rescues the mutant phenotype (Yanai et al. 2005). Thus, *STM* and cytokinin signalling form a positive feedback loop to maintain the optimum level of cytokinin and stem cell fate. In addition, STM directly binds to the promoter of *CUP SHAPED COTYLEDON (CUC1)* and activates its expression, and indirectly, influences the levels of *CUC2*, *CUC3*, and MIR164a (Spinelli et al. 2011). Thus, a positive feedback loop maintained by cytokinin-STM and a negative feedback loop maintained by *CUC-STM* is necessary for stem cell maintenance in the shoot apex.

1.3.3. Role of chromatin remodellers in SAM development

In eukaryotes, the genetic material is tightly packed into a stable nucleoprotein complex called chromatin. Chromatin is organized into a bead-like structure called nucleosomes. Transcription factors and transcription machinery to access the cis-element present within the DNA recruits chromatin remodelling factors to disrupt the nucleoprotein complex. SPLAYED (SYD), a SWI2/SNF2 chromatin remodelling ATPases involved in chromatin remodelling directly recruited to *WUS* locus and promotes *WUS* expression (Kwon, Chen, and Wagner 2005). In this process, histone chaperones are also needed to assist in depositing the H3, H4, H2A, and H2B subunits in the nucleosome. In Arabidopsis, CHROMATIN ASSEMBLY FACTOR 1 (CAF1) and NUCLEOSOME ASSEMBLY PROTEIN 1 (NAP1) are two conserved histone chaperones (Tripathi et al. 2015). CAF1 is involved in depositing H3/H4 and composed of three distinct subunits, namely, FASCIATA1 (FAS1), FASCIATA2 (FAS2), and MULTICOPY SUPPRESSOR OF IRA1 (MSI1) (De Koning et al. 2007). The double mutant of *fas1* and *fas2* show fascinated stem as well as disorganized SAM as a result of ectopic *WUS* expression (Kaya et al. 2001). In contrast, NAP1 is conserved evolutionarily from yeast to humans. NAP1 is involved in H2A/H2B deposition (Aguilar-Gurrieri et al. 2016). Arabidopsis genome contains four *NAP1* genes and two genes encoding *NAP1 RELATED PROTEIN 1* and *2* (*NRP1* and *NRP2*) involved in postembryonic root growth (Zhu et al. 2006; Zhu, Dong, and Shen 2007). Plant having mutation in other chromatin regulators like *CURLY LEAF (CLF), EMBRYONIC FLOWER 2 (EMF2),* and *INCURVATA2 (ICU2)* also show misexpression of *WUS* (Barrero et al. 2007; Wang et al. 2017; Yoshida et al. 2001). Recently It has been reported BRCA1-associated RING domain 1 (BARD1) acts as SYD binding protein and directly interacts with SYD to represses *WUS* expression (Han, Li, and Zhu 2008). Thus, Chromatin remodellers mediated regulation of *WUS* activity is essential for the stem cells homeostasis in the SAM.

1.3.4. Meristem maintenance by cytokinin

Cytokinins (CKs) were discovered 50 years ago. They control virtually every aspect of plant growth, including meristem maintenance, response to abiotic stress, cell division and differentiation. Increased level of cytokinin signalling in SAM leads to an elevated level of *WUS* (Gordon et al. 2009). Among the seven *IPT* genes, *IPT7* is activated by STM (Yanai et al. 2005). *stm* mutant plants get rescued when they are treated with exogenous cytokinin or by expressing *IPT7* directly under *STM* promoter (Yanai et al. 2005). IPTs catalyze the first step and rate-limiting step of CK biosynthesis (Kakimoto 2001; Takei, Sakakibara, and Sugiyama 2001). The inactive CK synthesized by IPTs is converted into the biologically active pool by LONELY GUY (LOG) enzymes (Kurakawa et al. 2007). The founding member of LOG family, *LOG1* was identified in rice based on the shoot meristem termination phenotype (Kurakawa et al. 2007). *LOG1* is expressed in the tip of the SAM in rice (*Oryza sativa*) and in the CZ of SAM in Arabidopsis (Yadav et al., 2009). *LOGs* display cell and tissue-specific expression patterns and thus affect CK signalling. Genetic studies combining gain of function and loss of function approaches revealed multiple functions of *LOGs* in various tissues during plant development (Kuroha et al. 2009). Arabidopsis genome encodes 9 LOGs enzyme (Kuroha et al. 2009). Among them, *LOG4* and *LOG7* are expressed in SAM and contributes for cytokinin biosynthesis in the SAM (Gruel et al. 2016).

To maintain the homeostasis in cytokinin signalling plants have evolved CYTOKININ OXIDASEs (CKXs), a class of enzymes that are involved in the degradation of active CK pool (Werner et al. 2006). In total, seven genes encoding CKXs were identified in the Arabidopsis genome. *CKX3* is expressed in the stem cell niche partially overlapping with the WUS expression domain, while *CKX5* shows slightly deeper expression in the SAM (Bartrina et al. 2011). Despite their subtle differences in expression patterns, double knockouts of *ckx3 ckx5* show significantly larger inflorescence and floral meristem due to an increase in *WUS*

transcription (Bartrina et al. 2011). Thus, cell and tissue-specific regulation of CK accumulation and degradation in plants is precisely regulated at multiple levels.

ARABIDOPSIS HISTIDINE KINASEs (AHKs) or CK receptors, (AHK2, AHK3 and AHK4) are expressed in the OC of SAM and perceive CK as a ligand. ARABIDOPSIS HISTIDINE PHOSPHOTRANSFER PROTEINs (AHPs) are involved in signal transfer below AHKs in response to CK (Kieber and Schaller 2018). The primary targets of this signalling cascade are two types of response regulators known as Type-B ARABIDOPSIS RESPONSE REGULATORs (ARRs) or Type-B ARRs. Type-B ARRs get activated after receiving the phosphate from AHPs and act as true transcription factor while Type-A ARRs are pseudo transcription factors, which receive the phosphate but lacks DNA binding domain thus compete with Type-B ARRs (Ferreira and Kieber 2005; Heyl and Schmülling 2003; Kakimoto 2003). Elevated CK signalling can be witnessed by *TCSn::GFP* reporter activity in the OC region of the SAM where Type-B ARRs activity is relatively high (Zürcher et al. 2013). As expected *TCSn::GFP* and *WUS* expression domains also coincide in the SAM from the early embryonic stage until the adulthood in SAM (Lenhard and Laux 1999; Zürcher and Müller 2016). Despite not having a strong mechanistic basis, it has been shown that WUS negatively regulates Type-A ARRs to promote CK responses positively in the OC (Leibfried et al. 2005). The Type-B ARRs, on the other hand, have been quite well studied for their role in positively regulating *WUS* levels (Meng et al. 2017; Wang et al. 2017; Zhang et al. 2017). This could be partly because there are repressive histone marks like H3K27me3 on the *WUS* regulatory region and those are removed to activate the *WUS* transcription in niche cells in response to CK signalling (Zhang et al. 2017).

1.3.5. Auxin and its role in plant development

1.3.5.1. Discovery of Auxin

In the 19th century, Julius Von Sachs, a German botanist, was first to introduce the concept of chemical messengers in the context of plant development. At that time, he was not aware of the chemical nature and identity of the chemical messenger. The activity of the plant hormone auxin was first revealed by Ciesielski (1872), but it came into limelight when Charles Darwin and his son showed its role in phototropism (Darwin & Darwin, 1892). Darwin showed that when unidirectional light was shone to the oat coleoptile, the tip bends towards the light signal. The bending of tip occurs due to a chemical substance which is released from the tip and moves towards the lower part of coleoptile; as a result coleoptile tip bends in the direction of light (Darwin 1880). In 1913, Peter Boysen-Jensen repeated Darwin's experiment in a different way; he cut off the coleoptile tip and found the coleoptile tip no longer bend towards the light. Later he placed the tip on an agar block and noticed that by putting the agar block, one could restore the bending towards the light. He proposed the presence of a chemical substance in the coleoptile tip, and it is water-soluble. In 1926, Fritz Went, a graduate student from Holland, isolated auxin. Many plant biologists such as Hermann Dolk, Jan Haagen-Smit, F. Kögl and Kenneth Thimann were engaged with this extraordinary chemical substance and named as indole acetic acid or "auxin".

1.3.5.2. Chemical nature of auxins

Native auxin molecules are normally synthesized from the Tryptophan (Trp) amino acid. The common feature of all the Auxin contains an aromatic and carboxylic acid side chain attached to it. The common auxin IAA can be seen below in the image (Fig1.2). The discovery of structure and chemical nature of auxin led to scientist develop the synthetic analogues. These synthetic analogues of auxin can be used for many applications, e.g. 1-Naphthaleneacetic acid

(NAA) is widely used to promote adventitious root formation in shoot cuttings in *A. paniculate*, which can help in fastening the cultivation process (Hossain and Urbi 2016). Another synthetic auxin is 2,4-Dichlorophenoxyacetic acid (2-4D) is widely used as a herbicide.

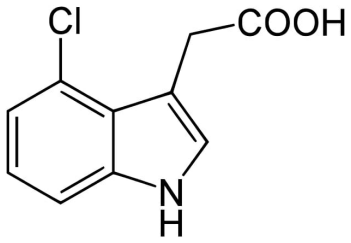

Figure 1.2. Structure of Indole Acetic Acid

1.3.5.3. *De-novo* auxin biosynthesis

Auxin levels are precisely controlled in plants. Plant regulates auxin biosynthesis primarily at the level of biosynthesis and degradation**.** Early molecular and genetic studies revealed the role of Trp dependent auxin biosynthesis pathway in plant development. Trp is an aromatic amino acid, and it is synthesized in various organism, including plants via shikimic acid pathway. Indole acetic acid (IAA) is mainly synthesized from the precursors, which are generated via the shikimate pathway; it is an essential pathway for secondary metabolite synthesis. The shikimate pathway is very well characterized and regulated at transcriptional and post-transcriptional levels (Tzin and Galili 2010). In this pathway, shikimate gets converted into chorismite, which further converted into anthranilate. The later step is catalyzed by a single enzyme consists of two subunits encoded by *ANTHRANILATE SYNTHASE ALPHA SUBUNIT (ASA1)* and *ANTHRANILATE SYNTHASE BETA SUBUNIT (ASB1)*. Physiological and isotope labelling studies have shown that Trp is the main precursor required for auxin biosynthesis. In early studies, it has been shown that Trp deficient mutants have no significant change in free IAA level in comparison to WT. However, the Trp deficient mutant can accumulate indole compounds in higher amount compared to WT (Clark et al. 1993; Gälweiler

et al. 1998). Feeding experiment using T[2H5] Trp suggested the existence of a Trp independent pathway in plants (Normanly, Cohent, and Fink 1993). In contrast to previous studies, Trp deficient mutant did not show a auxin related phenotypes similar to *pin1* or *mp* (Clark et al. 1993; Gälweiler et al. 1998). Early studies provided some clue about Trp dependent and independent pathways for auxin biosynthesis, but it was difficult to ascertain mutant defects due to lack of auxin biosynthesis, or It is caused because of deficiency of other amino acids and secondary metabolite, as L-Trp is also a key source for the biosynthesis of secondary metabolite and amino acids. It has been shown in plants from L-Trp four different pathways can synthesize IAA (Ljung 2013). Shikimate pathway also produces precursors for aromatic amino acids, metabolites, lignin and indoles **(**Fig.1). L-Trp is funnelled through four different pathways, which leads to IAA biosynthesis (Fig.1.3).

1. Indole Pyruvic (IPyA) acid pathway
2. Indole Acetamide (IAM) pathway
3. Indole Acetaldoxime (IOAx) pathway
4. Indole Tryptamine (TRA)pathway

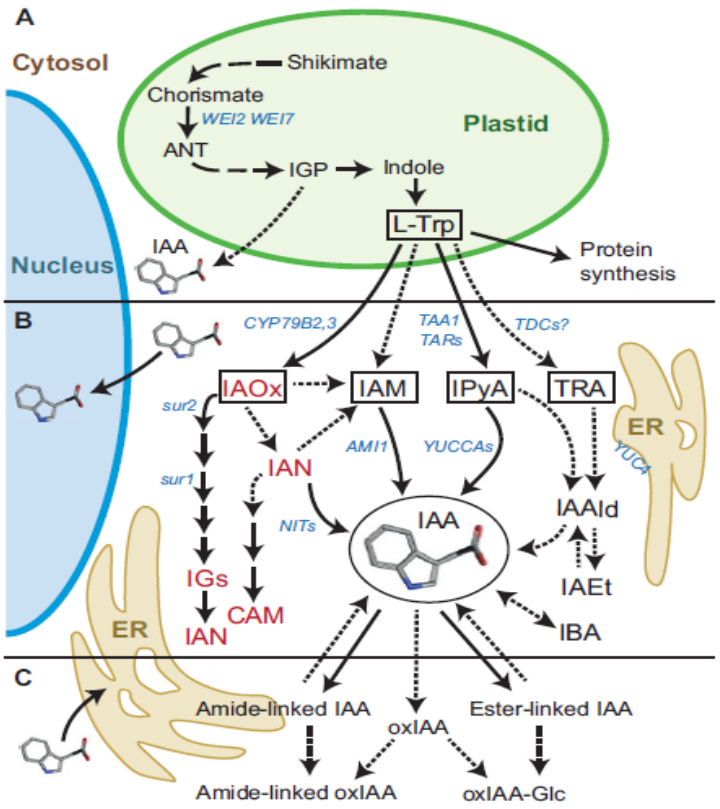

Figure 1.3. IAA metabolism in higher plants. (Courtesy: Ljung 2013)

1.3.5.3.1. Indole Pyruvic (IPyA) Acid pathway

Auxin is a key molecule which regulates different developmental and physiological aspects during plant growth and development. Indole-3-pyruvic acid (IPyA) is a two-step pathway and utilize Trp amino acid as a precursor to synthesize auxin. In this branch of auxin biosynthesis, *TRYPTOPHAN AMINOTRANSFERASES OF ARABIDOPSIS (TAA1)* and closely related *TRYPTOPHAN AMINOTRANSFERASES RELATED* (*TARs)* family genes play a critical role. TAA1 and TARs convert L-Trp into IPyA (Zhao 2012)(Figure 1.3). Two groups of researchers independently identified *TAA1* genes in different genetic screens and proposed the role of *TAA1* and *TARs* in various developmental processes like shade avoidance, ethylene insensitivity, root growth and floral organ patterning (Stepanova et al. 2008; Tao et al. 2008). When *taa1* was

combined with its closest paralogue *tar1* and *tar2,* the resulting double and triple mutant plants show severe phenotype related to auxin signalling (Stepanova et al. 2008).

Downstream of TAA1/TARs, YUCCA (YUC) flavin monooxygenases converts IPyA into IAA (Zhao et al., 2001). *YUC* genes were identified based on the overexpression phenotype. Arabidopsis genome encodes 11 *YUCs* genes. *YUC* overexpression defects are similar to auxin overproduction mutants in Arabidopsis (Zhao et al., 2001). Loss of function studies revealed that single mutant of *yuc* does not show any phenotype, but higher-order mutants lead to defect in auxin-related growth phenotypes in flower development, vascular patterning and embryogenesis (Cheng, Dai, and Zhao 2006; Y. Cheng, Dai, and Zhao 2007).

1.3.5.3.2. Indole Acetamide (IAM) pathway

Plants, fungi, plant-associated pathogenic and non-pathogenic bacteria utilize a two-step auxin biosynthesis pathway (Comai and Kosuge 2009; Lottspeich, Steglich, and Kahmann 1996; Ry 2008; Sardar and Kempken 2018; Tsavkelova et al. 2006). In the first step, plant pathogenic bacteria uses TRYPTOPHAN-2-MONOOXYGENASE (IaaM) enzyme to convert L-Trp into IAM. In the second step, IAM is converted into IAA by INDOLE ACETAMIDE HYDROLASE (IaaH) (Comai and Kosuge 2009). Later on, the presence of IaaH like enzymes, e.g. AMIDASE 1(AtAMI1) to AMIDASE 4 (AtAMI4) were reported in Arabidopsis, which can hydrolyze IAM into IAA (Nemoto et al. 2009; Pollmann et al. 2006). A second IAM hydrolase NtAMI was also identified and characterized in tobacco (Nemoto et al. 2009).

1.3.5.3.3. Indole Acetaldoxime (IOAx) pathway

The Indole Acetaldoxime **(**IOAx) pathway is exclusively present in Arabidopsis and Brassicaceae family. In this pathway, L-Trp is converted into IAOx using by Cytochrome P450 monooxygenases, *CYP79B2* and *CYP79B3* (Sugawara et al. 2009; Zhao et al. 2002). Both these enzymes were identified in Arabidopsis. IOAx is the main intermediate compound

present in this pathway. Elevated levels of IAA was seen in plant overexpressing *CYP79B2* and *CYP79B3.* A decrease in the free IAA was found in the *cyp79b2 cyp79b3* double mutant (Zhao et al. 2002). At the second step, IAOx is converted into Indole-3-Acetonitrile (IAN) and IAM intermediate compounds. Genetic studies suggested the role of Nitrilase encoded by *NIT1* gene for the conversion of IAN into IAA in Arabidopsis (Normanly et al. 1997) and ZmNIT2 in maize (Park et al. 2003). Besides IAA biosynthesis, IAOx is also known to function as a precursor in the biosynthesis of several secondary metabolites and camalexin using SUR1 and SUR2 enzymes (Fig.1.3). Loss of function mutants of *S-ALKYL-THIOHYDROSYMATE LYASE* (SUR1) and *S-ALKYL-THIOHYDROSYMATE LYASE* (SUR2) genes are defective in indole glucosinolate (IG) biosynthesis and accumulates IAA and IAA conjugates (Barlier et al. 2000; Mikkelsen, Naur, and Halkier 2004).

1.3.5.3.4. Indole Tryptamine (TRA) pathway

Initially, it was reported by Zhao et al., (2001, 2002) that *YUCCA* family of genes encodes an enzyme that can catalyze the formation of N-hydroxytryptamine from Tryptamine (TRA). Later on, this finding was questioned. In the first step, L-Trp is converted into TRA by TRYPTAMINE DECARBOXYLASES (TDC). At the biochemical and molecular level, TDC enzymes are well characterized. TDC enzymes were first isolated and characterized for serotonin biosynthesis in rice (Ueno et al. 2003). At the phenotypic level, overexpression plants did not show any obvious phenotype in rice; however, overexpressing plants lines have elevated level of serotonin and *TDC.* Knockdown of *TDC* reduced the serotonin compared to WT (Kang et al. 2009; Ueno et al. 2003). In Pea and Arabidopsis, TRA is present at a very low level. It is possible that TRA could function both as a precursor for IAA and in indole alkaloid and serotonin biosynthesis in different plant species (Mano and Nemoto 2012; Quittenden et al. 2009)

1.3.5.4. Auxin conjugation and degradation

Other than auxin biosynthesis, auxin levels are also regulated by conjugation and degradation (Normanly 2010; Ruiz Rosquete, Barbez, and Kleine-Vehn 2012). Proper coordination between auxin biosynthesis, conjugation and degradation are required to maintain auxin levels in specific cell type and tissues. Plants have three types of auxin conjugation (Bajguz and Piotrowska 2009). (i) Low molecular weight ester conjugates where IAA can be conjugated with ester sugar moieties using UDP glucose transferase, (ii) in low molecular weight amide conjugates, IAA forms the conjugates with some amino acid like alanine, leucine and phenylalanine and (iii) high molecular weight IAA conjugates, which contain protein and peptides attached with an amide bond reviewed in (Ludwig-Müller 2011). These conjugates can be hydrolyzed with the help of amino acid conjugate hydrolases when free IAA is required. Besides ester conjugates, amino acid and protein conjugates, plants also accumulate several inactive auxin in the form of conjugates like IBA, and the inactive methyl ester form of IAA MeIAA (Cohen and Bandurski 1982).

IBA was initially described as a synthetic Auxin, which can regulate many development processes similar to naturally occurring auxin, e.g. initiation of roots, leaf epinasty (Zimmerman and Wilcoxon 1935). On the basis of structure, IAA and IBA, are different, and because of structural dissimilarity, IBA is unable to bind the auxin receptor TIR/SCF complex. Previous studies based on plasma resonance surface analysis revealed that IBA molecule did not have any binding affinity for the auxin receptor (Uzunova et al. 2016). IBA can be converted into IAA by a mechanism similar to B-oxidation operates in peroxisomes in Arabidopsis. Genetic studies revealed that enzymes encoded by *INDOLE-3-BUTYRIC ACID RESPOSE1 (IBR1), ACYL-COA DEHYDROGENASE-LIKE (IBR10) AND PEROXISOMAL ENOYL-CONA HYDRATSE 2 (ECH2)* are responsible for the conversion of IBA into IAA (Katano et al. 2016; Zolman et al. 2008; Zolman, Nyberg, and Bartel 2007). IBA-derived auxin

has strong roles in various aspects of root development and shoot development. IBA derived IAA is required to maintain root auxin levels and in loss of function mutation in three major genes responsible for conversion of IBA into IAA leads to severe developmental defects in lateral root development, root hair elongation, cotyledon development, and pavement cell lobbing (Katano et al. 2016; Strader et al. 2010; Strader and Bartel 2011).

1.3.5.5. Auxin transport

Auxin is a major regulator of various developmental events. The function of auxin depends on the local maxima, which forms as a result of differential distribution of auxin within the tissues and organs. This heterogeneity in auxin distribution is partly contributed by transport. Auxin can travel to long distances in plant system using phloem. Local auxin production in young tissue of leaf and floral organ primordia in the SAM can be a good source of auxin. Polar transport of auxin is an intriguing phenomenon observed with respect to only auxin. Auxin is a weak acid. In the apoplast, it remains in IAAH form. According to this model, a non-polar form of IAAH can directly diffuse through the plasma membrane and enter into the cells very easily without any transport protein. Inside the cells, pH is more alkaline or neutral (pH 7). After entering the cell, IAAH gets deionized and dissociates into anionic form (IAA^-) and proton (H^+). In its anionic form, it cannot diffuse through the plasma membrane (Ljung 2013). Therefore, IAA^- requires efflux carrier (Ruiz Rosquete et al. 2012; Zazımalova 2015). The localization of transport protein within the cell membrane determines the directionality of auxin transport. Although the requirement of auxin influx carrier protein for transport was not proposed in this model. However, influx carrier-mediated auxin exit from the cell also considered in polar auxin transport (Benning 1986; Delbarre et al. 1996; Tanaka et al. 2006).

1. Auxin efflux carriers
2. Auxin influx carrier proteins
3. ABCB transporters

1.3.5.5.1. Auxin efflux carriers

The polar transport of auxin depends on the auxin efflux carrier proteins, mainly responsible for the transport of auxin from one cell to another cell. The polar localization of PINs within the cells would determine the direction of auxin transport in tissue. On the basis of structural differences in the hydrophilic loop present in the middle of the polypeptide chain, the eight *PIN* genes identified encode short and long PIN proteins (Křeček et al. 2009). Short PINs have a small or reduced hydrophilic loop in the middle (e.g. PIN5 and PIN8). Short PINs are involved in the intracellular auxin transport and are localized on the cell organelle membrane, mostly on the ER. PIN5 transports auxin to the ER lumen (Ganguly et al. 2014; Křeček et al. 2009). Other PINs belongs to long PINs subclass; they contain a long hydrophilic loop in the middle of the protein and localizes to the plasma membrane, and facilitates auxin transport (Ganguly et al. 2014). PIN6 is an exception and facilitates both inter and intracellular transport of auxin depending upon the cellular and subcellular localization (Ditengou et al. 2018; Simon et al. 2016). Expression of *PINs* is regulated at transcriptional and post-transcriptional levels. Auxin itself regulates the expression of *PINs* (Ganguly et al. 2014) except *PIN5*. *PIN5* expression is downregulated in response to auxin (Křeček et al. 2009; Mravec et al. 2009). Some of the transcription factors belonging to the MADS-box family can bind to *PIN1* and *PIN4* promoters, e.g. *XAL2/AGL14* (Garay-Arroyo et al. 2013). A recent study also suggested the role of *INDETERMINATE DOMAIN (IDD)* class of genes in modulating the auxin accumulation by directly influencing the expression of auxin biosynthesis (*TAA1* and *YUCs*) and transport genes to promote the organogenesis and gravitropic responses (Cui et al. 2013). *ARF3* is also shown to involved in the regulation of *PIN1*, *3* and *7* (Simonini et al. 2017). Beside auxin, cytokinin also takes part in regulating auxin transport. *CYTOKININ RESPONSE FACTORs (CRFs)* 6 and 7 are directly involved in regulating *PIN1* and *PIN7* expression

(Šimášková et al. 2015). Expression of *PINs* is also regulated by chromatin remodelling factors. BRAHMA, a SWI2/SNF2 chromatin remodelling ATPase directly, targets *PIN1* loci and activates its expression (Yang et al. 2015). PIN proteins are constitutively recycled between plasma membrane and endosomes, which defines the cellular localization of PINs (Adamowski and Friml 2015). Depending upon their precise expression and localization, PINs have specific functions. *PIN1* expresses in the SAM, and PIN1 protein polarly localized towards the emerging organ primordium, likewise in the root, lateral root organ primordium emerges as a result of polar localization in pericycle cells (Billou et al. 2005; Gälweiler et al. 1998; Okada et al. 1991). PIN2 is localized in the cortical cells in the meristematic region of root apical meristem and senses the gravity (Müller et al. 1998; Rahman et al. 2010). PIN3 protein is required to maintain the differential growth of shoot and root, phototropism, gravitropism, and apical hook formation (van Gelderen et al. 2018; Haga and Sakai 2012; Rakusová et al. 2016; Willige and Chory 2015). PIN4 is localized at the basal membrane in the root meristem and have a function in apical hook development (Willige and Chory 2015).

1.3.5.5.2. Auxin influx carriers

As the name suggests, auxin influx carrier mediates the transport of auxin inside the cell. Auxin influx carrier belonging to AUX/LAX (AUXIN RESISTANT1/LIKE AUX1) family of protein was identified in Arabidopsis. Four influx *AUX1, LAX1*, *LAX2* and *LAX3* are encoded by Arabidopsis genome (Péret et al. 2012). AUX1 is localized asymmetrically in the protophloem and facilitates acropetal transport of auxin in the root (Péret et al. 2012; Swarup et al. 2001). It is also localized in the columella cells of the root cap and promotes basipetal transport in the root apex in response to gravitropic responses (Swarup et al. 2005). *aux1* mutants are agravitropic (Swarup et al. 2005). *LAX1* and *LAX2* are expressed in the root vasculature tissues and weakly in the quiescent centre and columella cells (Péret et al. 2012), while *LAX3* expresses in columella cells, stele, and its expression is also influenced by auxin (Péret et al. 2012;

Swarup et al. 2008). Loss of function studies revealed the role of *AUX1* and *LAX3* in lateral root formation. The *aux1 lax3* double mutant plants fail to form lateral roots 14 DAG (Swarup et al. 2008). Genetic studies also revealed the role of *AUX1/LAX* in phyllotactic patterning, organogenesis, vascular development (Fàbregas et al. 2015; Péret et al. 2012), seed germination (Wang et al. 2016) and apical hook development (Vandenbussche et al. 2010; Žádníkova et al. 2010).

1.3.5.5.3. ABCB transporters

ABCB (ATP BINDING CASSETTE/ MULTI-DRUG RESISTANCE/ POLYGLYCOPROTEIN) transporters family of genes are present in all living organisms from bacteria to humans. Twenty-one genes encoding ABCB proteins were identified in Arabidopsis genome. Structurally, these transport proteins contain two domains, connected by a 60aa long linker. One domain is called the transmembrane domain (TMD), and another half domain is known as the nucleotide-binding domain (NBD) (Geisler and Murphy 2006). ABCB1, ABCB4 and ABCB19 are well characterized, and studied for their role in auxin transport. ABCB 1 and ABCB 19 are localized to the plasma membrane. ABCB1 expresses in the root differentiation zone and is required for hypocotyl elongation (Sidler et al. 1998). ABCB19 is a closet homologue of ABCB1, and its expression is found in the cotyledon node, epidermis, cortex, and stele region of the root (Blakeslee et al. 2007). *abcb1 abcb19* double mutant plants are dwarf with short inflorescences and have the defects in axillary and secondary inflorescences formation. They form reduced numbers of the rosette and cauline leaves (Blakeslee et al. 2007). The other well-characterized member of this family is ABCB4, and known to have a role in auxin transport in roots. It is highly expressed in the primary root tip and lateral root primordia. *abcb4* mutant show increased lateral root formation (Santelia et al. 2005; Terasaka et al. 2005).

1.3.5.6. Auxin perception and signalling

Auxin regulates the auxin responses at the cellular level by a well-defined auxin signalling pathway. In response to auxin signalling, hundreds of genes get either upregulated or downregulated (Ivan A. Paponov et al. 2008). Inside the cells, for the activation of auxin signalling three different components come together, the first component, depending upon auxin levels inside the cell they can make a complex with different component like auxin, ubiquitin ligase complex SCF and AUX/IAAs. At low auxin concentration within the cell, AUX/IAA forms dimers with ARFs and does not allow the auxin-dependent activation and repression of auxin responsive genes (Fig.1.4). However, at high auxin concentration, auxin directly binds to TIR1/AFB complex, and thus, auxin acts as glue for TIR1/AFB-AUX/IAA complex, which is recognized by SCF-type ubiquitin-protein ligase complex. Ubiquitination of AUX-IAA leads to 26S proteasomal degradation of AUX/IAAs by TIR/AFB (Fig.1.4). Now, in the free state ARFs can recruit the chromatin remodelling complex (SWI/SNF) and can convert the chromatin into more open state and can directly interact with the auxin responsive elements (AuxRE) present within the promoter of the auxin responsive genes and activate or repress their transcription (Fig.1.4). On the basis of this mechanism, auxin signalling can change the expression of the auxin responsive gene at the level of transcription. Auxin signalling pathway contains three major components to execute signalling.

1. Auxin receptors
2. AUX/IAAs
3. Auxin Responsive Factors

1.3.5.6.1. *TIR1/AFBs* or auxin receptor

One of the important component of auxin signalling pathway is the auxin receptor. *TRANSPORT INHIBITOR RESPONSE1 / AUXIN SIGNALING F-BOX (TIR1/AFB)* is a F-box protein. TIR1 is the auxin receptor and binds with auxin directly (Dharmasiri, Dharmasiri, and

Estelle 2005; Kepinski and Leyser 2005). Plants, which do not have the *TIR/AFB* proteins are unable to sense auxin. Previous phylogenetic analysis suggested that these proteins are conserved in all land plants (Mutte et al. 2018). *TIR1* belongs to a small family, in addition, *AFB1*, *AFB2, AFB3, AFB4* and *AFB5* also belongs to the same gene family and function in auxin perception (Dharmasiri, Dharmasiri, Weijers, et al. 2005). Structure of TIR1 was first resolved by Tan et al. (2007). TIR1/AFB protein shares a similar structure with AUX/IAA. At the N-terminal contains a F-BOX domain and rest of the region includes 18 Leucine-Rich Repeats (LRR). AFB4 and AFB5 consist of an extra N-terminal extension which is not present in TIR1 and other AFBs. The F-BOX domain is essential to facilitate interaction between TIR1/AFBs and AUX/IAA proteins (Tan et al. 2007). The LRR repeats containing domain acts as a binding pocket for auxin (Tan et al. 2007). *TIR1, AFB1-AFB5* are actively expressed during different developmental stages like emerging lateral roots seedling root tips, vascular bundles, cotyledons and mature leaves, and in floral organs (Dharmasiri, Dharmasiri, Weijers, et al. 2005). Single and double mutant of *TIR1* and *AFB1-AFB5* did not show any phenotype because of functional redundancy. However, higher-order mutants *tir1-1 afb2-1 afb3-1* and *tir1 afb1 afb2 afb3* show severe defects in root and root meristem development (Dharmasiri, Dharmasiri, Weijers, et al. 2005).

1.3.5.6.2. AUX/IAAs repressors of Auxin signalling

AUX/IAAs are the negative regulator of auxin signalling (T Ulmasov et al. 1997). AUX/IAA are classified as short-lived nuclear-localized proteins, required for auxin-dependent regulation of auxin responsive genes. Arabidopsis encodes 29 AUX/IAA (Paponov et al. 2008). AUX/IAA proteins composed of four conserved domains referred to as domain I, II, III and IV (Hagen and Guilfoyle 2002). Among these, domain I consists of an EAR motif and designated as a repression domain (Tiwari, Hagen, and Guilfoyle 2004). Domain II is called a degron

domain and consists of "GWPPV" conserved motif. This domain interacts specifically with SCF-TIR1-auxin receptor complex and promotes auxin-dependent degradation of AUX/IAAs (Kepinski and Leyser 2005; Ramos et al. 2001). Recently it has been shown that lysine residues in the flanking region of the degron domain are associated with ubiquitinoylation mediated degradation of AUX/IAAs by TIR1/SCF complex (Winkler et al. 2017). Domain III and domain IV collectively called as PB1 domain. Domain III is consists of βαα-fold and facilitates the homodimerization between AUX/IAAs and heterodimerization between AUX/IAAs and ARFs (Heologis 1997; Morgan et al. 1999). Domain IV is consist of an SV40 type NLS (PKKKRKV) signal (Guilfoyle and Hagen 2012). Domain III and domain IV collectively called as PB1 domain. The presence of specific residues at the at N and C terminal of PB1 domain is essential to mediate the protein-protein interaction between two PB1 domains either by electrostatic interaction or through hydrogen bonding (Kim, Harter, and Theologis 1997; Noda et al. 2003). Structurally, the majority of AUX/IAAs and ARFs have the same PB1 domain.

1.3.5.6.3. Auxin responsive factors or output factors regulating the auxin signalling

The mechanism of auxin signalling relies on the output signal transmitted through Auxin Responsive Factors (ARFs) to auxin responsive genes. Phylogenetic studies revealed the presence of 23 *ARFs* in Arabidopsis genome, belongs to three different subclasses, namely, class A, B and C. All the ARFs contains three conserved domains, and designated as DNA binding domain at the N-terminal, a middle region (MR) in the centre and a PB1 domain at the C-terminus (Ulmasov, Hagen, and Guilfoyle 1999a, 1999b Tiwari et al 2003). Crystal structure of ARF1 and ARF5 revealed that the N- terminal DNA binding domain has three subdomains. A B3 subdomain is required for sequence-specific interaction of ARFs with auxin-responsive elements (AuxRE). An ancillary domain (AD) and a DNA dimerization (DD) domain are

essential for ARF-ARF homodimerization (Boer et al. 2014). In contrast to the DBD domain, MR regions are not conserved in all the ARFs. *ARFs* are defined in the different subclasses on the basis of amino acids present in the MR region. Class A *ARFs* are called as activators, and consists of glutamine-rich MR region, whereas class B and C are called as repressors, and they contain serine, prolines, and threonine in MR region (Roosjen, Paque, and Weijers 2018, Tiwari et al 2003). Crystallographic studies revealed the presence of a C-terminal CTD domain. It is required for oligomerization of AUX/IAA and ARFs through protein-protein interactions (Kim et al. 1997).

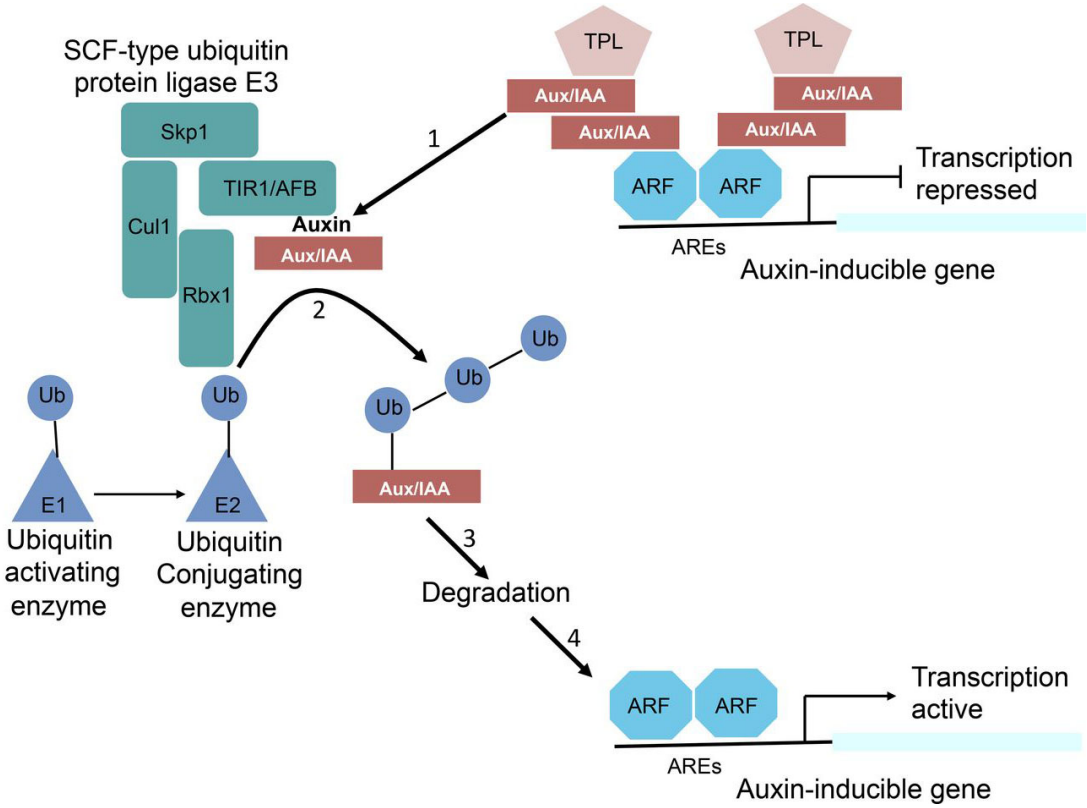

Figure 1.4. Schematic showing main auxin signalling pathway. Courtesy:(Leyser 2018)

1.4. Auxin a central regulator of phyllotaxy and organogenesis

Higher plants can produce tissues and organs such as leaves and stem post embryonically. Lateral organ development relies on spatially and temporally coordinated cell proliferation of

the primordium cells, which resides in the SAM. Stem cells present in CZ of SAM divide continuously, and their daughter cells enter into the PZ where new organ primordia arise. In Arabidopsis, the beginning of organ initiation is marked by the selection of a population of cells, called as primordia founder cells. Later, these cells receive a signal, in response to it they form the primordium, then fully differentiated organ. Cells from both the epidermal cell layer and subepidermal cell layer participate in the new organ primordium formation. A previous live imaging study suggested that cells undergo oriented cell divisions and cell expansion during primordial growth (Reddy et al. 2004). However, cells present at the organ boundaries show reduced cell division and cell expansion (Reddy et al. 2004). At the genetic level, genes for meristem identity, such as *STM* gets downregulated in these primordia founder cells (Lenhard et al. 2002; Long et al. 1996) and genes which are associated with organ formation and organ boundary separation like *LEAFY, ANT, CUC1, CUC2, CUC3* starts to express in those cells which are committed to form the organ (M Aida et al. 1997; Elliott et al. 1996; Heisler et al. 2005; Hibara et al. 2006; Takada et al. 2001; Vroemen et al. 2003).

Researchers proposed various models and mechanisms underlying the phyllotaxy and how primordia are positioned in SAM. Auxin plays an essential role in primordia initiation and proper phyllotactic patterning. Mutants which are defective in auxin transport show defects in lateral organ formation and these defects can be partially rescued by application of exogenous auxin (Okada et al. 1991, Reinhardt, Mandel, and Kuhlemeier 2000). High auxin maxima decide the position of lateral organs. Moreover, the region of high DR5 responses in SAM correlates with organ initiation sites (Heisler et al. 2005). Next question arises how these high auxin maxima forms and how the organ initiation starts. The mechanisms for the formation of auxin maxima to generate lateral organs are very complex and regulated at the level of auxin transport and biosynthesis. This auxin maxima is perceived by components of auxin signalling. When auxin levels are low, AUX/IAA negative regulator of auxin signalling remain bound

with *ARF5/MP* and recruits co-repressor TOPLESS(TPL), which makes a complex with HDA19 to keep the transcription off (Long et al. 2006; Szemenyei, Hannon, and Long 2008). In the primordium founder cells, when auxin concentration is high, AUX/IAAs will undergo for ubiquitin-mediated degradation. Once AUX/ IAAs are degraded, in the free form ARF5/MP recruit chromatin remodellers BRAHMA and SPLAYED (SYD) and activates the transcription of target genes (Wu et al. 2015; Yamaguchi et al. 2013). MP belongs to class A ARFs, and by interacting with auxin responsive elements (AuxRE) present in the promoter of auxin responsive genes it activates transcription in the presence of auxin (Cole et al. 2009; Konishi et al. 2015). *ARF3* and *ARF4* are highly expressed in the PZ of SAM in the organ founder cells (Vernoux et al. 2011). *ARF3* and *ARF4* both belong to Class B family and consider as a repressor for auxin signalling (Ulmasov et al. 1999a; Weijers and Wagner 2016). Previous studies revealed the role of *ARF3* and *ARF4* in lateral root initiation, and in abaxial identity (Marin et al. 2010; Pekker, Alvarez, and Eshed 2005). In a recent study, it has been shown that the *ARF3* and *ARF4* mediated repression of *STM* is required to promote organ initiation at the peripheral zone of SAM. Hence, *ARF3* and *ARF4* act together with MP to promote the organogenesis (Chung et al. 2019).

Previous studies were mainly focused on PIN-FORMED1 (PIN1) mediated auxin transport, and it defines the local auxin maxima. The (PIN) auxin efflux carriers, of which PIN1 is known to most critical for the initiation of lateral primordia during the reproductive phase of plant development and phyllotactic patterning in SAM. *pin1* mutants fail to form the lateral organ and generate pin-like inflorescence meristem (Okada et al. 1991). Plants treated with auxin transport inhibitor drugs also have a similar phenotype (Reinhardt et al. 2003b). External application of auxin to *pin1* and NPA treated plants restore the organogenesis, suggesting that accumulation of auxin at the shoot apex is required for the formation of organs. Localization of PIN1 also changes according to the stage of primordia development (Heisler et al. 2005).

Besides auxin transport, auxin biosynthesis also plays an important role in the initiation of lateral primordia. In maize, *VANISHING TASSEL2* (VT2) and *SPARSE INFLORESCENCE1* (*SPI1*) encodes for an ortholog of *TRYPTOPHAN AMINOTRANSFERASE OF ARABIDOPSIS1* (*TAA1*) and a monocot-specific YUCCA-like enzyme, respectively (Gallavotti et al. 2008; Phillips et al. 2011). *VT2* and *SPI1* display distinct spatiotemporal expression pattern in the SAM. *SPI1* expresses in the newly emerging organ primordia, whereas *VT* expresses in the epidermal cell layer of emerging organ primordia (Gallavotti et al. 2008; Phillips et al. 2011). The double mutant *vt spl1* plants show less number of lateral organ, suggesting the role of auxin biosynthesis in lateral organ formation in maize (Gallavotti et al. 2008; Phillips et al. 2011). In Arabidopsis, *YUCCA* class of genes were reported to maintain auxin threshold in SAM, and are involved in organ formation (Cheng et al. 2006). However, previous studies did not characterize the role of *TAA1* and *TARs* in organ formation.

1.5. Thesis Objectives

It is already well established that auxin can trigger various non-transcriptional processes, like activation of the ion channels and proton pump of the plasma membrane (Perrot-Rechenmann 2010). There are reasonably well-documented experiments suggesting the role of polar auxin transport in organ formation. However, there are very few studies to suggest the role of local auxin biosynthesis in setting up auxin gradients and auxin maxima in specific cell types. Auxin is mainly synthesized from L-Trp in plants (Ljung 2013). The enzymes encoded by *TAA1* and its closely related *TARs* genes are involved in catalyzing the conversion of L-Trp into IPyA. YUC monooxygenases convert IPyA into IAA (Zhao 2010). The single mutant of neither *TAA1/TARs* nor *YUCs* shows any phenotype owing to their high genetic redundancy. However, when higher-order mutants are generated, they display a defect in embryonic and postembryonic development related to auxin signalling (Youfa Cheng, Dai, and Zhao 2007; Stepanova et al. 2008). From the previous studies, it is well established that local auxin

biosynthesis is essential for the establishment of local auxin maxima and its maintenance in roots (Brumos et al. 2018). From the previous studies, it is not clear where and when *TARs* genes are expressed in the SAM and whether their activity contributes in maintenance of local auxin maxima in the SAM. Further, it is not clear how auxin biosynthesis genes are regulated in the SAM. I have addressed two specific questions related to this in this thesis:

1. What *TAA1* and *TAR2* mediated auxin biosynthesis signifies in the SAM?
2. How WUS mediated regulation of auxin biosynthesis in SAM relevant for plant growth and meristem functioning?

Here, in this study, I report *TAA1* and *TAR2* both are expressed in the different zones of SAM and contribute to the formation of local auxin maxima to the lateral organ formation. Disruption in the function of *TAA1* and *TAR2* genes affects meristem organization and organogenesis in SAM. Furthermore, interference in the auxin transport enhances the SAM patterning defect, and repeal in the differentiation of stem cell daughters into PZ cell types. *TAR2* is a direct target of WUS, whose expression is repressed in CZ and RM cell types by WUS. Conversely, miss expression of *TAR2* in the PZ cell types reduces the total number of stem cells and their descendants, hence perturbing the relative ratio of CZ and PZ cell number in SAM. We show that auxin synthesized by *TAA1* and *TAR2* is required for auxin responses in PZ. To maintain the fate of stem cells, WUS negatively regulates auxin responses in the CZ by directly regulating auxin biosynthesis, and thus, affecting the expression of auxin signalling genes to counter the differentiation pathways. We believe that these novel findings will pave the way to increase our knowledge about our understanding of meristem function.

Chapter 2
Material and Methods

2.1. Plant work

2.1.1. Plant growth media and conditions

For plant growth work, the seeds were either sown on Murashige and Skoog (MS) medium, containing 0.8% Bacto-agar, 1% (w/v) sucrose and 0.1% (w/v) MES or directly on the soil, a mixture of soilrite (KELTECH Energies Ltd. India) containing perlite and vermicompost in 4:1:1 ratio. Seeds were kept for vernalization in darkness at 4°C for three-four days on wet soil and then transferred to the plant growth chambers (Conviron, Canada and Percival Scientific, USA). Plant growth chambers were equipped with Philips fluorescent tube lights (write full name and model). Plants were grown under 16 h light / 8 h dark cycle, 70% relative humidity, at 22°C temperature with 120 $\mu M/m^2/s^{-1}$ light intensity.

2.1.2. Seeds sterilization

Seeds were surface-sterilized before plating on MS agar plates with 70% ethanol for one min, followed by 4% (v/v) sodium hypochlorite containing 0.03% Triton X-100 for 3-min and washed four times with sterile distilled water. Plates were kept for vernalization in the dark for 3-4 days for stratification of seeds.

2.1.3. Plant material

Arabidopsis thaliana Columbia-0 (Col-0) and Landsberg *erecta* (L*er)* ecotypes were used as wild type strains and were obtained from Arabidopsis Biological Resource Center (ABRC, Ohio University, USA). T-DNA insertion alleles for *TAA1* and *TAR2* used in this study are in Col-0 background and were obtained from ABRC. The *pin1*-5 allele is in L*er* background and obtained from ABRC. *clv3-2* mutant seeds having *pCLV3::H2B-YFP* and *pWUS::eGFP-WUS* transgenes and *35S:WUS-GR* lines were shared by Dr Venu Reddy (University of California Riverside) (Yadav et al. 2010). *pTAA1::TAA1-Ypet*, *taa1-1-/- tar2-1-/-* rescued line was a kind gift by Dr. Anna Stepanova (North Carolina State University, USA) (Brumos et al. 2018).

pRPS5A-DII-n3xVenus and *R2D2* (*pRPS5A-mDII-ntdTomato, RPS5A-DII-n3×Venus*) seeds were obtained from Teva Vernoux laboratory (Liao et al. 2015). *pCLV3::mGFP-ER*, *pPIN1::PIN1-GFP*; *pDR5rev::3XVENUS-N7 reporter* lines and *clv3-2* mutant were available in the lab, was previously used in (Yadav et al. 2010).

T-DNA insertion mutants of *taa1-1 tar2-1* (CS16413), *tar2-1* (CS16404), and *pin1-5* (CS69067) were obtained from Arabidopsis Biological Resource Center (ABRC, Ohio, USA). To confirm the presence of T-DNA allele in the mutant lines, genomic DNA was isolated using a modified CTAB method. T-DNA PCR was set up, and finally, the PCR product was sequenced to ascertain the insertion. *taa1-1* single mutant was isolated from the segregating population of *taa1-1-/- tar2-1+/-* and was confirmed both by genotyping and sequencing. Primers used for genotyping are listed in Table 2.5. To generate the double mutants of *pin1 taa1, pin1 tar2* and triple mutant of *pin1 taa1 tar2*, *pin1-5-/-* was crossed with *taa1-/- tar2+/-* line. Seeds from the crosses were self-pollinated in the F1 generation. Plants in the F2 generation were analyzed on the basis of genotype and phenotype. In the F2, *pin1-5* allele was identified based on the flower phenotype in *pin1 taa1* and *pin1 tar2* double mutants, while the *taa1-1* and *tar2-1* alleles were confirmed using T-DNA PCR. In the above population, I identified *pin1 taa1 tar2* triple mutant plants based on the novel phenotype having a mound of cells on the shoot apex tip. The *pin1-5* allele was confirmed by Sanger sequencing in the *pin1-5 taa1-1 tar2-1* triple mutant whereas *taa1-1* and *tar2-1* alleles were confirmed by T-DNA PCR as described above. Since *pin1-5-/- taa1-1-/- tar2-/-1* triple mutant plants were rare and did not produce seeds, *pin1-5-/- tar2-1-/- taa1-1+/-* segregating lines were used for isolating triple mutant for experimental work.

To combine *pTAR2::H2B-YFP, pWUS::mCHEERY* and *pTAR2::H2B-YFP, pCLV3:mGFP-ER* reporters. Genetic Crosses were made between *pTAR2::H2B-YFP x pWUS::mCHEERY* and *pTAR2::H2B-YFP x pCLV3:mGFP-ER* reporter lines. Seeds from the crosses were grown first

on to MS plate, after 12-14 days of germination transferred on to the soil. F1 plants were checked for the fluorescence and plants carrying *pTAR2::H2B-YFP x pWUS::mCHEERY* and *pCLV3:mGFP-ER x pTAR2::H2B-YFP* together followed in the F2 generation and used for confocal imaging.

To investigate the stem cells fate, auxin input and output *taa1-1-/- tar2-1+/-* mutant line was crossed with *pCLV3:mGFP-ER, pIN1:PIN1:GFP, pDR5rev::3XVENUS-N7*, and *pRPS5A::DII-Venus* reporters respectively. Plants from these crosses were allowed self-pollination in F1. F2 seeds were collected separately for each independent line, and subsequently, 5 to 6 independent lines were followed up in F2 generation. Plants were genotyped for all the allelic combination *taa1-1-/-, tar2-1-/-, taa1-1+/- tar2-1+/-, taa1-1-/- tar2-1+/-, taa1-1+/- tar2-1+/-, taa1-1+/- tar2-1-/-, taa1-1+/- tar2-1+/+, taa1-1+/+ tar2-1+/- , taa1-1+/- tar2-1+/+, taa1-1+/+ tar2-1+/-, taa1-1+/+, tar2-1+/+* in F2 generation using the primers listed in Table 2.2. Two independent lines of WT, *tar2-1-/-, taa1-1-/-, and taa1-1-/- tar2-1+/-* having respective reporter line isolated from F2 generation, and followed up to F5 generation and used for confocal imaging.

2.1.4. Plant transformation

Agrobacterium-mediated floral dip method was followed for plant transformations (Clough and Bent 1998). *Agrobacterium tumefaciens* GV3101 strain was used for plant transformations in the present study. The plasmid containing transgene of interest was transformed in *Agrobacterium* by electro-transformation. Transformed cells were rescued on gentamycin, rifampicin and plates containing antibiotic required for plasmid of interest selection. Plates were kept at 30ºC for 48 h. Colony PCR was performed to confirm the presence of the transgene in *Agrobacterium* strain. Positive colonies were inoculated in 5 ml LB medium with antibiotics and were grown for 24 h at 30ºC. The Secondary culture was inoculated with 1% primary culture and kept for shaking at 30ºC for 18-20 h. Once the OD of the cells is reached

to 0.8-1.0, cells were harvested by centrifugation and resuspended in 5% sucrose. 0.05% SILWET L-77 solution was added to the suspended cells. Arabidopsis inflorescences were dipped into the Agrobacterium solution, and plants were kept at the bottom of the plant tray in the dark covered with another inverted tray on top for overnight at RT. Next morning, plants were returned to the plant growth chamber. Plant transformation was repeated one more time after 8-9 days to increase the efficiency of transformation.

2.1.5. Selection of transgenic lines

Seeds were collected and kept in a desiccator for drying for 4-5 days, and later on, either plated on MS medium supplemented with respective selection marker listed in Table 2.1 or on soil with BASTA. After 10-12 days transgenic plants were transferred to soil in fresh pots. In order to make plants homozygote for respective transgenes, T1 transgenic plants lines were put on selective antibiotics until T3 generation. Two-three independent homozygous lines were used for phenotypic and promoter-reporter analysis.

Table 2.1. Transgenic lines generated in the present study

Construct name	Genetic background	Selection marker in planta	Selection marker in bacteria	T1 selected lines.
pTAR2::H2B-YFP	WT-L*er*	Basta	Kanamycin	18
pTAR2(ΔWUS)*::H2B-YFP*	WT-L*er*	Basta	Kanamycin	16
pTAR2(m1)*::H2B-YFP*	WT-L*er*	Basta	Kanamycin	22
pTAR2(m2)*::H2B-YFP*	WT-L*er*	Basta	Kanamycin	6
35S::TAR2	WT-L*er*	Hygromycin	Kanamycin	17
6xpOp:TAR2 x CLV3s::LhG4	WT-L*er*	Gentamycin	Gentamycin	48
6xpOp:TAR2 x WUS::Lhg4	WT-L*er*	Gentamycin	Gentamycin	40
pTAR2::TAR2, pGreen 0229	WT-L*er*	Basta	Kanamycin	24
pTAR2(ΔWUS)*::TAR2, pGreen 0229*	WT-L*er*	Basta	Kanamycin	24
pTAR2::TAR2, pMDC32	*pCLV3::mGFP-ER*	Hygromycin	Kanamycin	21
pTAR2::TAR2, pMDC32,	*taa1-1 tar2-1*	Hygromycin	Kanamycin	6
pTAR2(ΔWUS)*::TAR2, pMDC32*	*pCLV3::mGFP-ER*	Hygromycin	Kanamycin	21
pWUS::mCHEERY	WT-L*er*	Kanamycin	Kanamycin	7

2.2. Molecular biology techniques

2.2.1. Primers

Primers used in this study were designed using Vector NTI 2.0 software. Primers for genotyping of *taa1-1* and *tar2-1* T-DNA lines were used as reported in (Stepanova et al. 2008). Primers used for qRT-PCR were designed manually. All the primers were ordered either from Sigma Aldrich (India) or Integrated DNA Technologies (IDT, India)). Primers for EMSA experiments were synthesized with 50nM concentration (Sigma Aldrich, India). Primers used for cloning, qRT-PCR and genotyping were synthesized with standard 25nM concentration. All the primers used for this study are listed in Table 2.2 to 2.7.

Table 2.2. Primers used for clonings

Transgene		Primer sequence
pTAR2:H2B-YFP WT	Forward	CACCTCAAAGAAAGAAAAACCACACCCTG
	Reverse	TTTCTCTCAAAACTAAAACACAAAACCA
TAR2 CDS	Forward	CACCATGGGACAGATTCCGAGGTTTCTTT
	Reverse	TACAAAGTTGAATTAAAGGAAGAT
TAA1 CDS	Forward	CACCATGGTGAAACTGGAGAACTCGAGG
	Reverse	CTAAAGGTCAATGCTTTTAATGAGCTTC
ARF3 CDS	Forward	CACCATGGGTGGTTTAATCGATCTG
	Reverse	CTAGAGAGCAATGTCTAGCAACATG
ARF4 CDS	Forward	CACCATGGAATTTGACTTGAATACTGAG
	Reverse	TCAAACCCTAGTGATTGTAGGAGAAGAA
ARF5 CDS	Forward	CACCATGATGGCTTCATTGTCTTGTGTT
	Reverse	TTATGAAACAGAAGTCTTAAGATCGTTA
CUC1 CDS	Forward	CACCATGGATGTTGATGTGTTTAACGGTT
	Reverse	TCAGAGAGTAAACGGCCACACACTCACG
WUS-FL CDS	Forward	CACCATATGATGGAGCCGCCACAGCATCA
	Reverse	ATCTCGAGCTAGTTCAGACGTAGCTCA
CLV3 CDS	Forward	CACCATGAGAAGACATGATATCATCATC
	Reverse	TCAGTGTTTGACCGGTGGGTGACGATTT
pWUS::mCHEERY	Forward	CACCGGCGCGCCATGGTGAGCAAGGGCGAGGAGG
	Reverse	GATATCTTACTCTTCTTCTTGATCAGCTTC
SP/TAR2 CDS/Spe1	Forward	GAGCTCTTACAAAGTTGAATTAAAGGAA
ASP/TAR2 CDS/Sac1	Reverse	GTTGTGTGGAATTGTGAGCGGATAACAA
SP/TAR2 CDS/Sbf1	Forward	CCTGCAGGGCTCTTTCAAAGAAAGAAAA
SP/TAR2 CDS/Asc1	Reverse	GGCGCGCCTTTCTCTCAAAACTAAAACA

Table 2.3. Primers used for probe synthesis for In-situ hybridization

Primer name		Primer sequence
pENTER/D-TOPO/T7sense	Forward	CTCGGGCCCTAATACGACTCACTATAGG
pENTER/DTOPO/T7/sense	Reverse	GCCAACTTTGTACAAGAAAGCTGGGTCG
pENTER/DTOPO/T7/antisense	Forward	GACCATGTAATACGACTCACTATAGGGGATATCAG
pENTER/DTOPO/T7/antisense	Reverse	AAAGCAGGCTCCGCGGCCGCCCCCTTCACC

Table 2.4. Primers used for qRT-PCR

Gene name		Primer sequence
TAR2	Forward	CCCTTCTTCACACTTAAACC
	Reverse	GGATTGGATGGGCTTT
TAA1	Forward	CTTACCCTGCGTTTGCGT
	Reverse	CTTCATGTTGGCGAGTCTCT
ARF1	Forward	CATCTGGTCCTGTTACTCCAGA
	Reverse	CAAAAAGCCTACAGACATTTCCATTA
ARF2	Forward	GCTTACCAGAGAAGGTACAACTAA
	Reverse	AAAGCCGGAGAGCAAATCTG
ARF3	Forward	CTGTCTCTGAGGGGATTCGC
	Reverse	TTGCAAGACCTTATGGAAACCATA
ARF4	Forward	CCCATAACAAAAAGGGGTGGT
	Reverse	TACAAACTCACCAAATCGATCCT
ARF5	Forward	CTTACTTTGCTGGTGAAACTGAA
	Reverse	TAGCAAACCTCCATTCCCCAT
ARF6	Forward	CATCTTTCCATGGCCTTAAAGAAG
	Reverse	AATTTTGGAACTGAAGAAGTGAAGC
ARF7	Forward	GGAATGCCAGATGATGAGACT
	Reverse	TCTGAAAGCTCAGTAACTTGGA
ARF8	Forward	CATCTTTGCCTGATGGAAGGG
	Reverse	TATGGGAAGCTGATTGTTGAAGAT
ARF9	Forward	ATCTGCACTTGATGTAGGCAT
	Reverse	CTCGACTGGGGAAACCATTTG
ARF10	Forward	CGTCTCCTTCAGGTAGCTTG

	Reverse	GACAGATAACACATGGACTCG
ARF11	Forward	GACCAATCTCAGAAATCACAGG
	Reverse	CCACACTTATTAGCTGCTTGTC
ARF18	Forward	GAGGTCATTGCAGGTACAATG
	Reverse	TGGATCTTGAAACAGTTTAAGGG

Table 2.5. Primers used for genotyping

T-DNA allele		Primer sequence
tar2-1/42670-F1	Forward	GCACGCAAGTGAAGCTCCAAGC
tar2-1/42670-R1	Reverse	ATACTGTGGCCAATAGTAAGCC
taa1-1	Forward	CATACTCATTGCTGATCCATGTAGATTTCC
taa1-1	Reverse	GCTTTTAATGAGCTTCATGTTGG
taa1-1	Forward	CATCAGAGAGACGGTGGTGAAC
SALK_LBb3	Reverse	ATTTTGCCGATTTCGGAACCACCATCAAA

Table 2.6. Oligos used for EMSA

Primer name		Primer Sequence
pTAR2 BS1	Forward	TGGATCATTTATCTATTTTAATGTTACCCTTGCAGAGATT
	Reverse	AATCTCTGCAAGGGTAACATTAAAATAGATAAATGATCCA
pTAR2 BS2	Forward	CTCGCAAACCCTAGATATTAATTGTGAGAATCGAACGAAGA
	Reverse	TCTTCGTTCGATTCTCACAATTAATATCTAGGGTTTGCGAG
pTAR2 BS1M	Forward	TGGATCATTTATCTATTTTGGTGTTACCCTTGCAGAGATT
	Reverse	AATCTCTGCAAGGGTAACACCAAAATAGATAAATGATCCA
pTAR2 BS2 M	Forward	CTCGCAAACCCTAGATATTGGTTGTGAGAATCGAACGAAGA
	Reverse	TCTTCGTTCGATTCTCACAACCAATATCTAGGGTTTGCGAG

Table 2.7. Primers used for site directed mutagenesis

Gene name		Primer Sequence
pTAR2 /BS1M	Forward	CATGGATCATTTATCTATTACCCTTGCAGAGATT
	Reverse	AATCTCTGCAAGGGTAATAGATAAATGATCCATG
pTAR2/ BS2M	Forward	GTCCTCGCAAACCCTAGATGAGAATCGAACGAAG
	Reverse	CTTCGTTCGATTCTCATCTAGGGTTTGCGAGGAC

2.2.2. Plasmid DNA extraction

Plasmid DNA isolation was performed using accuprep Accuprep plasmid mini extraction kit (Bioneer Corp). All the steps were followed according to manufacturer's protocol. A single colony was inoculated in 5ml LB liquid media with 1µg/ml respective antibiotic and grown at 37°C with shaking for overnight (12-16 h). For all high copy number plasmids, 5ml culture was set up whereas for low copy number plasmids like *WUS-pET28* 15-20ml culture was set up for overnight growth to isolate the plasmid DNA. Overnight grown bacterial culture was pelleted by centrifugation in 2ml eppendorf. Cells were resuspended in 250µl P1 buffer (containing RNaseI) and vortexed vigorously. In the second step, 250µl P2 buffer was added, and after thorough mixing, the sample was left for cell lysis for 5 min at RT. In the end, 350µl neutralization buffer was added to stop the lysis reaction. The contents of the tube were mixed thoroughly by inverting the tube 3-4 times. The contents were spun at 14000rpm for 10 mins. The upper layer lysate was applied to a fresh silica column inserted into a collection tube. Contents of the column were centrifuged at 14000 rpm for 1 min and then washed with washing buffer containing 70% ethanol. After spin-drying the column twice, it was placed into a new eppendorf tube, and finally, plasmid was eluted in two steps by applying 25µl ddH_2O or elution buffer. Plasmid concentration was checked using Bio-spectrophotometer (Eppendrof, Germany).

2.2.3. Total RNA Isolation

RNA isolation was performed using ReliaPrep™ RNA Miniprep Systems (Promega). All the steps for purification were followed according to manufacturer's protocol. Shoot apices from 4-weeks old plants were dissected, and ~30-35 mg tissue was collected in an RNase free microcentrifuge tube. The dissected tissue sample was snap-frozen in liquid N_2. Further, it was grounded down in liquid N_2 using an autoclaved pestle. 600µl TGA buffer containing

thioglycerol was added to the grounded sample and mixed thoroughly in the microcentrifuge tube. Microcentrifuge tubes were spun at 14000 rpm for 1 min at 4ºC to pellet down the solid tissue, the upper layer of the tube was transferred to a fresh tube and RNA was precipitated by adding 700µl isopropanol and mixed gently by inverting microcentrifuge 4-5 times. The clear lysate was applied to a silica column, and a quick wash was performed by applying 500µl washing buffer. After washing, on column DNase-I treatment was performed for 15 mins to remove all the genomic DNA contamination. Two quick washes were carried out to flush out the DNaseI. Next, RNA was eluted in 30µl RNase free water. Prior to cDNA synthesis reaction, RNA concentration was checked using a spectrophotometer.

2.2.4. Genomic DNA extraction

For plant genomic DNA isolation, a modified CTAB buffer method was used (Murray and Thompson 1980). CTAB buffer (5M NaCl, 0.5M EDTA, 1M Tris-HCl, 2% CTAB w/v) was prepared, First, preferably 1-2 young leaves were plucked in 1.5ml eppendorf and frozen into liquid nitrogen. Frozen tissue was grounded down in liquid nitrogen, and 600ml of CTAB buffer containing 1ml/µl β-Mercaptoethanol was added. The contents of the tube were incubated at 65°C for 30 mins in thermomixer (Eppendorf, Germany). A cocktail of Phenol Chloroform: Isoamyl alcohol (24:5:1) in an equal amount was added to the incubated tissue sample. The contents of the tube were mixed thoroughly and centrifuged at 14000 rpm for 10 mins. The upper aqueous layer was transferred into a fresh tube and 600ml of Chloroform: Isoamyl alcohol (24:1) was added and repeated the above-mentioned step once again. For the genomic DNA precipitation, chilled isopropanol was added to the supernatant, and it was mixed thoroughly by gently inverting the tube 4-5 times. Precipitated DNA was pelleted down at 14000 rpm for 10 mins. The supernatant was discarded without disturbing the pellet, followed by a wash with chilled 70% ethanol for 10 mins at 14000 rpm. Pellet was dried at

99°C for 1 min and resuspended in 40µl of sterile ddH_2O or TE (10mM Tris pH.8, 1mM EDTA). It was stored at -20oC for further experiments.

2.2.5. Purification of DNA fragment from agarose gel

For PCR product and gel purification, Accuprep mini gel extraction kit was used (Bioneer Corp.), and the manufacturer's protocol was followed. First PCR product was checked by running the reaction mixture on 0.8% agarose gel. In the remaining PCR product, 200ml of PCR binding buffer was added and mixed thoroughly. Later the mixture was applied to silica spin columns and spun at 14000 rpm for 1 min. Washing buffer was applied to the spin column and dried by centrifugation. For DNA gel purification, after running the agarose gel, DNA fragments were excised neatly with a scalpel keeping in mind the product size. The gel slices were weighed, and 3x volume of gel binding buffer was added to the excised slices. The mixture was incubated at 55°C for 10-15min. Once the gel is dissolved completely, the contents were passed through the spin column. 700ml wash buffer was added to the column for washing. After two washes, the DNA was eluted in 25ml of sterile ddH2O and stored at -20°C.

2.2.6. Molecular Clonings

2.2.6.1. Preparation of competent cells

Chemical ultra-competent (*DH5α, DB3.1*) cells were used for all cloning experiments in this study. *Rosetta™(DE3)* strain was used for protein expression. However, electrocompetent cells were used for Agrobacterium strain.

For the preparation of ultracompetent cells, the following buffers were prepared in sterile conditions.

Transformation Buffer 1

Component	Final Conc.	Amount
1M MOPS (pH 6.5)	10mM	1ml
1M KCl	100mM	10ml
1M MnCl2	45mM	1ml
1M CaCl2	10mM	1ml
1M KAc	10mM	4.5ml
Sterile ddH_2O		To the final volume 100ml

Transformation Buffer 2

Component	Final Conc.	Amount
1M MOPS(pH.6.5)	10mM	1ml
1M KCl	100mM	10ml
1M MnCl2	45mM	4.5ml
1M CaCl2	10mM	1ml
1M KAc	10mM	1ml
Glycerol	80%	
Sterile ddH_2O		To the final volume 100ml

Firstly, a single colony was picked up from the streaked plate, and inoculated in 5ml LB broth overnight at 37^{o}C. 1% of primary culture was added to 100ml of SOB medium and kept at 37°C until the OD reached 0.5. Cells were kept on ice for 15 mins and later pelleted down at 3500 rpm for 10 mins at 4^{o}C. After centrifugation, cells were resuspended in 25ml of chilled transformation buffer 1 and kept on ice for 10mins. The mixture was centrifuged at 3500 rpm for 10 mins at 4^{o}C, and the supernatant was discarded. Cells were resuspended in 3 ml chilled transformation buffer 2 and 280µl of DMSO was added and mixed. Cells were kept on ice for 15mins. Again 280 µl of DMSO was added to the cells. Aliquots were made and stored at -80^{o}C for further use.

For the preparation of Agrobacterium electrocompetent cells. 1% Primary inoculum of overnight grown Agrobacterium was added to of 500ml in a flask containing LB media plus gentamycin (50µg/ml), rifampicin (50µg/ml) and tetracycline (12.5µg/ml). The culture was grown at 28°C for 20 h, and cells were harvested by centrifugation at 4000rpm at 4°C for 15 mins. The pellet was resuspended in 500 ml chilled 10% glycerol, and the centrifugation step was performed as described above. In the next round, the volume of chilled 10% glycerol for cell suspension was reduced to 250 ml followed with 10 ml keeping the rest of the steps same. In the end, cells were resuspended again in 2-3 ml of 10% glycerol and cells were aliquoted into 100µl aliquots and stored at -80°C.

2.2.6.2. Bacterial transformation

2.2.6.2.1. Transformation in Agrobacterium using electroporation

The electroporation was done using a Bio-Rad Gene Pulser Xcell (Bio-Rad, USA). 0.2 µl of the plasmid was added to 50µl of Agrobacterium electrocompetent cells. The cells were mixed with plasmid DNA and placed in between the two electrodes (1mm cuvette). Electric pulse was applied @ 1.8kV, capacitance of 25µF and 200Ω resistance. The cells were rescued immediately after the pulse by adding 700µl LB media in the cuvette. The content of the cuvette was transferred into a 1.5ml eppendorf tube and kept for shaking at 30°C for 1 h in the incubator. ~ 50µl of the culture was plated on the LB plates containing rifampicin, gentamycin and selection marker. Plates were kept at 30°C for 36-48 h and screened for positive colonies using colony PCR.

2.2.2.6.2. Transformation of DH5α and Rosetta using chemical transformation

For chemical transformation, *DB3.1* (for cloning), *DH5α* (for cloning), and Rosetta strain of *E.coli* (for protein expression) were used in the present study. Ligation mix (3-8 µl) / 0.5 to 1 µl in case of supercoiled plasmid DNA were added to competent cells (70µl) and gently mixed

by tapping the tube. Competent cells, along with DNA, were kept on ice for 30 min. Heat shock was given at 42ºC in the water bath for 1 min 30 secs, cells were rescued immediately first by putting on ice for 5 mins, and later 700µl of LB media was applied. The mixture was incubated at 37ºC for one hour in an incubator with shaking. In the end, cells were spread onto LB plate containing the appropriate antibiotic selection marker and incubated at 37ºC for overnight.

2.2.6.3. PCR

All Primes used for cloning listed in Table 2.2. Three different types of PCR was setup.

(a) Phusion PCR

(b) Colony PCR or plasmid PCR

(c) PCR for T-DNA genotyping

All PCR reactions were either set up in standard PCR strips or single tubes. Suitable buffers were used depending upon the DNA polymerase, e.g. Phusion requires HF buffer, which is supplied by manufacturer. T-DNA PCR and colony PCR were setup using home-made Taq-polymerase and reaction buffer. For Phusion polymerase, the initial denaturation step was performed at 98ºC for 5 min, followed at 98ºC for 30 sec for successive steps. Annealing was done at 55ºC for 30 sec, followed by extension at 72ºC at the rate of 1kb/30 sec. Usually, 29-30 cycles were performed for PCR based cloning experiments whereas for colony PCR and genotyping the number of cycles varied from 30-35. For colony PCR, initial denaturation was performed at 95ºC for 3 minutes, followed with denaturation step at 95ºC and annealing at 55ºC for 30 sec each. Extension was carried out at 72ºC @ 1kb/min and final extension step was carried for 10 minutes. For genotyping annealing step was performed at 65ºC for 30 secs.

2.2.6.4.Restriction digestion

All restriction enzymes were brought from New England Biolabs (NEB, USA) and used according to manufacturer's instructions. For restriction digestion, Following components were added in a nuclease-free microcentrifuge tube.

Components	Amount
DNA	3-4µg
Restriction enzyme buffer	5µl
Restriction enzyme 1	2µl
Restriction enzyme 2	2µl
Nuclease free water	To the final volume to 50µl

Insert and vector backbone were digested with respective enzymes for 2-3 h at 37°C, followed by addition of alkaline phosphatase in digested vector for 1 h. Vector and insert both were run on the 0.8% agarose gel. Bands were excised from the gel and purified

2.2.6.5. Ligation reaction

For all DNA ligation reactions, T4 DNA ligase enzyme was used. The concentration of purified products of insert and vector were checked using a spectrophotometer (Eppendorf Germany). For each ligation reaction, insert to vector ratio was determined based on the insert and vector size (in kb). The reaction was set up in a 0.2 ml PCR tube.

Components	Amount
Vector	70-100ng
Insert	250-300ng
10x Ligation Buffer	1µl
T4 DNA ligase	0.5µl
Nuclease free water	To the final volume to 10µl

The reaction was kept at 25°C for 1 h in a thermomixer (Eppendrof Germany), subsequently transformed into ultracompetent $DH5\alpha$ cells.

2.2.6.6. Gateway cloning

All the reagents for Gateway cloning were purchased from Invitrogen (USA)/Thermofisher (USA). All the steps of gateway cloning were performed according to Molecular Cloning Manual (Sambrook and Maniatis, 1989).

2.2.6.6.1. TOPO Cloning Reaction

Promoter and cDNA fragments were rescued by cloning them into *pENTRY* vector. For this, blunt-end PCR product having 5'CACC overhang was used to setup ligation. An entry reaction was set up using this protocol.

Component	Amount
PCR product insert	30-40 ng
pENTER/D/TOPO vector	0.5µl
1x salt solution	0.5µl
Nuclease free water	To the final volume 3µl

The reaction was kept at 25ºC for 1 h. The reaction mixture was immediately transformed into DH5α ultracompetent cells and was plated on LB and kanamycin plates. Plates were kept at 37°C for overnight. Transformants were screened using an internal forward primer which binds to the gene of interest and M13R reverse primer specific to the *pENTER/D/TOPO* vector. Positive clones were inoculated in LB medium for plasmid isolation. Furthermore, clones were verified by restriction digestion and sequencing.

2.2.6.6.2. LR recombination reaction

To perform LR recombination, *pENTRY* vector with the gene of interest was linearized using a restriction endonuclease in a 50µl reaction and gel purified. The following components were added into a 0.2ml PCR tube to set up the LR reaction.

Components	Amount
Linearized Entry vector	70-80 ng
Destination vector	70-80 ng
TE pH8.0	0.5 µl
LR clonase	0.5 µl
Sterile ddH_2O	To the final volume 3µl

The reaction was kept at 25°C for 1 h and subsequently transformed in *DH5α* ultracompetent cells. After transformation, 100µl of bacterial culture was spread on LB agar kanamycin plates and incubated at 37°C for overnight. Recombinants were screened by colony PCR, confirmed by digestion and sequencing.

2.2.7. Plasmids

Following plasmids were created in the present study.

For *pTAR2::H2B-YFP* transcriptional reporter construct, a 3 kb promoter fragment was amplified from the WT-L*er* genomic DNA including the upstream 5' transcriptional start site of *TAR2* gene (primer sequences are given in Table 2.2). This promoter fragment was cloned into *pENTR/D/TOPO* vector, and clones were confirmed by restriction digestion followed by sequencing. *pENTRD/TOPO* clone carrying *TAR2* promoter was used as an entry vector while *pGreen 0229* having *H2B-YFP* reporter gene was used as a destination vector for the LR reaction. The subcloning of *TAR2* promoter was confirmed in destination vector by PCR and sequencing. Subsequently, the construct was transformed into 4-weeks old WT-L*er* Arabidopsis plants. Transgenic lines were selected on BASTA, and 18 independent lines were checked for the reporter activity using a confocal microscope.

35S::TAR2 construct was assembled in the pMDC32 vector. For this, the *TAR2* coding sequence was amplified and cloned into pENTER/D/TOPO (primer sequences are given in Table 2.2). An LR reaction was set up between the *pMDC32* destination vector and entry clone

carrying the *TAR2* coding sequence. Resulting clones were confirmed by sequencing and transformed in WT-L*er*. Transformants were selected on hygromycin (50µg/ml). For ectopic expression of *TAR2* in CZ and niche cells. pENTER/D/TOPO vector carrying *TAR2* CDS was used as an entry vector to set up an LR reaction with *6XpOp* gateway compatible vector as reported in(Yadav et al. 2010). Clones were sequenced and subsequently transformed into *pCLV3::LhG4* and *pWUS::LhG4* driver lines, respectively. Transgenics were selected on gentamycin (20µg/ml) and were transferred on the soil. Plants showed termination of the shoot apex in the vegetative phase and stayed green on soil for 2-3 weeks were transferred on to the soil.

For WUS protein expression, I cloned *WUS CDS* in *pET28a* vector containing 6xHis tag at N-terminus. The *WUS CDS* was PCR amplified and cloned into *Nde*I and *Xho*I restriction sites in *pET28a* vector (primer sequences are given in Table 2.2).

For Cloning of *WUS*, *CLV3*, *TAA1*, *TAR2*, *CUC1*, *ARF3*, *ARF4*, and *ARF5* clones for *in situ* hybridization firstly from WT-L*er,* total RNA was isolated and used for cDNA library preparation. Coding regions of *WUS, CLV3, TAA1, TAR2, CUC1, ARF3, ARF4* and *ARF5* were amplified directly from cDNA library, and cloned into *pENTER/D/TOPO* vector (primer sequences are given in Table 2.3). cDNA clones were sequenced and were used subsequently to amplify the template for setting up *in-vitro* transcription reaction. For antisense and sense probe synthesis primers were designed in such a way that at least one of the forward primer contains T7 RNA polymerase binding site. The PCR product was gel purified and used for setting up the *in-vitro* transcription reaction.

To understand the functional relevance of WUS binding sequence in the *TAR2* promoter, *pTAR2::TAR2* and *pTAR2*(ΔWUS)*::TAR2* cassettes were assembled in *pGreen 0229 vector*. In the *pTAR2::H2B-YFP pGreen 0229* vector, *H2B-YFP* reporter gene was replaced with *TAR2* coding sequence using *Spe*I and *Sac*I restriction sites (primer sequences are given in Table 2.2).

This vector *pTAR2::TAR2 pGreen 0229* was used further to clone *pTAR2*(ΔWUS) by replacing *pTAR2*. Both the constructs were transformed in WT-L*er*. In T1, 21 independent lines were selected on BASTA both the constructs. Three to four independent homozygous lines were followed till F3 generation and were used for confocal imaging to measure the SAM size. To rescue the double mutant phenotype, I made another construct. Since the *pGreen 0229 pTAR2::TAR2* vector backbone has BASTA resistance in planta, and *taa1-1* T-DNA allele also has the same resistance. To overcome this challenge, I assembled *pTAR2::TAR2* and *pTAR2*(ΔWUS)*::TAR2* cassettes in *pMDC32* vector (primer sequences are given in Table 2.2). First, I replaced 35S promoter with *pTAR2* and *pTAR2*(ΔWUS), respectively, in *Sbf*I and *Asc*I restriction sites in pMDC32. *Sbf*I and *Asc*I sites were introduced in *pTAR2 and pTAR2*(ΔWUS) by PCR (primer sequences are given in Table 2.2). Second, *pENTRY* clone having *TAR2* CDS was used to set up an LR reaction with *pTAR2 pMDC32* and *pTAR2(ΔWUS) pMDC32* constructs, respectively. This resulted in *pTAR2::TAR2 pMDC32* and *pTAR2(ΔWUS)::TAR2 pMDC32* constructs. Both the constructs were transformed in *taa1-1 +/- tar2-1-/-* and *pCLV3::mGFP-ER* reporter by floral dip method. Seeds were collected, and transgenics were selected on hygromycin (50µg/ml). To recuse the double mutant phenotype more than 100 plants were selected on hygromycin and genotyped for *taa1-1* and *tar2-1* T-DNA alleles in the T1 generation. Total 6 T1 lines having *taa1-1 tar2-1* double homozygous T-DNA alleles showed complete rescue in the T1 generation and set seeds. In next generation seeds from two different plants were further grown in soil parallelly with Col-0 and *taa1 tar2* double mutant plants to capture the images and SAM imaging.

To generate *pWUS::mCHERRY* transcriptional fusion, *pWUS::SUB-myc pCAMBIA2300* backbone having 5.6 kb 5' and 1.2 kb 3'WUS regulatory elements was digested with *Asc*I and *Stu*I, SUB-myc was replaced with *mCHERRY-NLS*. Seven T1 lines were isolated after putting

them on kanamycin plates and, two independent lines were followed up further for the experiments.

2.2.8. Site-directed mutagenesis

For Site-directed PCR mutagenesis, the PCR reaction was set up using the following protocol.

Components	Amount
5xGC rich buffer	10µl
10µm dNTPs	3µl
Forward primer	2µl
Reverse primer	2µl
Phusion High fidelity DNA polymerase	2µl
Nuclease free water	To the final volume to 25µl

2µl PCR product was checked on 0.8% agarose gel to see the amplification. PCR product was treated with 1µl *Dpn*I restriction enzyme to cut the circular template plasmid DNA into linear to prevent transformation. *Dpn*I digested PCR product was transformed into *DH5α,* and colonies were screened with gradient PCR, and plasmid was prepared for sequencing. Mutated positive clones were confirmed by sequencing and subsequently transformed in Arabidopsis WT-L*er* plants using Agrobacterium-mediated floral dip method.

2.2.9. cDNA synthesis and qRT PCRs

iScript cDNA synthesis kit (Bio-Rad USA) was used for cDNA synthesis. 3µg of total RNA was used as starting material. The following components were added in an RNase free PCR tube to set up cDNA synthesis reaction.

Components	Amount
RNA	3µg
5XiScript reaction mix	4µl
iScript reverse transcriptase	1µl
RNase free water	final volume to 20µl

The reaction mix was incubated in a thermocycler. Priming was done at 25°C for 5 mins, followed by a reverse transcription at 46°C for 20 mins and finally, Reverse transcriptase was inactivated at 95°C for 1 min. Aliquots of cDNA were made and stored in -20°C for further experiments.

qRT-PCR experiments were performed using a BioRad CFX6 machine (BioRad, USA). Reactions were set up in 96 well plates (Bio-Rad USA). All the steps were performed according to manufacturer's instructions using the following protocol.

Components	Amount
cDNA 1:5 times diluted	1µl
Forward primer	0.5µl
Reverse primer	0.5µl
iTaq Universal SYBR Green Supermix	5µl
Nuclease Free water	3µl
Total volume	10µl

The reactions were kept on the BioRad CFX6 machine, and a three-step amplification protocol was followed up for all qRT-PCR assays. The initial denaturation step was performed at 95°C for 5 mins, followed at 95°C for 30 secs, annealing was done at 60°C for 30 secs. These two steps were repeated for 40 cycles. Next, the denaturation was repeated at 95°C for 15secs, followed by a ramp cycle at 60-95 °C for 20 mins. The final step was carried out at 95 °C for 15secs. *UBQ10* gene was used as an internal control for all the experiments. Gene expression

analysis was done for three to four biological replicates and three technical replicates. Primer efficiency was calculated using standard curves for each primer pair, and values are represented in graphs by the efficiency corrected quantification model as described by (Sparks et al. 2016). (Primer sequences information is described in Table 2.4)

2.3.Protein biochemistry techniques

2.3.1. WUS protein induction

For WUS protein expression, *WUS* coding sequence was cloned into *Nde*I and *Xho*I restriction endonucleases sites to make N-terminal translational fusion with 6×His tag in *pET28a* vector. The plasmid was transformed in Rosetta strain of *E.coli.* For protein induction, one single colony inoculated from the plate in 5ml LB having Kanamycin (50µg/ml) and chloramphenicol (34µg/ml). The secondary culture was inoculated with 1% of overnight grown primary culture. Protein was induced with 1mM IPTG when the OD reached to 0.5-0.6 and kept at 30°C for 6 h. The bacterial cells were harvested by centrifugation at 4000rpm for 10 mins. The pellet was resuspended in 1x PBS. Sonication was performed to lyse the cells, and the contents of the tube were centrifuged for 30 mins at 14000 rpm at 4ºC. SDS-PAGE gel was prepared according to Molecular Cloning Manual (Sambrook and Maniatis, 1989). Protein induction was checked on a 12% separating gel. The samples were prepared by adding 5µl of 4x protein loading buffer (250 Tris-HCl, 2%(w/v) SDS, 20%(v/v) β-mercaptoethanol, 40%(v/v)glycerol,) in 20µl of protein sample. The samples were heated at 99°C for 10 mins, cooled and loaded onto the 5% stacking gel. The gel was run at 90V initially, and then at 120 V for 1h in 1x SDS gel running buffer (25mM Tris-HCl, 192mM glycine and 1% (w/v) SDS). The gel was stained in freshly prepared staining solution (50% methanol, 10% glacial acetic acid, and 1% w/v Coomassie brilliant blue) for 10 mins at RT with shaking and immediately destained with the

destaining solution (50% methanol, 10% glacial acetic acid) until the bands were clearly visible.

2.3.2. Western blotting

The protein was run on SDS-PAGE gel and transferred to a nitrocellulose membrane. All the steps were followed up according to Molecular Cloning Manual (Sambrook and Maniatis, 1989). The transfer was performed in chilled 1x transfer buffer (25mM Tris, 192mM Glycine, 20% (v/v) methanol). The protein was blocked on to the membrane with 0.5% skimmed milk for 1 h at RT with shaking. Later on, the membrane was washed four times with 1x TBST (50mM Tris-Cl, pH.7.5, 150mM NaCl, 0.1% Tween20) and subsequently incubated with 1:5000 times diluted anti-His antibody for 3 h at 4°C with gentle shaking. The membrane was washed four times again with 1x TBST and incubated with anti-rabbit secondary antibody, followed by four washes with 1x TBST. Finally, the blot was developed using X-Ray imager.

2.3.3. Electrophoretic mobility shift assay (EMSA)

The supernatant having 6×His-WUS protein was used to perform gel shift assay. EtBr based EMSA assays were performed to check the DNA-protein interactions. First, forward and reverse primer having binding sites were hybridized to make the double-stranded probe (sequences listed in Table.2.7). DNA-protein interaction was performed in a reaction tube containing 5x binding buffer (20mM HEPES pH7.8, 100mM KCl, 1mM EDTA, 0.1% BSA, 10% v/v glycerol, 10 ng Herring sperm DNA) and hybridized double-stranded DNA probe. The reaction was set up in a 1.5ml eppendorf using the following components. (Oligonucleotide sequences is described in Table 2.6).

Components	Amount
5x Binding buffer	3µl
Protein	200ng
DNA	1.5µl
Nuclease free water	To the final volume 15µl

The reaction was incubated for 30 mins at RT. Samples were immediately kept on ice and loaded on 8% native polyacrylamide gel. The gel was run in a vertical electrophoresis unit (Bio-Rad Mini PROTEAN Tetracell) in 1x TBE buffer (0.089M Tris Base, 0.089M Boric Acid, and 0.002M EDTA) at 100V for 90 mins. The gel was stained in 1% EtBr solution for 10 mins, and images were captured using molecular imager Gel Doc XR+ imaging system (Biorad, USA).

2.4. Confocal Laser Scanning Microscopy of SAM

For the present study, confocal imaging was done for three different tissues of respective transgenic lines.

2.4.1. Confocal imaging of SAMs

For confocal imaging of shoot apex plants were first grown under controlled light conditions having 16 h light / 8 h dark cycle for 4-5 weeks. Once the bolting was induced, shoot apices of plants were plucked and placed in a box containing 1.5% solidified agar. First shoot apices were carefully dissected under the stereomicroscope. Older flower buds were clipped with fine forceps. Before capturing the images, shoot apices were stained with Propidium Iodide (PI) (1mg/ml). The SAMs were scanned, and images were captured using a 63× long-distance water dipping lens in an upright confocal microscope (Leica SP8, Germany). For reporter lines, emission and excitation spectra were collected according to tagged fluorescence reporter. YFP, Venus, yPet were excited at 515 nm wavelength with argon laser lines at 9-10% laser power, and the emission spectra were collected between 525–545 nm by adjusting the variable

bandpass filter. GFP was excited at 488 nm, and emission spectra were collected at 500–540 nm. PI was used for staining the cell outline, and it was excited using 561 nm laser line, and emission spectra were filtered with 600-650 nm adjustable bandpass filter. 3D stacks were created using a processing tool of Leica software (Leica X).

2.4.2. Confocal imaging of embryos

For embryo imaging, the homozygous lines positive for fluorescence in inflorescence meristem imaging were used. Siliques with immature seeds of approximately 6-7 weeks old plants were used for embryo imaging. Dissection of Siliques was performed on a glass slide in distilled water. The ovules were stripped from the ovary wall and placed into FM4-64FX (Invitrogen) solution on a microscope slide. Embryos were popped out with the help of insulin syringes under a stereomicroscope. Isolated embryos on a microscope slide were covered with a coverslip and sealed with nail polish. Imaging was done immediately under a 63x oil immersion lens in Leica SP8 upright confocal microscope according to the settings mentioned above.

2.4.3. Confocal imaging of seedling shoot apex

For seedling shoot apex imaging, seeds were surface sterilized and put on MS media, kept in the darkness at 4^{o}C for 2-3 days. Plates were kept in the chamber for 3 days at 22^{o}C. Germinated seedlings at their earliest stages (mostly with unopened / semi-opened cotyledons) were selected for the experiments and directly transferred in the 1.5% solidified agar in magenta boxes. Seedlings were pushed into the pre-created holes into agar leaving their top outside. Shoot apical meristem was dissected and exposed by gently removing one cotyledon with the help of fine tweezers (5TI, Dumont, Switzerland) and oriented vertically to visualize under the upright confocal nose piece. Propidium iodide (10µg/ml, Invitrogen) drops

were used to stain the cell outline. Autoclaved distilled water was poured over the seedlings to submerge. Images were captured under the Leica SP8 confocal microscope equipped with a long-distance water dipping lens (63X objective). Rest of the confocal microscope settings were followed as described above

2.5. SAM size measurement

For SAM size measurements, confocal image stacks were captured with 0.35µm step size from 4-weeks old plants of respective genotypes and analyzed using Morphograph X as described earlier (Reuille et al. 2015). SAM surface was extracted using marching cubes, and single seed was used to mark the meristem area, excluding emerging primordia and propagated using watershed segmentation algorithm.

2.6. In-situ hybridization assay

A modified non-radioactive based protocol was used to perform all *in-situ* hybridization assays. All the steps were followed according to the protocol posted on the website (http://www.its.caltech.edu/~plantlab/protocols/insitu.pdf,) with some modifications.

2.6.1. Fixation and embedding of tissues

To perform the in-situ hybridization assays, shoot apices of the 28-30 days old plants were fixed in 4% (w/v) paraformaldehyde. Before preparing fixative, 10x PBS pH.7.0 was made in sterile ddH_2O. The solution was autoclaved and kept for further use.

For fixative preparation, 1x PBS was diluted from 10x PBS in DEPC treated ddH_2O. To adjust the pH of 1x PBS to 10-11, 2-3 NaOH pellets were added in 1x PBS and heated at 50-60°C for 2-3 mins. Then, 4% paraformaldehyde was dissolved in 1x PBS in a fume hood using a magnetic stirrer. Once PFA was completely dissolved, the solution was cool-down on ice and pH was readjusted to 7 by adding H_2SO_4. Tissues were collected in ice-chilled PFA in glass

scintillation vials, and vacuum infiltered until the tissue sank (20-30 mins are sufficient for SAM tissues). Fixative in the tissues was replaced with fresh PFA pH.7.0 and kept at 4°C for overnight with gentle shaking.

Next day, all the steps were carried out at 4°C with gentle shaking. All the steps were followed as below.

1. Tissues were rinsed with freshly diluted 1x PBS in DEPC treated ddH_2O. Each washing step was carried out for 30 mins at 4°C with gentle shaking.
2. Tissues were dehydrated with ethanol series (30%, 40%, 50%, 60%, 70%, 85%). Ethanol was diluted using DEPC treated ddH_2O. Each washing step was carried out for 1 h. In the 70% ethanol tissues can be stored for 2-3 weeks at 4°C. I preferred not to stop at this step for better results.
3. At the final step, tissues were kept at 4°C for overnight with gentle shaking in 95% ethanol. 4-5 drops of eosin dye were added to visualize the shoot apex while making sections.

   Next day, the following steps were performed at the RT.

1. 95% ethanol was discarded, and tissues were washed with 100% ethanol twice. Each step was carried out for 30 mins at RT.
2. Next, tissues were again washed with 100% ethanol twice for 1 h each at RT with gentle shaking at the orbital shaker.
3. A mixture of 75% ethanol and 25 % Histoclear was prepared in a fresh RNase free falcon and tissues were washed with it for 30mins.
4. Tissues were again washed again with 50% ethanol + 50% histoclear, followed by a wash of 25% ethanol + 75 % histoclear. Both the washings were carried out for 30 mins each.
5. Next, two washes of histoclear were given for 1 h each with gentle shaking.

6. At the final step, tissues were kept in 100% histoclear with ¼ volume of paraplast. Next day, tissues were kept at 42°C until the paraplast chips got completely melted and then transferred to 60°C for 5-6 h. Several wax changes were carried out at 60°C for 3-4 days (twice in a day). Finally, tissues were embedded as molds in molten paraplast and kept at 4°C for further use. Tissue can be stored at this stage for 6-7 months.

2.6.2. Tissue sectioning

Pre-cleaned and lysine coated probe on-plus slides were used. 8µm thick sections were cut using a microtome (Leica) and put in the slightly warm water on the slides. Slides were baked at 42°C for overnight on a heating plate (Leica) and stored in 4°C for further use. All the machines and blades were pre-cleaned with 70% ethanol to avoid RNase contamination.

2.6.3. Composition of stock solutions

All the stock solution were prepared in autoclaved ddH_2O and autoclaved again to avoid any RNase contamination. The following solutions were mad prior to the experiment.

1. 1M Tris-HCl pH.8.0, 1M Tris-HCl pH.7.5 and 1M Tris-HCl pH.9.5**:** To prepare Tris-HCl 60.57 gm Trizma was added to 400 ml of sterile ddH_20, pH was adjusted using HCl. Further, the volume was made up to 500 ml.
2. 0.5 M EDTA: 93.06 gm of EDTA was added to 400 ml of sterile ddH_20, NaOH pellets were added slowly to adjust the pH.8.0. Volume was made up to 500 ml.
3. 0.5M MgCl2: 50.825 gm of MgCl2 was dissolved in 450ml of sterile ddH_2O, and volume was made up to 500 ml.
4. 20X SSC (3M NaCl, 300mM Na citrate): 175.32 gm NaCl and 88.23 gm Sodium citrate were dissolved in 900 ml sterile ddH_2O, and the final volume was made up to 1000 ml.

5. 10X PBS (1.3M NaCl, 70mM Na_2HPO4, 30mM NaH_2PO4)**:** 75.972 gm NaCl, 9.9 gm Na_2HPO4, 3.5 gm NaH_2PO4 were added in 900ml sterile ddH_20, pH.7 was adjusted with 5N NaOH. Then, the volume was made up to 500 ml.
6. 1 M Sodium Phosphate Buffer: Firstly, Two buffers were prepared separately.
    A. 1M NaH_2PO4 (5.99 gm of NaH_2PO4 was dissolved in 40ml of sterile ddH_20, and the volume made up to 50 ml).
    B. 1M Na_2HPO4 (7.098gm of Na_2HPO4 was dissolved in 40ml of sterile ddH_20, and volume was adjusted to 50 ml made up the volume 50ml).

Now, 50 ml Na-phosphate buffer (pH.6.8) was prepared by adding 25.5 ml of 1M NaH_2PO4 and 24.5 Na_2HPO4 and autoclaved.

7. 5M NaCl: 292.2 gm of NaCl was dissolved in 900 ml of sterile ddH_20, and the final volume was adjusted to 1000ml.
8. 50% w/v Dextran sulphate: 5 gm of Dextran sulphate was added to 7 ml of DEPC treated ddH_20 in a fresh RNase free 50 ml falcon, and the solution was kept at 55°C until it completely gets dissolved. Volume was made up to 10 ml. Aliquots were made in RNase free eppendorfs and kept at -20°C.
9. t-RNA (100mg/ml): 50 mg t-RNA was dissolved in 500 ul of DEPC treated ddH_20 and aliquots were made in RNase free eppendorf and stored at -20°C.
10. In-situ salts: The following components were added into a 50ml RNase free falcon. *In-situ* salts were stored at room temperature.

Components	**Final conc.**	**Amount**
5M NaCl	3M	30ml
1 M Tris pH.8	100mM	5ml
Na-Phosphate buffer pH.6.8	100mM	10ml
0.5M EDTA	50mM	5ml
Total volume		50ml

11. 4M Ammonium Acetate (NH4Ac): 4.62gm NH4Ac (Sigma-Aldrich Catalogue No. A1542) was added to 10ml of DEPC treated water and made up the volume 15ml). Freshly prepared 4M NH4Ac gave good results for probe synthesis.
12. 3M Sodium acetate (NaAc) (pH.5.2): 24.609 gm of NaAc (Sigma-Aldrich Catalogue No. S5636) was dissolved in 80ml of autoclaved dd$H_2$0. pH was adjusted to 5.2, and volume was made up to 100ml.
13. Triethanolamine: 18.565 gm of Triethanolamine (was dissolved in 900ml of DEPC treated ddH_2O. pH was adjusted to 8 using 5N NaOH. pH strips were used to check the pH at this step.

2.6.4. *In-vitro* transcription

For RNA probes synthesis, A set of primer pair; one for antisense and another for sense (primer sequences are given in Table.2.4) were synthesized (Sigma Aldrich). First, a PCR reaction was set up to prepare the template using the following reaction components.

Components	**Amount**
Template plasmid	20-30ng
10XPCR Buffer	75µl
dNTPS	6µl
Forward primer	3µl
Reverse primer	3µl
$Mgcl_2$	2.55µl
Nuclease free ddH_2O	To the final volume 75µl

The amplified PCR product was run on the agarose gel to check the presence of the desired product. Size of the PCR product will always be slightly more than the actual size of the genes of interest. PCR product was purified using a gel extraction kit (Bioneer, South Korea) and at

the last step DNA was eluted in DEPC treated ddH_2O and stored in -20°C. Later on, this PCR product was used for setting up *in-vitro* transcription reaction.

The following components are mixed in an RNase free eppendorf to set up *in-vitro* transcription reaction.

Components	**Amount**
PCR product	1- 1.5µg
DIG-UTP	1.25µl
T7 RNA polymerase buffer	1.25µl
Protector RNase inhibitor	0.5µl
T7-RNA polymerase	0.5µl
DEPC treated ddH_2O	To make up volume
Total reaction volume	12.5µl

The reaction was kept at 37°C. 2% agarose gel was prepared in RNase free 1x TAE buffer. Gel running unit, combs, trays, etc., were treated with 0.2 N NaOH a night before RNA probe synthesis and cleaned with double distilled water three to four times to wash off NaOH solution. After 1 h, 1 µl of RNA probe was run on the 2% agarose gel at 100V. The gel was checked after 15 mins because the RNA gets degraded quickly, the remaining reaction was again kept at 37°C for 1 h.

After 2 h of probe synthesis, 75µl DEPC treated ddH_2O, 1µl 100mg/ml tRNA, 2µl RNase-free *DNase1* were added in the reaction to remove all DNA contamination and kept at 37°C for 10mins. RNA was precipitated using an equal volume of 4M NH4Ac (100µl) and two volumes of Ethanol (200µl) at -20°C for 2 h. After precipitation, the mixture was centrifuged at 14000 rpm for 20mins. The pellet will be visible after this step. The supernatant was discarded carefully without disturbing the pellet. Freshly prepared 70% chilled ethanol was added to the pellet and centrifuged at 14000 rpm for 20 min. Once the centrifugation was done, ethanol was removed completely by pipette, and the remaining amount was air-dried by leaving tubes at

the RT. Dried pellet was dissolved in 100 µl DEPC treated ddH_2O and 100 µl freshly prepared 2xCO_3 buffer and kept at 60°C for calculated time to chop RNA into 150bp long pieces. The second precipitation was done by adding 1/10 volume 3MNaAc (pH.5.2) (20µl) and two volumes of EtOH (440µl) in the sample. The sample was mixed by inverting tube gently 10-12 times. Now, the reaction was kept at -20°C for overnight. Next day, the mixture was pelleted for 20 mins at 4°C, followed by a wash with freshly prepared chilled 70% ethanol and drying at RT. Once the ethanol was evaporated from the sample, the pellet was dissolved in 50µl of 50% formamide and stored at -20°C for further use.

2.6.5. In-situs sections pre-treatment

All the stock solutions were made in sterile ddH_2O and diluted in DEPC treated ddH_2O. The following steps were performed on the first day for in-situs pre-treatment.

1. Slides were rinsed in histoclear twice for 1 min each.
2. Slides were dehydrated in ethanol series as follows 100% two times 1 min each, 95%, 90%, 80%, 60%, 30% for 1 min at each step.
3. Slides were then washed in 2xSSC solution for 15mins.
4. 35 ul Proteinase K was added in 250 ul pre-warmed (37°C) Tris/EDTA pH.8.0 buffer. Slides were dipped into this solution for 30mins.
5. Slides were rinsed then in 1x PBS/glycine solution for 2mins. To prepare 1x PBS/ glycine, 2mg/ml glycine was added to 1x PBS and mixed using a magnetic bead on a magnetic stirrer. Magnetic beads were treated with 0.1N NaOH overnight, washed with ddH_2O and autoclaved before use on the first day.
6. Slides were rinsed in 1xPBS twice for 5mins.
7. Slides were then again rinsed in 4% paraformaldehyde for 10 mins, followed by two washes of 1x PBS 5 mins for each.

8. Slides were then rinsed in triethanolamine/acetic anhydride solution. To prepare triethanolamine/acetic anhydride solution 5ml of acetic anhydride was added to 250ml of freshly prepared triethanolamine pH.8.0 and mixed using a magnetic bead. Slides were dipped immediately in the solution for 10 mins.
9. Slides were rinsed again in 1xPBS two times for 5 mins
10. At the final step, slides were again dehydrated in the ethanol series as follows 30%, 60%, 80%, 90%, 95%, and 100% ethanol for 30 secs at each step. Before hybridization, slides were kept at 4°C for 1-2 h. Meanwhile, hybridization solution was prepared.

2.6.6. Hybridization

After pre-treatment of the slides, hybridization (Hybe) solution was prepared using the following composition for 40 slides processed at one time.

Component	Amount
10x in-situ salts	990µl
Deionized formamide	3960µl
50% Dextran sulphate	1980µl
50% Denhardt's solution	198µl
t- RNA	99µl
DEPC treated ddH_2O	693µl

Before hybridization, 3µl probe and 57µl 50% formamide were added into an RNAse free microcentrifuge, mixed well by a short spin, and heated at 80°C for 2 mins. The probe/formamide mixture was immediately kept on ice. Then, 240 µl of hybe solution was added to probe/formamide mixture and mixed well with a short spin at 4°C. The total 150 µl of this probe/hybe solution was applied to each slide and spread all over it. Two slides having the same probe were sandwiched together and kept above the wet kim wipes in an airtight plastic container. Hybridization was performed at 55°C for overnight.

2.6.7. In-situ post-hybridization

Next day after overnight hybridization, the following steps were performed. All the solution for the second day were prepared in sterile ddH_2O.

1. Slides were separated carefully in 0.2x SSC solution.
2. Slides were washed three times in pre-warmed 0.2xSSC (55°C) solution with gentle shaking at 55°C. Each washing was carried out for 1 h.
3. Meanwhile, the following solutions were prepared in the autoclaved ddH_2O for 40 slides processed at one time.

Solution 1: Blocking solution

Stock	Final conc.	Amount
1M Tris/HCl pH.8.0	100 mM	30 ml
5M NaCl	150 mM	9 ml
Boehringer block	1%	3 gm
Sterile ddH_2O		To the final volume 300ml

Solution 2:

Stock	Final conc.	Amount
1M Tris/HCl pH.7.5	100mM	100ml
5M NaCl	150 mM	30ml
Triton X100	0.03%	3ml
BSA	1%	10gm
Sterile ddH_2O		To the final volume 1000ml

Solution 3:

Stock	Final conc.	Amount
1M Tris/HCl pH.9.5	100mM	50ml
5M NaCl	100mM	10ml
0.5M MgCl2	50mM	5ml
Sterile ddH_2O		To the final volume 500 ml

Solution 4:

Stock	Final conc.	Amount
1M Tris/HCl pH.9.5	100mM	5ml
5M NaCl	100mM	5ml
Sterile ddH_2O		To the final volume 50 ml

4. Slides were then blocked in solution 1 for 45 mins with gentle shaking at RT.
5. Four washes of solution 2 were given, each for 15 mins with gentile shaking at RT
6. After washing, 1:1250 times diluted anti-Digoxigenin-AP Fab fragments antibody was prepared in solution 2 and applied by spreading all over the slides. Slides were sandwiched together and kept above the wet kim wipes for 2 h.
7. Next, Slides were separated and washed again in solution 2 four times for 15mins each with gentle shaking in an orbital shaker at RT.
8. Slides were washed in solution 3 for 10 mins for each step with gentle shaking.
9. Slides were rinsed in solution 3 to wash off remaining triton-X100.
10. 20 µl of NBT-BCIP was added into 1ml of solution 4 and applied onto the slides. Again slides having the same probe were sandwiched together and kept above the wet paper towel in the dark until the signal develops.
11. Depending upon the signal intensity, the reaction was stopped using 1xTE (Tris/EDTA pH.8 buffer) and again pass through the ethanol series 30%, 60%, 80%, 90%, 95%, 100% ethanol twice and histoclear twice.
12. Slides were dried, mounted with 50% glycerol, covered with a coverslip and sealed with nail polish. Kept for drying overnight.
13. Next day, images were captured in DIC mode using 20X objective in Zeiss Axio Imager Z2 microscope.

2.7. Treatment of plants

For treatment experiments, Dexamethasone (10mM) and Cycloheximide (CYC) (10mM) stocks were prepared in 100% ethanol. Plants were treated with 10μm DEX and 0.03% L-77 silwet, and Mock (100% Ethanol) 0.03% L-77 silwet and 10μM DEX+CYC and 10μM CYC alone. After treatment plants were kept in the growth chamber depending upon the timepoint of the experiment. For L-Kynuriene (L-Kyn) and NPA treatments, 100mM stocks of L-kyn and NPA were prepared in 1% DMSO. 100μm of final concentration with 0.03% silwet was used for L-Kyn and NPA treatment for 48 hours.

2.8. Quantification of GFP +ve and GFP -ve cells in the SAM

Total number of *GFP* positive cells, *GFP* -ve cells, were counted in L1 layer after reconstructing 3D top view in Leica SP8 processing tool and using FiJI software. Firstly, 3D stack of confocal image was loaded and opened into FIJI software directly and all the primordia were marked (Supplementary Fig. 11a). P2 onward primordia were excluded from the quantification. One of representative example of *CLV3* positive cells are shown (Supplementary Fig 12). Area of interest was selected in the same image drawn by a white circle (Supplementary Fig.12b). Next, fluorescence positive cells were separated by drawing a yellow circle. The cells which are present in yellow circle were considered fluorescence positive cells and cells which are present between yellow and white boundaries were considered as florescence negative cells (supplementary Fig.12c) and counted by labelling each and individual cell manually in cell counter tool of FIJI software. Same protocol was followed up for quantification of all the images.

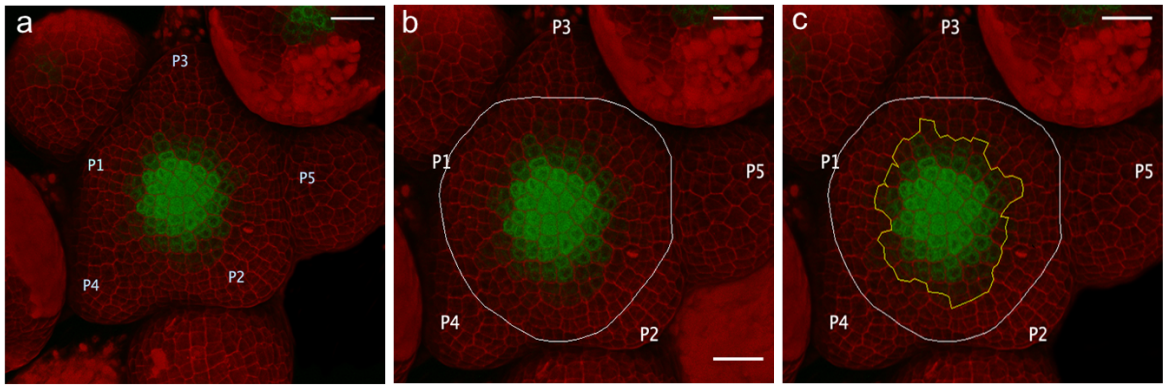

Figure 2.1. Tools used for quantification of stem cells (GFP +ve) and PZ cells (GFP -ve). Representative images showing the method of quantification for counting the GFP +ve and GFP -ve cells. For example; in Col-0 SAM, primordia were labelled **(a)**, SAM was marked with outline, and the area having GFP +ve cells was separated for stem cell counting **(b).** Remaining cells in the marked SAM were considered as GFP-ve cells **(c).** scale bar is 20µm.

2.9. Quantification of Auxin maxima in SAM

To quantify auxin maxima and DR5 positive cells in SAM of different mutants backgrounds and L-Kyn, NPA treatment experiments, following methods were used. 3D Confocal images of shoot apices expressing pDR5 reporter (Fig. 2.2 a) was loaded and opened into FIJI software directly and all the primordia were marked from P1 to P5 (Fig. 2.2 b). At the next step, auxin responses were marked on the individual incipient primordia and primordia P0 and P1 by giving them separate numbers (Fig. 2.2 c). P2 onwards primordia were excluded from the analysis.

For quatification of DR5 positive cells 3D Confocal images were opened in FIJI software, all the primordia were marked from P0 to P5 (Fig. 2.2 d, e). A white circle was drawn covering cells of SAM and P1 primordia (Fig. 2.2 f). DR5 positive cells in the white circle were counted in L1 layer using cell counter tool in FIJI software. P2 onwards primordia were excluded from the analysis.

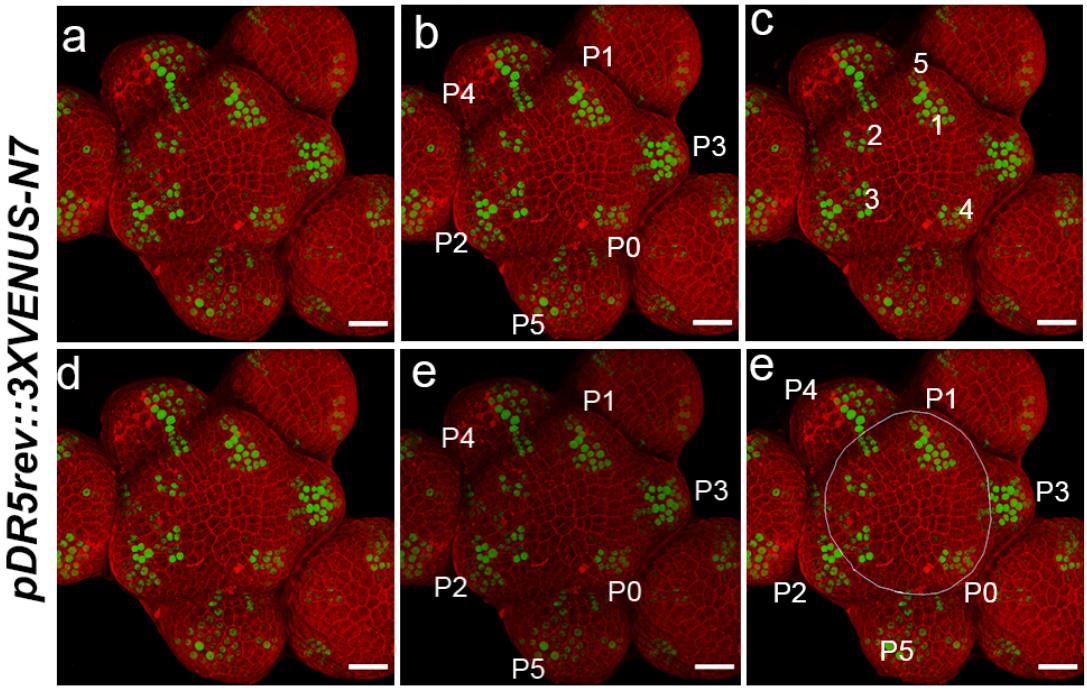

Figure 2. 2 Tools used for quantification of Auxin maxima and DR5 positive cells in the SAM. Representative images showing the method for quatification of auxin maxima and DR5 positive cells in the SAM. For example in one of the representative image **(a)**, Primordias were marked **(b)**, and auxin maxima were labelled with different numbers at the site of incipient primordia and primordia Po and P1 **(c)**. Similarly for quantification of DR5 positive cells representative 3D image showing the DR5 expression in the SAM **(d)**, primordia were marked from P1 to P5 **(e)**. Image showing the area of SAM included for quantification of DR5-postive cells. scale bar is 20µm

2.10. Quantification of data

Plants height, flower number, silique number and axillary meristem number were counted manually at 28 days and 35 days post vernalization. Total number of GFP positive cells, GFP -ve cells, H2B-YFP cells +ve and H2B-YFP cells -ve cells, D2 +ve and D2-ve cells, number of DR5 +ve and DR5-ve cells were counted in L1 layer after reconstructing 3D top view in Leica SP8 processing tool and using FiJI software. P2 onward primordia's were excluded from the quantification.

2.11. Statistical analysis

All bar graphs were generated using GraphPad Prism 6 Software.

In the present study two different statistical tests were applied using GraphPad Prism 6 software. Wherever a comparison was made between two samples unpaired student t-test was applied and statistically significant difference was represented by * sign. When a comparison was made between multiple samples, One way Anova followed by Tukey's multiple comparisons test was used, similar letters represent that the difference between samples are non-significant, however different letters represent the statistically significant difference.

Chapter 3

TAA1 and *TAR2* mediated auxin biosynthesis is essential for organogenesis and shoot development

3.1. Introduction

In plants, lateral organs arise at the flank of the meristem at defined positions. In the postembryonic phase of plant development, primordia formation begins with a coincidence of high auxin accumulation at the initiation site. The positioning of the primordia is dynamic in nature and at the same time, a self-regulating process. This arrangement of the primordia around the periphery of SAM is called as phyllotaxy. This auxin maxima is achieved by a combination of biosynthesis (Youfa Cheng et al. 2007) and transport (Reinhardt et al. 2003b). Auxin is transported acropetally by PIN1, an efflux carrier, in the shoot apex. Past studies have shown that the genes involved in auxin biosynthesis and transport are expressed in the floral and inflorescence meristem (Youfa Cheng et al. 2007; Heisler et al. 2005; Stepanova et al. 2008). Thus, genes involved in auxin biosynthesis and transport build auxin threshold at critical positions in the SAM so that proper phyllotactic patterns can emerge.

Previous molecular and genetic studies in Arabidopsis were largely focused on PIN1 to explain the mechanism behind primordium formation and their positioning. PIN1 is polarized towards the new organ primordium in SAM (Heisler et al. 2005). It was postulated that PIN1 is polarized towards the higher auxin concentration, and reinforces a positive feedback loop between PIN1 and auxin signalling network genes (Benková et al. 2003). A recent study has shown that polarization of PIN1 is regulated by MONOPTEROUS / AUXIN RESPONSE FACTOR5 (MP/ARF5) (Bhatia et al. 2016). *MP* encodes a transcription factor that gets activated in response to auxin signalling. This raises a question, how at the first place MP gets activated in the absence of auxin. Genetic studies looking at the *pin-1* mutant has also shown that the null alleles of *pin-1* lack lateral organs in the inflorescence meristem, however, they are able to make leaves in the vegetative phase (Reinhardt et al. 2000a; Vernoux et al. 2000), suggesting yet unknown mechanism that trigger organ initiation in SAM.

Auxin is produced from L-Tryptophan (L-Trp), an aromatic amino acid produced from chorismate (Ljung 2013). Although, it is well established that bulk of the auxin is mainly synthesized from L-Trp, however, a tryptophan independent pathway of auxin biosynthesis also exists in plants (Normanly et al. 1993; Tivendale, Ross, and Cohen 2014).

L-Trp is funnelled into four distinct sub pathways, and they are named based on the first metabolite produced from L-Trp, namely, indole-3-pyruvic acid (IPyA), indole-3-acetamide (IAM), tryptamine (TRA) and indole-3-acetaldoxime (IAOx) (Ljung 2013). Auxin biosynthesis from IPyA is mainly responsible for 80% of the auxin in plants. Arabidopsis plants appear to have two different families of genes involved in the IPyA pathway, and their spatiotemporal expression patterns determine the auxin accumulation in distinct cell types. IPyA pathway involves two families of genes, *YUCCA* (*YUC*) flavin monooxygenases and *TRYPTOPHAN AMINO TRANSFERASES OF ARABIDOPSISs* (*TAAs*). *TAA1* expresses in the QC of root, vasculature and in the apical hook region, while *TAR2* expression is reported in the lateral roots, cotyledons, and in the apical parts of hypocotyls (Stepanova et al. 2008). *YUC* family of genes are expressed in the shoot, root and hypocotyl, *YUC1*, *YUC2*, *YUC4* and *YUC6* are mainly expressed in the shoot whereas *YUC3*, *YUC5*, *YUC7*, *YUC8*, and *YUC9* are responsible for producing auxin in roots (Chen et al. 2014; Hofmann 2011).

Despite having knowledge about auxin biosynthesis pathways and genes involved the role of *TAA1* and *TAR2* mediated auxin biosynthesis in SAM development and lateral organ formation remained elusive. I began this study by elucidating the spatio-temporal expression of *TAA1* and *TAR2* during embryogenesis, vegetative and reproductive phase of plant development. This was followed up by investigating its importance in plant growth, SAM development and deciphering the combined role of auxin transport and biosynthesis for organogenesis and maintaining the auxin maxima and auxin signalling in the shoot apex.

My findings revealed that both *TAA1* and *TAR2* are expressed in SAM. *TAA1* mRNA expression is restricted to the epidermis in the apical region of early embryo and maintained in the seedling and SAM. In contrast, *TAR2* expression is found in the hypocotyl region of heart stage embryo, in the postembryonic development, *TAR2* is expressed in the lateral organs. The single mutants of *TAA1* and *TAR2* do not show any phenotype. However, double mutant plants show severe defects in SAM patterning and organogenesis. Interestingly, when plants are having either *taa1* or *tar2* mutation combined with *pin1*, they revealed distinct phenotypes. *taa1 pin1* double mutant plants display less severe organ formation defects in comparison to *tar2 pin1*. The most notable difference was noted on the stem height. *taa1 pin1* plants are affected in apical dominance, suggesting the role of SAM epidermal derived auxin in stem growth. *tar2 pin1* plants show severe defects in organogenesis, indicating the role of locally produced auxin in primordia initiation.

3.2. Results

3.2.1. *TAA1* expression is restricted to the epidermal cell layer

In order to understand the importance of locally produced auxin in SAM development, I studied the expression pattern of *TAA1*. First, I did in-situ experiments to determine the spatiotemporal expression pattern. *TAA1* sense and the antisense probes were applied to the cross-sections of 4-weeks old WT-L*er* shoot apices. Analysis of in-situ images revealed that *TAA1* expression was restricted to a few cells in the epidermal cell layer in the apex in the antisense probe. However, no signal was detected in the sense probe (Fig.3.1 a, b). To investigate the *TAA1* expression, I analyzed plants carrying *pTAA1::YPet-TAA1* construct, driving *TAA1* expression under its native promoter. In this construct, *YPet* was inserted in front of the *TAA1* coding sequence *(pTAA1::YPet-TAA1)*. This construct fully rescues the *taa1 tar2* double mutant phenotype (Ref)First, I checked the expression of this reporter in SAM. As observed in the in-situ study, plants carrying *pTAA1::YPet-TAA1* transgene show fluorescence in epidermal

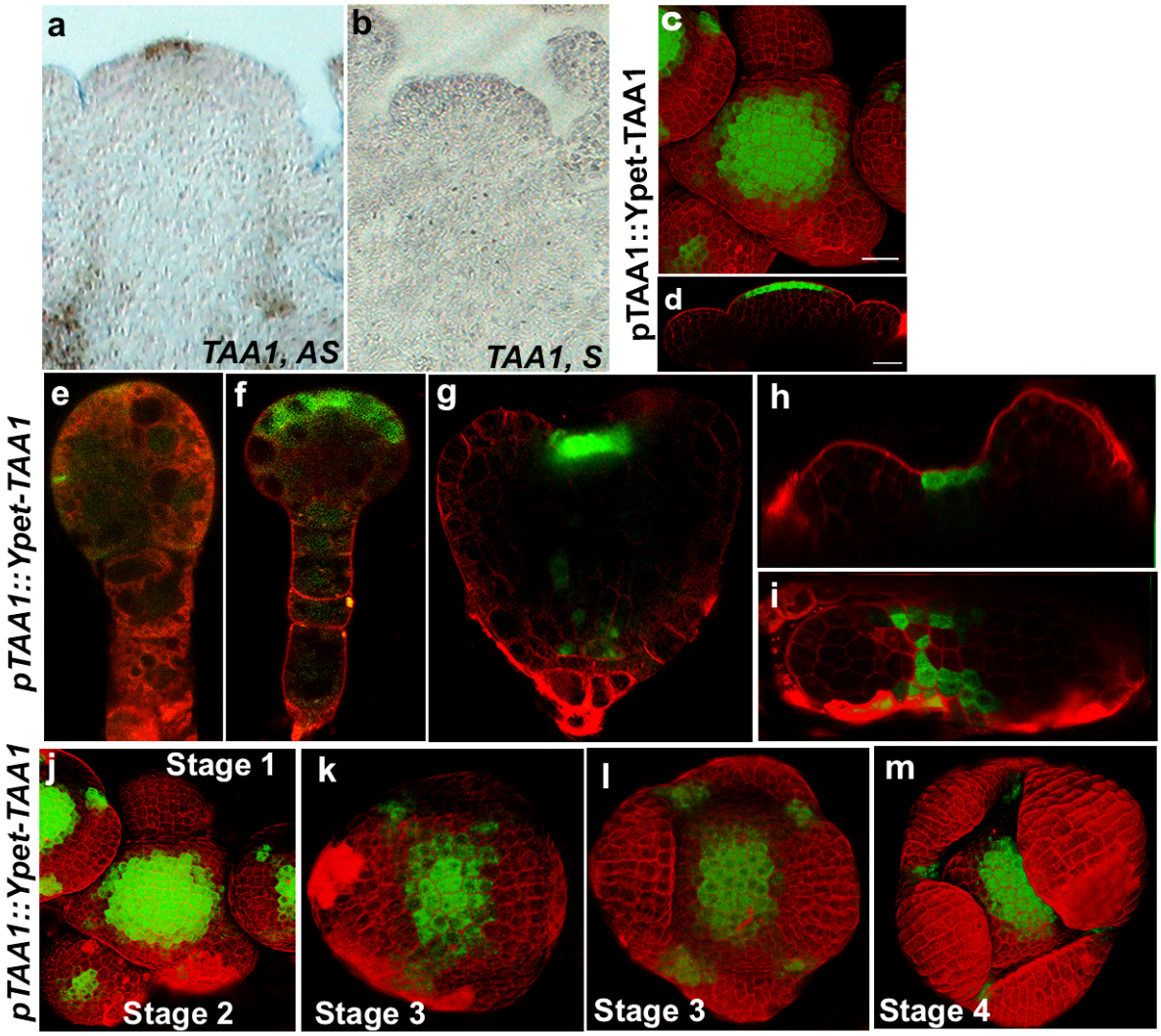

Figure 3.1. *TAA1* expression in embryo, vegetative and reproductive phases of plant development. *TAA1/WEI8* mRNA expresses in the epidermal cell layer of shoot apical meristem, antisense probe **(a),** and sense probe **(b).** Three dimensional (3D) reconstructed top view of SAM expressing translational fusion *pTAA1::Ypet-TAA1* **(c),** and side view **(d).** Ypet-TAA1 protein (in green) localized in the epidermal cell layer. Cell outlines were stained with propidium iodide (PI) (red). Confocal images of *TAA1* expression in the early globular stage **(e),** late globular stage **(f)**, and heart stage **(g)**. *TAA1* expression in 3 days old seedling SAM side view **(h)** and top view **(i)**. *TAA1* expression profile during different stages of flower development. Representative images are showing Ypet expression (in green) from in the floral meristem from stage 2 to stage 4 flower **(j-m).** Cell outlines are stained with propidium iodide (PI). Scale bars: 20µm.

cell layer of the shoot, indicating that *pTAA1* is able to capture *TAA1* native mRNA expression in the SAM (Fig.3.1 c, d). After establishing that *pTAA1::YPet-TAA1* is faithfully depicting the native *TAA1* expression in planta, I used this line to study the expression of *TAA1* in different stages of embryo development. YPet fluorescence was detected in the epidermis of globular

and heart stage embryo (Fig.3.1 e-g). Interestingly, the expression was restricted in the apical region of the embryo. In the postembryonic phases, expression of *pTAA1* was restricted to the epidermis in the meristematic region of seedling and adult SAM (Fig.3.1 h, i).

Next to understand, whether *TAA1* is expressed during flower development. The expression pattern of *pTAA1::YPet-TAA1* was captured with confocal laser-scanning microscopy at different stages of flower development. Analysis of 3D reconstructed top views of different stages of floral meristem revealed that *TAA1* expression appears first in stage 2 floral meristem in the epidermal cell layer, and continues until stage 4 of flower development (Fig.3.1 j-m). Taken together these results, suggest that *TAA1* expression is restricted to epidermal cell layer in embryonic and post embryonically phases of plant development.

3.2.2. *TAR2* expression coincides with incipient organ primordia in shoot and floral meristem

Similarly, to understand the importance of auxin produced via *TAR2* mediated pathway in shoot development, I studied the expression pattern of *TAR2* by in-situ hybridization and promoter-reporter studies. For in situ, *TAR2* antisense and sense probes were applied to the cross-sections of shoot apices for which inflorescence meristems were collected from 4-weeks old WT-L*er* plants. *TAR2* transcript was detected in the PZ of SAM. Interestingly, *TAR2* mRNA was missing completely from the cells of CZ and RM (Fig.3.2 a). No signal was detected in the sense probe (Fig.3.2 b). To study the expression pattern of *TAR2,* further, I made a transcriptional fusion of *TAR2* promoter with a yellow fluorescent protein (YFP) translationally fused with histone H2B in a modified *pGreen0229* vector. A 3 kb DNA fragment above the translation start site (TSS) was PCR amplified using Arabidopsis WT-L*er* genomic DNA as a template and placed in front of H2B-YFP sequence. Several independent T1 lines (n=18) were selected for *pTAR2::H2B-YFP* construct on BASTA. As expected *pTAR2::H2B-YFP* construct recapitulated the *TAR2* mRNA expression pattern as shown in the in-situs, indicating that the

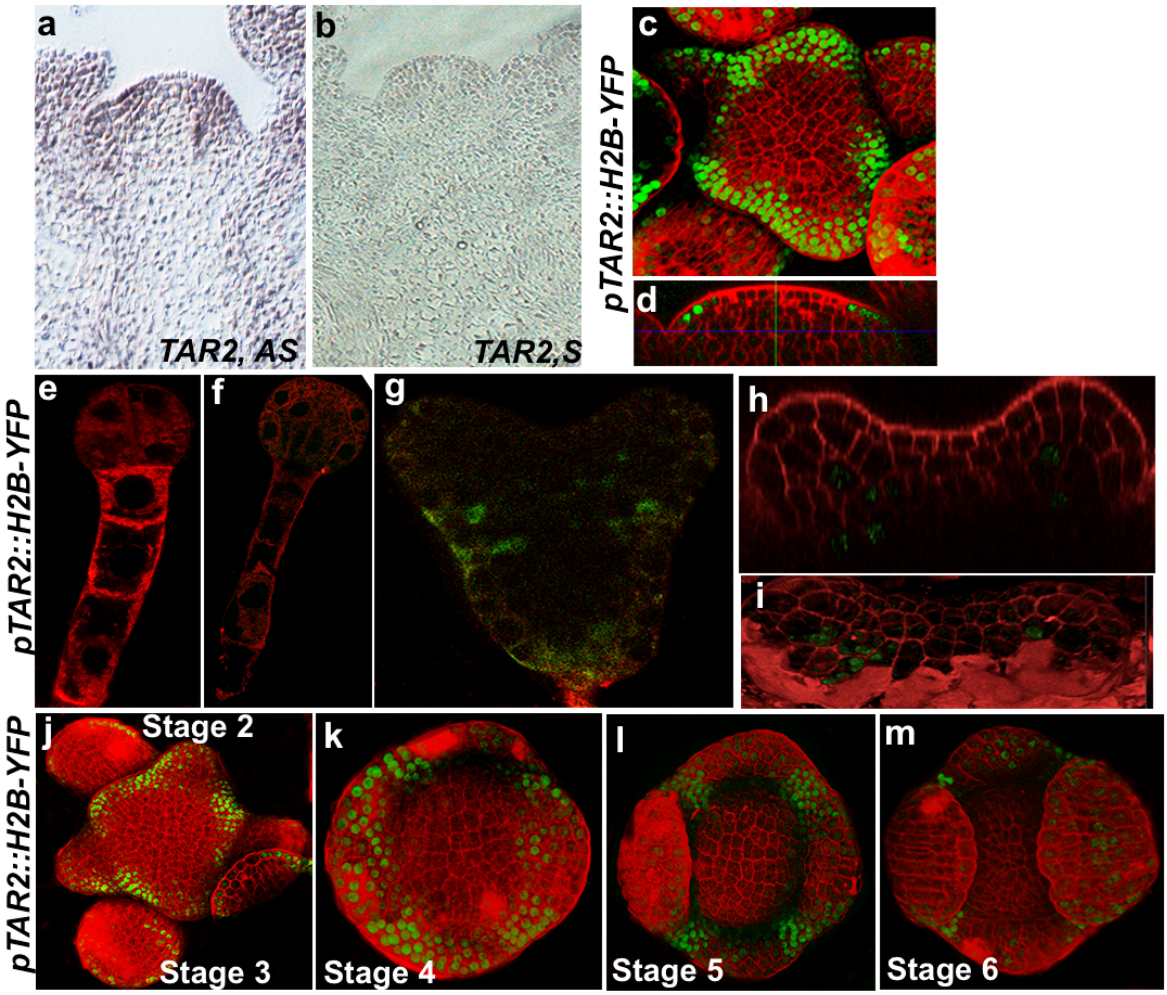

Figure 3.2. *TAR2* expression pattern during embryogenesis, vegetative and reproductive phase of plant development.
TAR2 mRNA detected in the periphery of the shoot apex, but not in the central zone cells antisense probe **(a),** and sense probe **(b).** 3D reconstructed top view of inflorescence meristem of 4-weeks old WT-Ler expressing *pTAR2::H2B-YFP* (green) top view **(c),** and side view **(d)**. Representative images of *TAR2* expression during embryogenesis early globular stage **(e),** late globular stage **(f),** and heart stage **(g)**. *TAR2* expression in 3 days old seedling restricted in cells of PZ side view **(h**), and top view **(i).** *TAR2* expression during different stage of flower development. Representative images are showing YFP expression in green from stage 2 to stage 4 flower **(j-m).** Cell outlines were stained with PI (red).

regulatory elements present within the 3 kb *TAR2* promoter are sufficient to capture its native mRNA expression pattern (Fig.3.2 c, d). Two independent lines of *pTAR2::H2B-YFP* construct were followed further, to make them homozygous for the transgene, and used further to study the expression of *TAR2* in the globular, heart and torpedo stages of embryo development. *TAR2* was not active in the globular stage of the embryo; however, in heart stage embryo *TAR2*

expression was detected in the presumptive hypocotyl region (Fig.3.2 e-g). In the seedling, expression of *TAR2* was mainly restricted to emerging leaf primordia, as the leaf primordium becomes more obvious, *TAR2* expression became stronger in the inner cells (Fig.3.2 h, i). In the SAM, *TAR2* expression was restricted to PZ cells; however, in the incipient primordia, its expression was stronger than the rest of the cells (Fig.3.2 c, d).

Unlike *TAA1*, *TAR2* is strongly expressed in stage 1, and 2 primordia. In the stage 1 primordium, *TAR2* expression is present in all the cell layers of the floral meristem, however, as the primordium turns to stage 2 of its development, its expression weakens in the inner cells, and get restricted to PZ of the floral meristem (Fig.3.2c). In stage-3, *TAR2* expression is conspicuously absent from the floral meristem but active in PZ where the floral organ primordia would appear (Fig.3.2 j). In stage 4, *TAR2* expression is found in the emerging sepals and in between the sepal primordia (Fig.3.2 k). In stage 4 as the primordia get more mature expression was restricted in the specified sepal primordia and completely absent from the centre of the meristem, where stem cells are active (Fig.3.2 i, m). Taken together these results suggest that *TAR2* expression coincides with organogenesis both in inflorescence and floral meristem. *TAR2* is strongly expressed everywhere in the early stages of primordia development. Moreover, as the stem cell specification starts in the flower meristem, its expression gets cleared from presumptive CZ of floral meristem and retained in the PZ cell types. Sepal primordia again start showing the *TAR2* expression similar to floral buttress everywhere, and later they maintain it.

3.2.3. *taa1 tar2* double mutant plants are dwarf and show reduced growth

Since *TAA1* and *TAR2* are the part of the IPyA branch of auxin biosynthesis pathway and both are expressed in SAM. I was intrigued by their non-overlapping expression patterns in the SAM and their function depending upon their expression domains. Past studies have shown

that single mutants of both *TAA1* and *TAR2* do not show any phenotype. However, the double mutant shows pleiotropic phenotypes (Stepanova et al. 2008). None of the past studies investigated shoot and organ defect phenotypes in depth. T-DNA insertion lines *tar2-1* (CS16404) and *taa1-1-/- tar2-1*+/- (CS16413) were obtained from ABRC and confirmed by genotyping, single mutant *taa1-1* was isolated in house from of *taa1-1-/- tar2-1*+/- segregating population confirmed by genotyping and sequencing. Double mutant plants had defects in floral organs, and inflorescence meristem patterning, identified from the segregating population of *taa1-1-/- tar2-1*+/- plants on the basis of phenotype reported in (Stepanova et al. 2008).

First to see the effect of loss of auxin biosynthesis on plant growth and development Col-0, *taa1, tar2* single and *taa1 tar2* double mutants plants were grown on soil parallelly under 16 h light/8 h dark cycle. After 4-5 weeks, plants were observed for their plant height and growth. Plants harbouring either *taa1-1* or *tar2-1* mutations showed normal growth similar to Col-0 plants with respect to inflorescence meristem development, plant height, growth and flower formation (Fig.3.3 a-c, i-k). However, *taa1 tar2* double mutant plants showed severe growth and developmental defects (Fig.3.3 d, l). Double mutant plants were completely sterile and dwarf (Fig.3.3 l).

To characterize further the role of *TAA1* and *TAR2* in SAM development and patterning. Shoots apices of 4-weeks old Col-0, *taa1, tar2* single and *taa1 tar2* double mutant were dissected under a stereomicroscope and stained for 5-6 minutes with propidium iodide (PI, 1mg/ml). Dissected shoots were imaged in an upright confocal microscope (Leica SP8, Germany). Confocal images were analyzed using Leica-X and Morphograph X software. The three dimensional (3D) images of the SAM revealed that *taa1* and *tar2* single mutants SAM

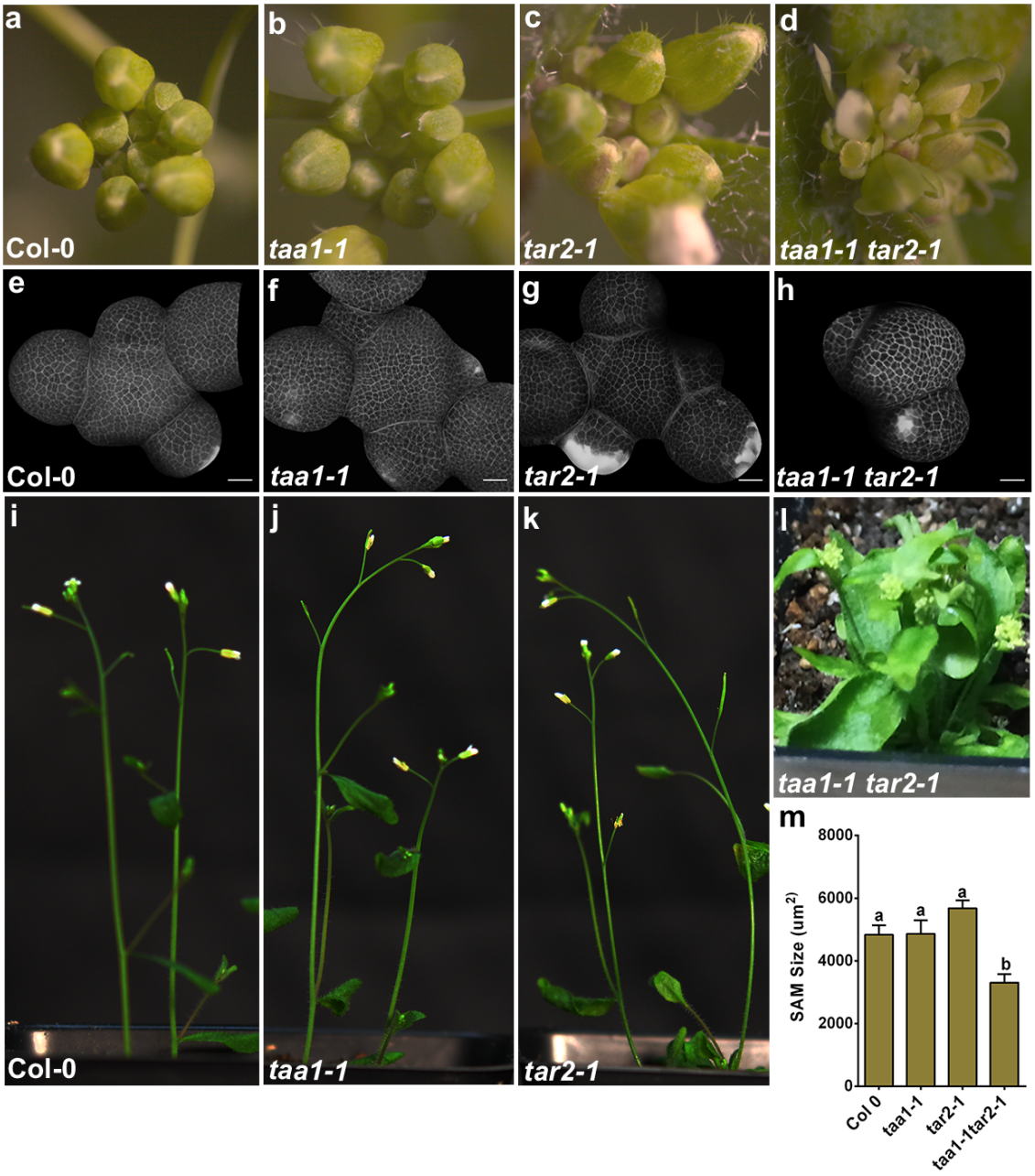

Figure 3. 3 *taa1 tar2* double mutant plant shows smaller shoot size.
Representative images of inflorescence meristems of 4-weeks old Col-0 **(a),** *taa1-1* **(b),** *tar2-1* **(c),** and *taa1-1 tar2-1* double mutant **(d)** plants n=15. Shoot apices of 4-weeks Col-0 **(e)** *taa1-1* **(f)** *tar2-1* **(g),** and *taa1-1 tar2-1* **(h)** plants. Representative images of 4-5 weeks old adults plants of Col-0 **(i),** *taa1-1* **(j),** *tar2-1* **(k)** and *taa1 tar2-1* **(l)**. Note: Double mutant shows growth defects and smaller SAM size. Graph showing SAM size measurement of Col-0 (n=6), *taa1-1* (n=7), *tar2-1* (n=7), *taa1-1 tar2-1* (n=7). Error bars show SEM. Statistical test: One way Anova followed by Tukey's multiple comparisons test, different letters represent the statistically significant difference ($p<0.05$). Scale bars: 20µm.

are similar to Col-0 (Fig.3.3 e-g). In contrast, the double mutant plants harbouring *taa1-1-/- tar2-1-/-* alleles displayed a spherical SAM (Fig.3.3 h). SAM size measurement was performed in Morphograph X software. The SAM size measurement analysis revealed that there was no significant change in the SAM sizes of *taa1* and *tar2* single mutants compared to Col-0 control plants (Fig.3.3 m). But *taa1 tar2* double mutant plants show a significant decrease in SAM size compared to Col-0 and their respective single mutants (Fig.3.3 m).

A closer examination of *taa1 tar2* double mutant shoot apices also revealed defects in organ boundaries and organ patterning. In Col-0 plants, the organ boundaries were properly separated, however in *taa1 tar2* double mutant organ boundaries were not properly patterned (Fig.3.4 a-c). The outgrowth and polarity of floral organ primordia were also compromised in double mutant plants compared to control (Fig.3.4 a-c). Taken together these results, I found that auxin synthesized by *TAA1* and *TAR2* is not only essential for plant growth and development, but it also plays a critical role in organ boundaries formation and SAM patterning.

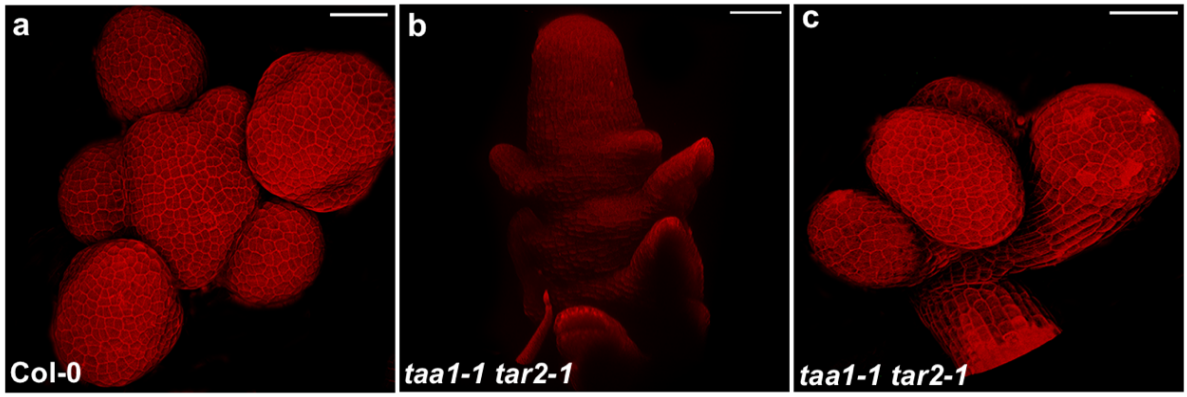

Figure 3.4. Organ patterning defects in *taa1 tar2* double mutant.
3D reconstructed top views of Shoot apices of Col-0 **(a),** and *taa1-1 tar2-1* double mutant **(b-c).** Cell outlines are stained with PI. Scale bars: 20µm

After uncovering that the *taa1 tar2* double mutant has smaller SAM and defects in organ patterning, I asked whether the stem cell pool is maintained in the double mutant SAM. To test this, I have crossed the *taa1-1 -/- tar2-1 -/+* with stem cells marker *pCLV3::mGFP-ER*,

reporter line. F1 plants were propagated and in F2 generation Col-0 and single mutants of *taa1* and *tar2* having *pCLV3::mGFP-ER* were identified after genotyping. The double mutant

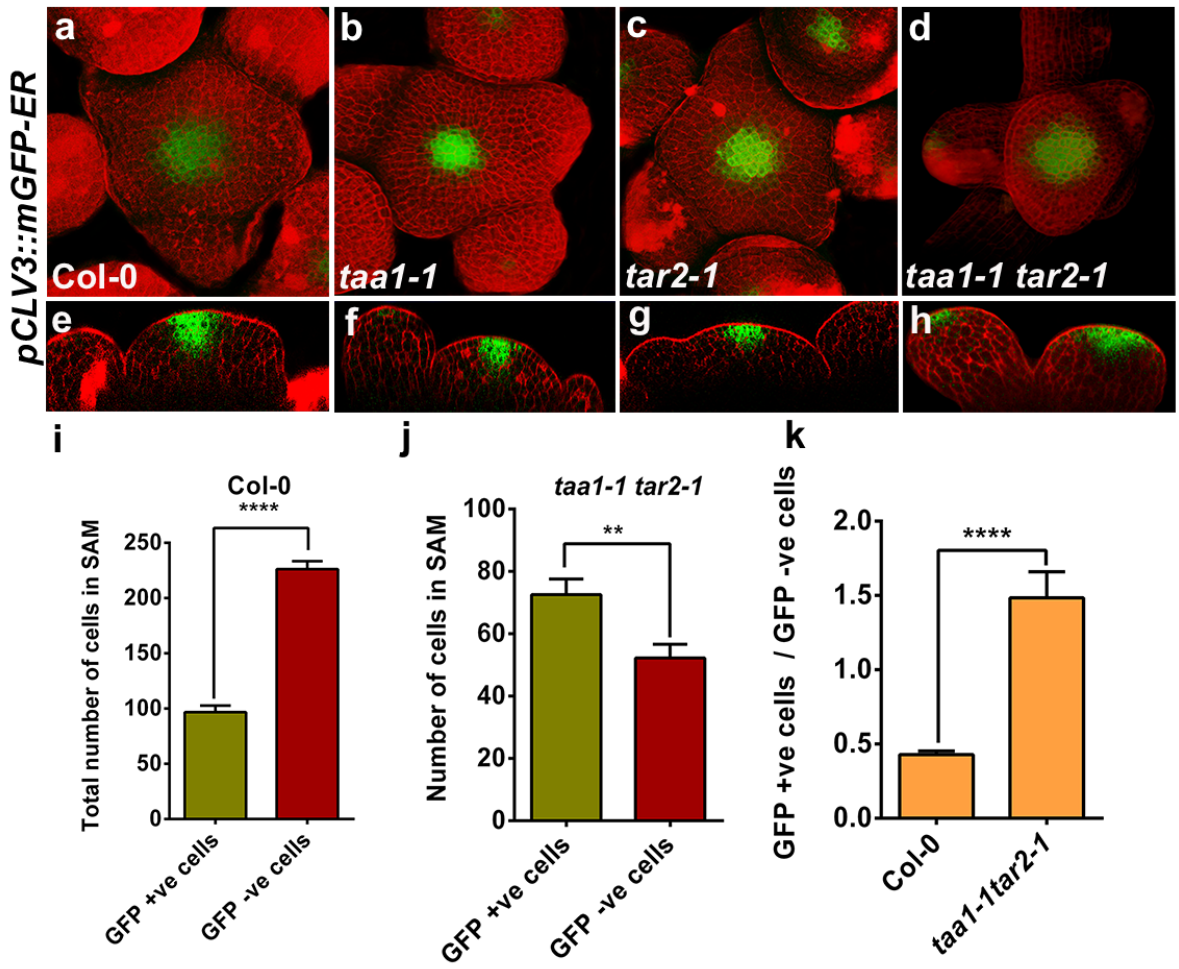

Figure 3.5. Stem cells (CZ cells) and Peripheral zone (PZ) cells fate in auxin biosynthesis mutants. 3D reconstructed top views of SAM expressing *pCLV3::mGFP-ER* (green) in Col-0 **(a)**, *taa1-1* **(b)**, *tar2-1* **(c),** and *taa1-1 tar2-1* **(d),** and side views of the same images are shown in **(e-h)**. Propidium iodide PI (in red) was used to visualize cell outlines. Graphs are showing quantification of GFP +ve (CZ cells) and GFP-ve (PZ cells) in Col-0 (n=9**) (i),** and *taa1-1 tar2-1* double mutant (n=9) **(j)** and relative ratio of GFP +ve (CZ cells) and GFP-ve (PZ cells) **(k).** Error bars show SEM, asterisk marks represent the statistically significant difference among the tested samples, Statistical test: Student t-Test ($p < 0.005$).

plants *taa1-1 tar2-1* were identified on the basis of phenotype. SAMs of Col-0, *taa1, tar2* single mutants and *taa1 tar2* double mutant having *pCLV3::mGFP-ER* reporter were imaged with similar settings on Leica SP8 confocal microscope. A closer examination of *CLV3* expression pattern in *taa1* and *tar2* single mutant plants revealed that its expression does not

differ significantly compared to Col-0 plants (Fig.3.5 a-c, e-g). But in the double mutant *CLV3* domain was slightly expanded (Fig.3.5 a-d, e-h). Parallelly, for the in-depth analysis, I quantified the number of GFP +ve cells (CZ cells) and GFP-ve cells (PZ cells). This analysis shows that *taa1 tar2* double mutant plants do not show a noticeable change in GFP +ve cells (CZ cells), but the number of GFP-ve cells (PZ cells) and size of PZ have got reduced compared to Col-0 plants (Fig.3.5 i-j). Hence, the relative ratio of GFP+ve cells/GFP-ve cells has got increased in the double mutant of *taa1 tar2* compared to Col-0 plants (Fig.3.5 k). This result indicates that reduction in auxin biosynthesis has perturbed the relative size of the CZ to PZ, and thus, the size of the shoot apex. Taken together, these results suggest local auxin biosynthesis plays a critical role in lateral organ formation, shoot apex patterning, stem growth, and axillary meristem formation.

3.2.4. Expression of *TAR2* in the PZ of SAM is sufficient for organogenesis and SAM development

Deficiency in the active pool of auxin leads to severe developmental defects in SAM patterning and organogenesis. To restore the developmental defects in *taa1 tar2* caused because of the deficiency of auxin biosynthesis, *TAR2* expression was driven under its native 3 kb promoter. The resulting construct *pTAR2::TAR2* was dipped in *tar2-1-/- taa1-1+/-* plants. More than 100 transgenic lines were selected on hygromycin and genotyped for the presence of *taa1-1-/- tar2-1-/-* alleles. Of the 100, six lines were confirmed for *taa1-1-/- tar2-1-/-* T-DNA insertion by PCR, and the isolated lines showed the complete rescue of *taa1 tar2* double mutant phenotype (Fig.3.6 d-f), suggesting that synthesis of auxin in the PZ of SAM is sufficient to restore the normal growth of the plastochron. Two of the lines were followed up and grown on the soil parallelly with Col-0 and *taa1 tar2* double mutant to check whether *pTAR2::TAR2* construct can also rescue the SAM defects. Interestingly, the *pTAR2::TAR2* construct was able to restore the growth defects in SAM development and organ patterning (Fig.3.6 a-c). Taken together,

these results suggest that the 3kb *pTAR2* not only recapitulated *TAR2* mRNA expression pattern but also rescued the double mutant phenotype. These results indicate that the cis-regulatory elements present within 3 kb *pTAR2* are sufficient for its proper spatio-temporal expression within the shoot apex and to rescue the *taa1 tar2* double mutant. Phenotype.

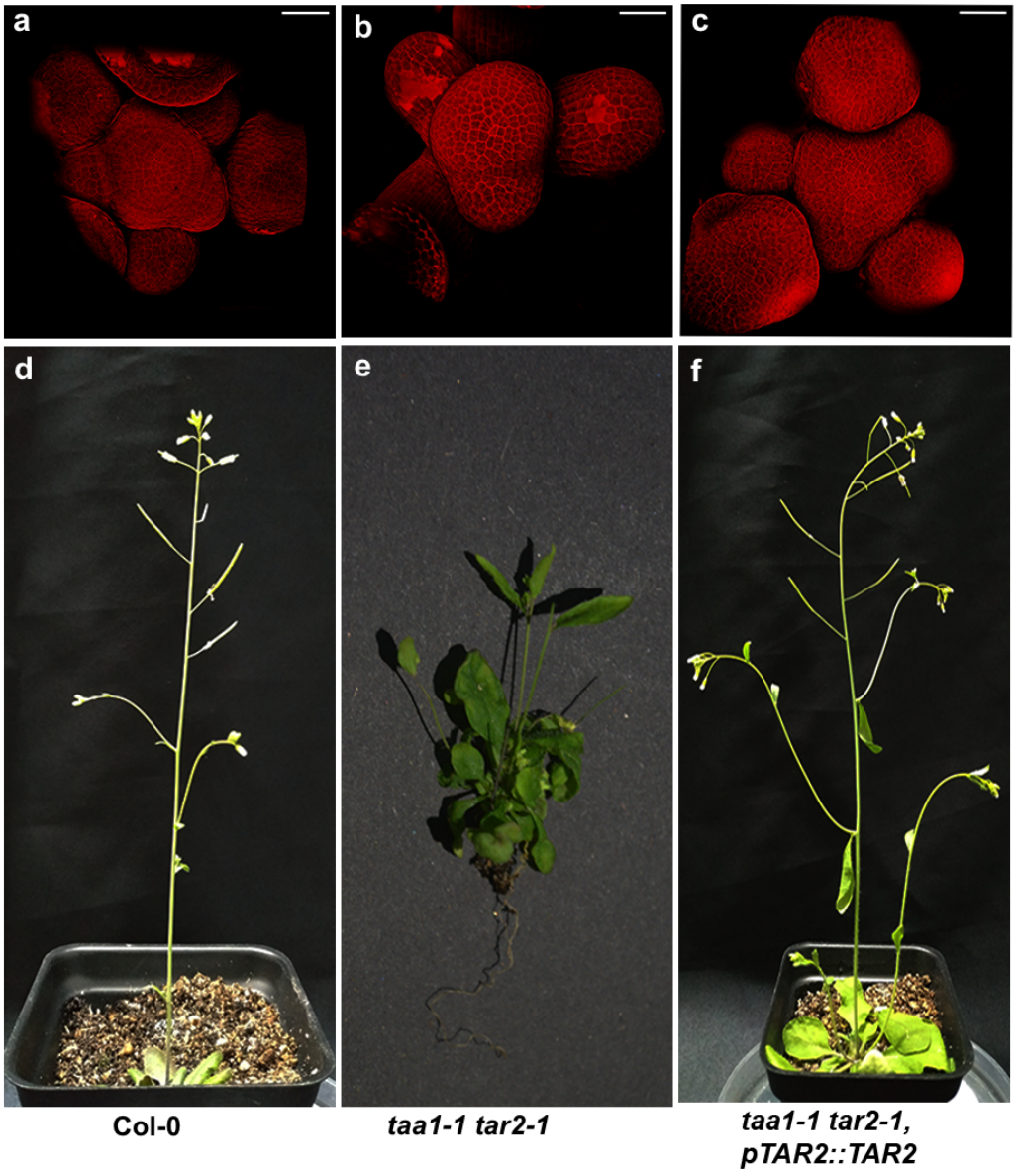

Figure 3.6. *TAR2* expression pattern in PZ is essential for proper plant growth and shoot development.
3D reconstructed top views of shoot apices of soil grown 4-weeks old Col-0 **(a)** *taa1-1 tar2-1* **(b),** and *taa1-1 tar2-1* double mutant phenotype rescued by *pTAR2::TAR2* construct **(c).** Cell outlines are stained with PI. Phenotypes of adult plants grown parallelly in soil Col-0 **(d),** *taa1-1 tar2-1* **(e),** and a complete rescue of *taa1-1 tar2-1* double mutant phenotype by *pTAR2::TAR2* construct **(f).** Scale bar: 20μm.

3.3. *TAA1*/*TAR2* mediated auxin biosynthesis is essential to maintain auxin responses in SAM

At the cellular level, auxin levels and auxin signalling can be detected within living tissues using different auxin sensors. In previous studies, to detect the auxin level (auxin input) DII-VENUS auxin sensor was designed, where an auxin sensitive DII domain of IAA28 was fused with a yellow fluorescent a reporter gene in plants, (Liao et al. 2015), depending upon the auxin concentration DII domain can be degraded within the tissues. Another auxin sensor, which is based on the auxin signalling output, contains concatemerized auxin response factor (ARF) binding sites also called as auxin response element (AuxRE) were fused with reporter gene to monitor auxin responses within a tissue (Tim Ulmasov et al. 1997). This AuxRE containing reporter provides information about auxin sensitive activation and repression of ARFs during different developmental process in the plant (Li et al. 2016). Here, for this study to check auxin input and output in SAM, *DII::VENUS* and *pDR5rev::3×VENUS-N7* reporters were used respectively

3.3.1. Auxin levels and auxin responses are perturbed in *taa1 tar2* double mutant

In the SAM, auxin maxima define the position of primordia emergence and lateral organ formation. *TAA1* and *TAR2* are involved in IPyA pathway of auxin biosynthesis, and thus, required for the organ initiation and patterning. To understand the role of locally produced auxin in organogenesis and their patterning, auxin levels and auxin responses were analyzed in *taa1, tar2* single and *taa1 tar2* double mutant plants. For this, I crossed the line harbouring *taa1-/- tar2-1+/-* T-DNA alleles with *pDR5rev::3×VENUS-N7* and *DII-VENUS* reporter lines, respectively. F1 plants were raised, and F2 seeds were obtained. F2 plants carrying either *pDR5rev::3×VENUS-N7* or *DII-VENUS* transgene were genotyped to identify *taa1* and *tar2* single mutants. For all the genotypes plants having *pDR5rev::3×VENUS-N7* and *DII-VENUS*

reporters from two independent crosses were followed up to F4 generation to make them homozygous. Since the double mutant of *taa1 tar2* did not give seeds, So, to get the double mutant, the line harbouring *taa1-1-/- tar2-1+/- pDR5rev::3×VENUS-N7* and *taa1-1-/- tar2-1+/- DII-VENUS* were identified in segregating population after genotyping and followed up in next-generation for confocal imaging.

To find out whether auxin responses are affected in the *taa1, tar2* single and *taa1 tar2* double mutant plants SAM due to auxin deficiency, I examined the confocal images of SAMs of *taa1, tar2* single and *taa1 tar2* double mutant plants, carrying *pDR5rev::3×VENUS-N7* and compared with Col-0. *pDR5* expression was not affected in the *taa1* and *tar2* single mutants; however, in *taa1 tar2* double mutant *DR5* expression was significantly decreased compared to control and respective single mutants (Fig.3.7 a-d, e-h). To make this observation more rigorous, auxin maxima formed at the peripheral zone was counted in the SAMs of Col-0, *taa1*, *tar2* single and *taa1 tar2* double mutant. This analysis revealed a drastic decrease in auxin maxima formation at the flank of the meristem (Fig.3.7 q), suggesting that *TAA1/TAR2* mediated auxin biosynthesis is required for the generation of auxin maxima in the SAM. The formation of auxin maxima in specific locations of SAM occur due to local auxin biosynthesis as well; however, it is not clear how these maxima get stabilized in specific locations in SAM. After confirming the role of *TAA1* and *TAR2* mediated auxin biosynthesis in maintaining the auxin output, I wanted to know whether a decrease in *DR5* expression in *taa1 tar2* mutant results in the corresponding stabilization of *DII-VENUS* input sensor. For this, confocal images of shoot apices of *taa1*, *tar2* single mutant, and *taa1 tar2* double mutant plants, carrying *DII-VENUS* reporter were analyzed and quantified. The input sensor activity was drastically altered in the *taa1 tar2* double mutant compared to single mutant and control, *DII-VENUS* expression became wider and stable all over the shoot apex (Fig.3.7 i-l, m-p). Which represents a low auxin zone is now established in the shoot apex in the absence of local auxin biosynthesis.

Quantification of *DII-VENUS* positive cells has revealed a significant increase in the *DII-VENUS* positive cells in *taa1 tar2* double mutant compared to Col-0, *taa1* and *tar2* single mutants in the meristematic area. Taken together these findings, I have concluded how precisely *TAA1* and *TAR2* collectively influence the auxin responses. It is also possible that auxin synthesized in other parts of the plants by these two genes also get affected in the double mutant; therefore the transport of auxin will be impaired, and that would result in overall decrease in auxin levels in the SAM.

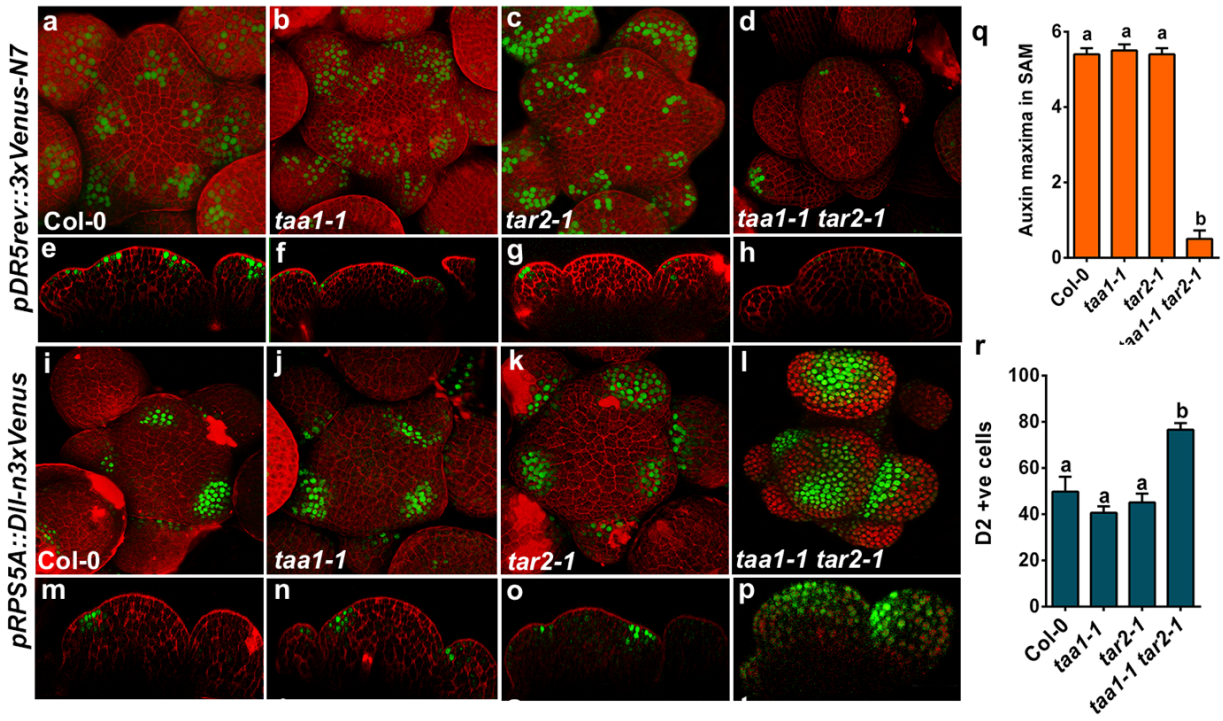

Figure 3.7. Locally produced auxin required for maintaining auxin input and auxin output in the SAM.

3D reconstructed views of Arabidopsis SAMs showing the expression of the auxin responsive marker *pDR5rev::3XVENUS-N7* (green) in Col-0, *taa1-1, tar2-1 and taa1-1 tar2-1* double mutant respectively, top views **(a-d)** and side views **(e-h).** The double mutant shows less auxin responses at the periphery of SAM. SAMs of Col-0, *taa1-1, tar2-1, and taa1-1 tar2-1*mutants carrying *DII-VENUS* (green), top views **(i-l)** and side views **(m-p).** Cell outlines are stained with PI. Graph showing quantification of auxin maxima for Col-0 (n=9*), taa1-1* (n=9), *tar2-1* (n=9), *taa1-1 tar2-1* (n=9) and Quantification of *DII-VENUS* positive cells in Col-0 (n=8), *taa1-1* (n=8), *tar2-1* (n=8), *taa1-1 tar2-1*(n=7) **(q-r).** Error bars show SEM. Statistical test: One way Anova followed by Tukey's multiple comparisons test, different letters represent the statistically significant difference ($p<0.05$).

3.3.2. Auxin biosynthesis and transport inhibitors drugs show less DR5 responses in the shoot apex

I showed that the *TAA1/TAR2* mediated auxin biosynthesis is required for maintaining optimum responses in the SAM. To investigate this further, I resorted to drug treatment. The idea behind these experiments to see whether transient inhibition of auxin biosynthesis enzyme TAA1/TAR2 results in alternation in SAM morphology and organogenesis. Since L-Kynurenine (Kyn) was identified as an alternative substrate for TAA1/TAR2, and it competitively inhibits the activity of these enzymes. Molecular and biochemical studies suggest that L-Kyn can specifically interact with active sites of TAA1/TAR2 but not with other aminotransferases (He et al. 2011).

To investigate how L-Kyn affects the auxin responses in SAM. 4-weeks old SAM of Col-0, *taa1* and *tar2* single mutants having *DR5* reporter were treated with 100µM L-Kyn. Mock plants were treated in parallel with 100µM DMSO. Two days after the treatment (~ 48 h), shoot apices were dissected and visualized under Confocal Microscope. For each genotype shoots of ten plants were examined. I found that compared to control (DMSO treatment), Col-0 shoot apices treated with L-Kyn showed a dramatic decrease in the *DR5* foci in the SAM, indicating that the L-Kyn treatment was effective and it can penetrate the cells despite having cuticle on the surface (Fig.3.8 a, b). A similar decrease was also observed in the number of *DR5* positive cells in *taa1* and *tar2* single mutants SAM (Fig.3.8 d-e, g-h). The difference in the number of *DR5* positive cells between the Col-0, *taa1* and *tar2* mutants SAM treated with L-Kyn was not significant, indicating that L-Kyn does not alter the *DR5* responses drastically in *taa1* and *tar2* single mutants (Fig.3.8 j). Despite blocking the activity of TAA1/TARs, I did not see a significant decrease in the number of *DR5* positive cells. This could be due to transport of auxin in the SAM by PIN1 is still active. I also treated Col-0, *taa1* and *tar2* mutant shoot apices with 100µM NPA for 48 h to see the sensitivity of *DR5* reporter activity. NPA

blocks the polar auxin transport; therefore I expected less auxin responses. However, auxin measurement studies in Arabidopsis root revealed 40% increase in auxin content after blocking the polar transport of auxin by NPA treatment, suggesting that the increase in auxin content is perhaps due to biosynthesis, and thus, blocking the auxin transport from the cells would lead an increase in its overall content. Taken together, my studies on the shoot apices of Col-0, *taa1* and *tar*2 revealed that auxin responses are not abrogated completely when L-Kyn or NPA is applied, suggesting that the interplay between auxin biosynthesis and transport is complex. It is difficult to discern the exact effect of L-Kyn from NPA.

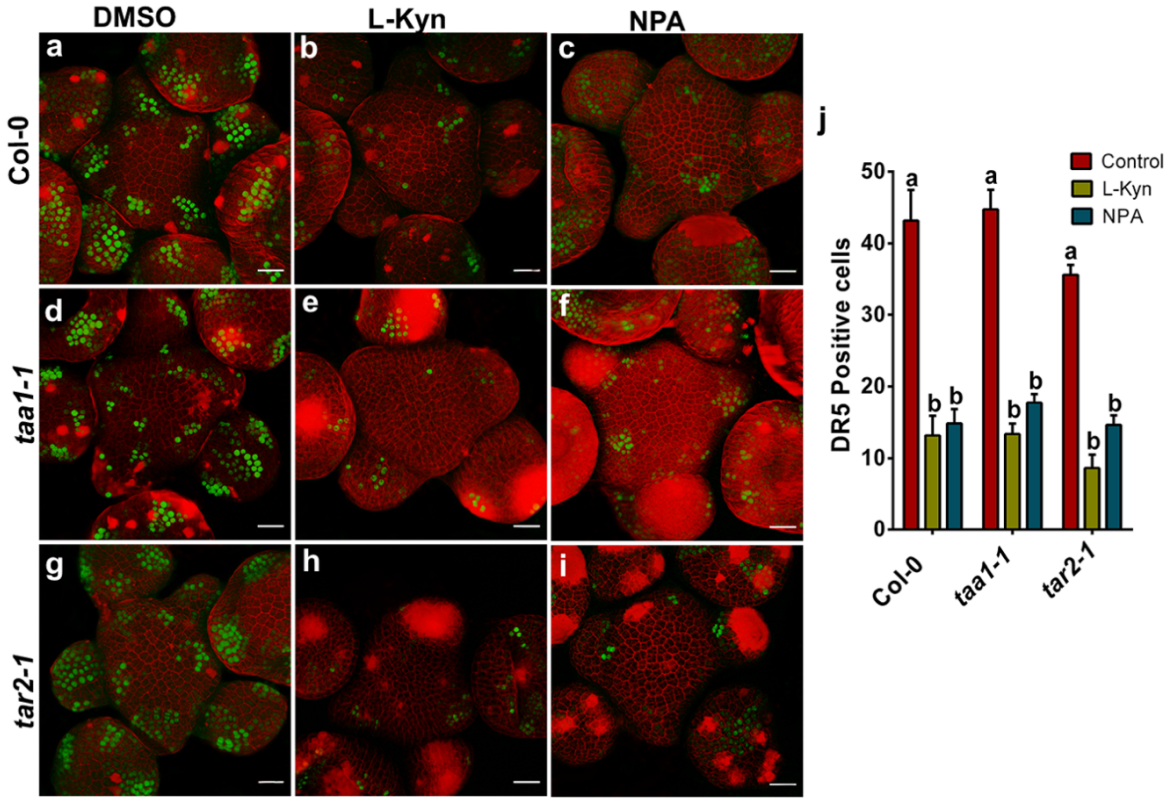

Figure 3.8. L-Kyn and NPA treatment lead to lesser DR5 responses in SAM.
Representative images of 3D reconstructed top views of SAMs showing the expression of auxin responsive marker *pDR5rev::3XVENUS-N7* (green*)* in Col-0 (n=10), *taa1-1*, (n=10) and *tar2-1* (n=10) respectively. treated with 100µm DMSO **(a, d, g)**, 100µm L-kyn **(b, e, h)** and 100µm NPA **(c, f, i)** for 48 hrs. Cell outlines are stained with PI. A graph **(j)** is showing the quantification of DR5 positive cells in control L-Kyn and NPA treated Col-0, *taa1-1* and *tar2-1* plants. Statistical test: One way Anova followed by Tukey's multiple comparisons test. Different letters represent the statistically significant difference ($p<0.05$). Scale bars: 20µm.

3.4. Auxin biosynthesis and transport both are required for SAM maintenance and patterning

Genetic and molecular studies suggested the role of polar auxin transport in lateral organ formation and phyllotactic patterning in the SAM. *pin formed 1* (*pin1*) mutant plants fail to form lateral organs and form pin-shaped shoot apices; however, they form rosette leaves, and stem does grow like WT (Okada et al. 1991; Reinhardt, Mandel, and Kuhlemeier 2000b). In addition, the overall layering and zonal organization of the SAM is maintained (Vernoux et al. 2000). Plants treated with auxin transport inhibitor NPA also have a phenotype similar to *pin1* mutant in tomato (Reinhardt et al. 2003b). External application of auxin to the shoot apices of *pin1* mutant can rescue the phenotype (Reinhardt et al. 2003b). Despite having severe defects in the organogenesis in the reproductive phase, *pin1* mutant plants can still make the lateral organs such as leaves during the vegetative phase. I asked If PIN1 mediated polar auxin transport is the only major contributor for organogenesis and maintaining phyllotactic patterning, then why *pin1* mutant plants grow and make the leaves and maintained the functional zones at the shoot apex. On the other side, *taa1 tar2* double mutant lacks *DR5* responses in SAM and show a defect in stem growth. Keeping the role of auxin in mind, it is important to understand how auxin transport and biosynthesis tie the knot together in the SAM development. Since *TAA1* and *TAR2* are expressed in two complementary domains of shoots, it is important to understand the relative contribution of biosynthesis in the absence of transport.

3.4.1. *TAA1*/ *TAR2* mediated auxin biosynthesis contributes for activation of MP and PIN1 in SAM

Past studies have shown that the phyllotactic patterning, which determines organ position in the SAM is regulated by auxin. Expression of *PIN1* is upregulated by auxin, a feedback loop between auxin and its own transport mediated through MP/ARF5 determines phyllotactic

patterning and initiation site of organ primordia, tightly regulates phyllotactic pattering in the SAM. (Bhatia, Bozorg, Ohno, et al. 2016; Jönsson et al. 2010; Okada et al. 1991; Reinhardt et al. 2000b; Stoma et al. 2008). In the present study, I hypothesized that auxin levels which required for MP activation, then PIN1 protein localization and polarity also contributed by *TAA1* and *TAR2* mediated auxin biosynthesis. To test this hypothesis, First, transcript of *MP (ARF5)* was checked in the shoot apex of Col-0 and *taa1 tar2* double mutant by qRT-PCR. RNA was isolated from the shoot apices of 4-weeks old Col-0 and *taa1 tar2* double mutant plants. cDNA was synthesized and used for qRT-PCR assays. I observed a significant decrease in *MP (ARF5)* transcript levels in *taa1 tar2* double mutant compared to control (Fig.3.9 a). To further confirm this observation, I carried out in-situ hybridization on 4-weeks old Col-0 and *taa1 tar2* double mutant plants, using *MP (ARF5)* antisense probe. Analysis of *in-situs* images revealed that the expression pattern of *MP (ARF5)* was maintained in the shoot apex, but quantitatively the expression weakened in *taa1 tar2* double mutant compared to control plants (Fig.3.9 b, c), which also supports qRT-PCR experiment as well.

Further to dissect the role of auxin biosynthesis, on PIN1 localization and its polarity in the *taa1 tar2* double mutant. I performed two experiments, First, I checked the expression level of *PIN1* in *taa1 tar2* double mutant shoot apices. The qRT-PCR experiments revealed a significant decrease in the *PIN1* transcript levels in *taa1 tar2* compared to control (Fig.3.9 d). Next, I checked the PIN1 localization by crossing the *PIN1:PIN1-GFP* translational fusion line by with *taa1-1-/- tar2-1+/-* plants. Plants carrying *pPIN1::PIN1-GFP* transgenes were identified in Col-0, *taa1-1*, *tar2-1* single mutants, and *taa1-1-/- tar2-1 +/-* line with *pPIN1::PIN1-GFP* reporter was followed to get the *taa1 tar2* double mutant. A closer examination of shoot apices in *taa1, tar2* single and *taa1 tar2* double mutant plants having *pPIN1::PIN1-GFP* transgene revealed that PIN1 localization is maintained in *taa1-1* and *tar2-1* single mutants similar to control plants, however, a decrease in *pPIN1:PIN:GFP* expression

was followed with non-polar localization of PIN1 in *taa1 tar2* double mutant (Fig.3.9 e-h, i-l) Taken together, these results suggest that auxin synthesized by *TAA1/TAR2* mediated pathway contributes to the expression of *MP/ARF5* and *PIN1*. In the absence of auxin biosynthesis, the positive feedback loop reinforcing the MP-PIN1 further get weakened, which reflect on the PIN1 localization.

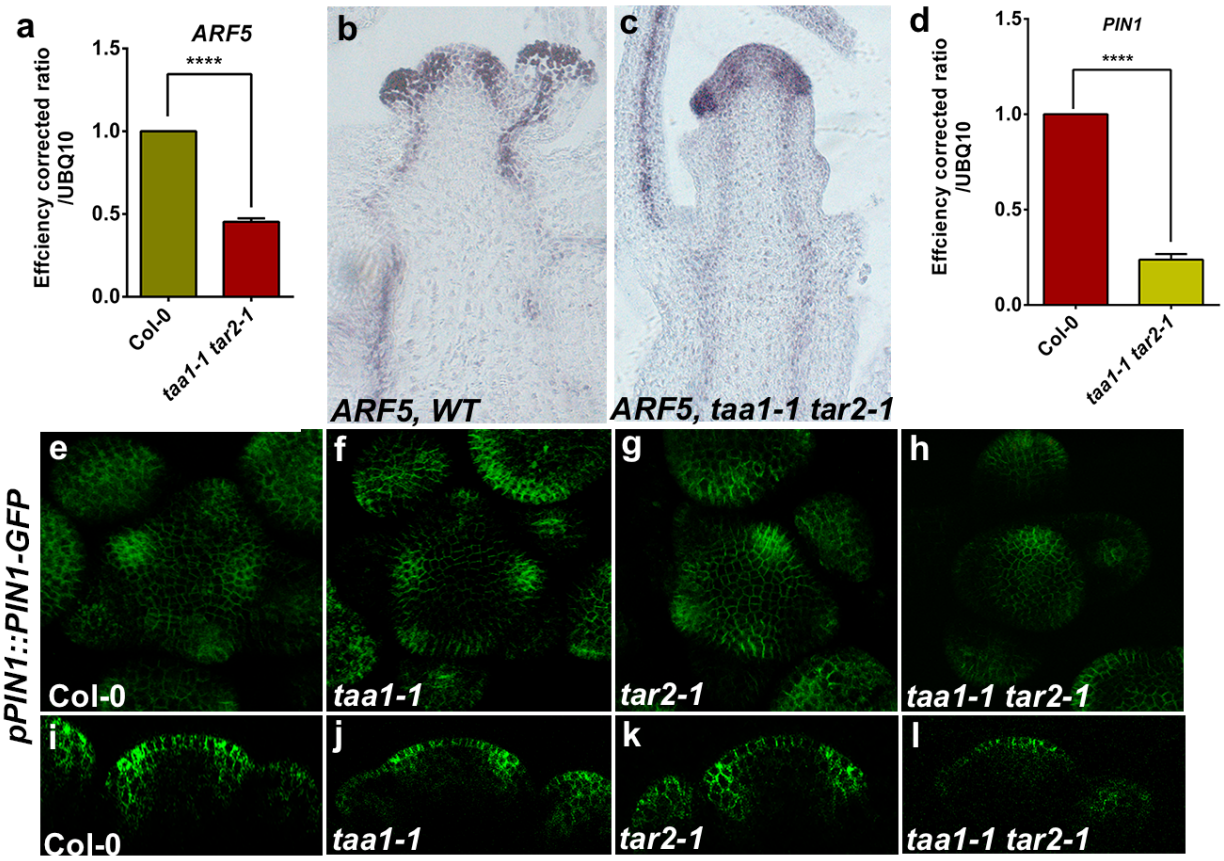

Figure 3.9. *TAA1/TAR2* mediated auxin biosynthesis is required to maintain *MP* and *PIN1* expression.
Graph showing qRT-PCR of *ARF5* in *taa1-1 tar2-1* double mutant in comparison to control Col-0 plants **(a).** In-situ hybridization images of *ARF5* antisense probe in Col-0 **(b)** and in *taa1-1 tar2-1* **(c)** qRT-PCR data is showing *PIN1* expression in *taa1-1 tar2-1* double mutant compared to control Col-0 plants **(d).** Representative images of 28 days old shoot apices of plants carrying *pPIN::PIN1-GFP* in Col-0, *taa1-1*, *tar2-1* and *taa1-1 tar2-1*, top views **(e-h)** and side views for the same images **(i-l).**

3.4.2. Correlation between auxin biosynthesis and signalling in SAM

Previous work has shown that MP (ARF5) polarizes PIN1 in the SAM non-cell autonomously (Bhatia, Bozorg, Larsson, et al. 2016). Since the results presented in the previous section show

PIN1::PIN1-GFP localization is partially dependent on auxin biosynthesis mediated by *TAA1/TAR2* pathway. Early expression of MP (ARF5) coincide with PIN1 polarization**,** I asked the question, Is the expression of *MP* correlate with auxin biosynthesis (*TAR2* expression) in SAM? In order to investigate the correlation between *ARF5*, *TAR2* and *PIN1*expression. I imaged the SAMs of plants carrying *pTAR2:H2B-YFP*, *pMP::MP-GFP* and *pPIN1::PIN1-GFP* transgenes. *pTAR2:H2B-YFP* marks the incipient primordia and expresses uniformly in I3 to P1 stage (Fig.3.10 b-e). Here, *TAR2* expression overlaps with MP-GFP localization (Fig.3.10 b-e, j-m). Expression of *TAR2* was detected in the L1/epidermal, L2/subepidermal and L3/corpus cell layers of I3 to P2 stage of primordia (Fig.3.10 b-f). In later stages, *TAR2* expression disappears from inner cell layers, especially from L2 and L3 / corpus(Fig.3.10 g-h). Although MP-GFP expression is maintained in the epidermal and subepidermal cell layer, its expression gets attenuated in the inner cell layer (Fig.3.10 o-p). This observation clearly suggests that *MP* expression partly overlaps with auxin biosynthesis. In the I3 primordium *pPIN1::PIN1-GFP* expression is weak; however, in I1 it shows the highest expression, which also coincides with primordium specification (Fig.3.10 r-x). Taken together these results, my data suggest Auxin biosynthesis mediated by *TAR2* in incipient primordium accumulates first, this partly activates the expression of MP/ARF5 in the first place, which leads to the further polarization of PIN1 in SAM. This self-sustaining feedback loop between *TAR2*, *MP* and *PIN1* is crucial to maintain the auxin maxima and auxin signalling in the organ founder cells at the flanks of the meristem. A strong perturbation in either of the components breaks this self-correcting feedback loop and has consequences on organogenesis.

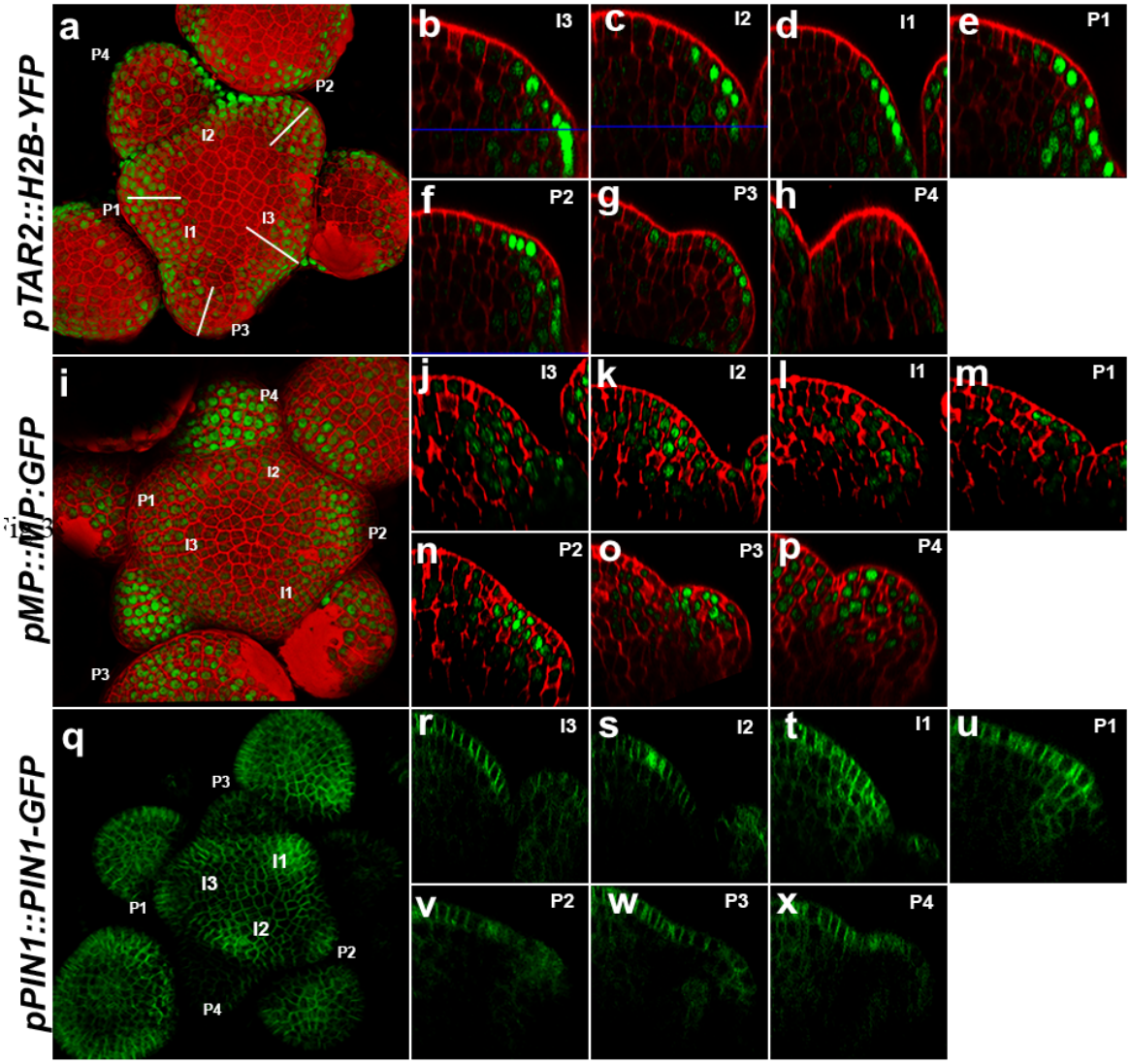

Figure 3.10. Overlapping expression pattern of *TAR2*, MP and PIN1 in SAM.
3D reconstructed top views of WT inflorescence meristem showing expression of *pTAR2::H2B-YFP* (green) **(a)** *pMP::MP:GFP* (green) **(i)**. and localization of *pPIN1::PIN1-GFP* **(q)**. *pTAR2::H2B-YFP* **(b-h)** *pMP::MP-GFP* **(j-p)** and *pPIN1::PIN1-GFP* **(r-x)** showing longitudinal sections of primordia. Cell outlines are stained with PI in (red)

3.4.3. Auxin biosynthesis in the incipient organ primordia is critical for lateral organ initiation

By considering the *TAA1* and *TAR2* spatiotemporal expression patterns in SAM, I hypothesized that *TAR2* would have more influence on lateral organ formation than *TAA1*. Despite its expression in emerging organ primordia, *tar2* single mutant plants do not show any phenotype related to organ formation. PIN1 is polarized towards the PZ cells, and this could very well

mask the apparent function of *TAR2* in organ formation. To test this hypothesis, I made crosses of *pin1-5* (a weak allele of *pin1*) with *taa1-/- tar2* +/- line. F1 plants were self-fertilised and propagated. In the F2, I identified *pin1-5-/- taa1-1-/-, pin1-5-/- tar2-1-/-,* and *pin-5-1-/- taa1-1+/- tar2-1-/-* allelic combination by T-DNA PCR. In the F2 generation, WT-L*er, pin1, pin1 taa1, pin1 tar2* plants were grown parallelly on the soil in similar conditions. Once the bolting started, shoot apices for WT-L*er*, *pin1-5, pin1-5 taa1-1,* and *pin1-5 tar2-1* were examined and dissected under the stereomicroscope, stained with propidium iodide and confocal imaging was performed. Analysis of confocal images revealed, *pin1-5* plants never make the pin-like apices and, their shoot apex appear similar to WT-L*er* plants with some defects in the organ formation (Fig.3.11 a-b, e-f). Moreover, the double mutants of *pin1-5 taa1-1*, and *pin1-5 tar2-1* did not make any lateral organ. They make the complete naked pin-like structure at the place of SAM (Fig.3.11 c-d, g-h).

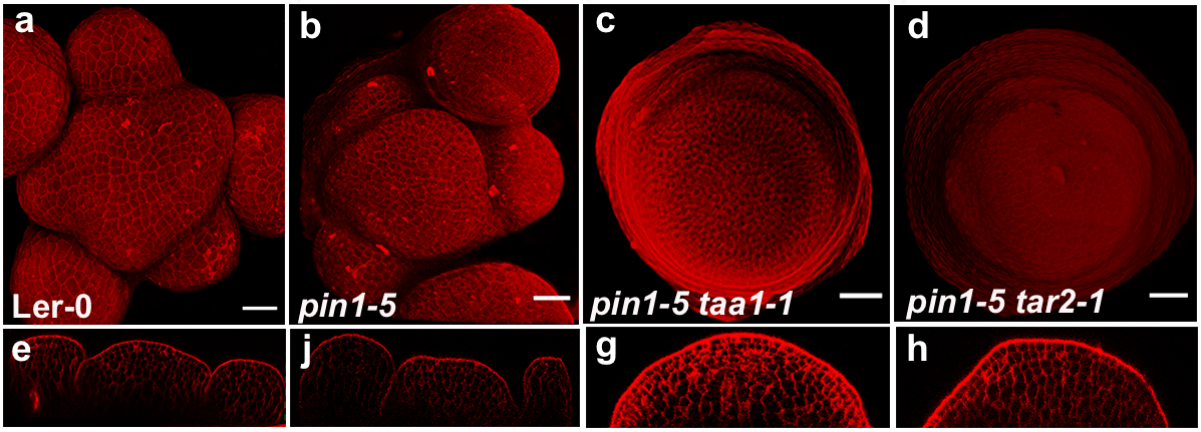

Figure 3.11. Auxin biosynthesis and transport both contribute to lateral organ formation. Representative confocal images of shoot apices of WT-L*er***,** *pin1-5, pin1-5 taa1, and pin1-5 tar2-1* plants, respectively, top views **(a-d)** and side views **(e-h).** *pin1-5* never forms PIN like inflorescence. Scale bars: 20µm.

To further understand the effect the *TAA1/TAR2* mediated auxin biosynthesis on lateral organ formation. Plants for all the genotypes were grown in soil and examined 28DAG and 35DAG. *pin1-5* single mutant did not show many differences in terms of plants growth compared to

WT-L*er* plants (Fig.3.12 a, b). As the plants grew old *pin1 tar2* double mutant plants were discernible from *pin1 taa1*. Twenty-eight DAG, *pin1 tar2,* and *pin1 taa1* both make the small pin-like structure at the shoot apex (Fig.3.12 c, d). Although *pin1-5* single mutant grew normally like WT-L*er* plants, without any pin-like structure the tip (Fig.3.12 a, b), When plants were observed 35 DAG, interestingly, I found that *pin1 tar2* double mutant plants show more severe defect in producing lateral organs and display pin-like apices without making any lateral organs at the periphery compared to WT-L*er* and *pin1* (Fig.3.12 e, f, h). In contrast to this, *pin1 taa1* double mutant plants also terminate in pin-like structure, but they are short and do not grow (Fig.3.12 c, g).

WT L*er*, *pin1, pin taa1, pin1 tar2* were also analyzed to quantify the number of the axillary meristem, lateral organ and stem height. This analysis revealed that *pin1 tar2* double mutant plants make significantly less number of axillary meristem compare to *pin1, pin1 taa1* and control plants (Fig.3.12 i). I also noticed an overall decrease in the number of lateral organs in 35 days old *pin1 tar2* double mutant compared to *pin1* and *pin1 taa1* plants (Fig.3.12 j, k). Interestingly, the stem height of *pin1 taa1* double mutant plants was significantly reduced compared to *pin1 tar2* and *pin1* single mutant (Fig.3.12 l). Taken together these results, I demonstrate that *TAR2* is more critical for organogenesis, whereas *TAA1* is required for apical dominance and stem growth.

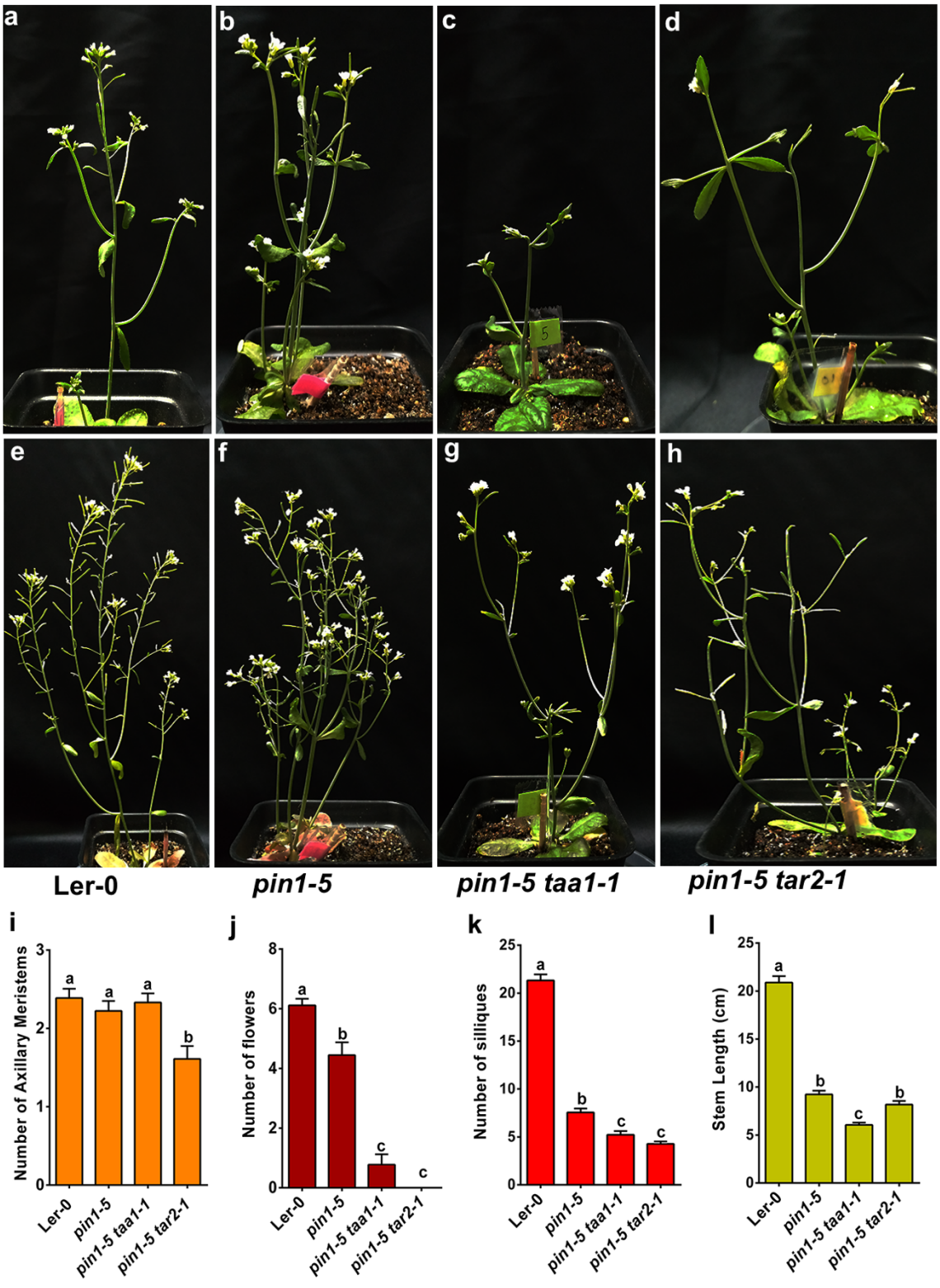

Figure 3.12. ***TAA1/TAR2*** **mediated local auxin biosynthesis and PIN1 mediated auxin transport both are required for organ formation and SAM development**.

From left to right, Phenotypes of 28 days old adult plants of WT-L*er pin1-5, pin1-5 taa1-1,* and *pin1-5 tar2-1* **(a-d),** and 35 days old plants of WT-L*er*, *pin1-5, pin1-5 taa1-1, and pin1-5 tar2-1* **(e-h).** Graphs are showing quantification of axillary meristems, siliques numbers, flower numbers and stem length respectively, in WT-L*er* (n=18), *pin1-5* (n=18), *pin1-5 taa1-1* (n=18), and *pin1-5 tar2-1* (n=18)

genotypes **(i-l).** Statistical test: One way ANOVA followed by Tukey's multiple comparisons test, different letters represent the statistically significant difference ($p<0.05$).

3.4.4. Auxin biosynthesis and transport both are essential for both shoot and root development

I found that *TAA1* and *TAR2* auxin biosynthesis genes mutant together with auxin transport mutant *pin1-5* display defect in stem growth and organogenesis. Both these phenotypes are distinct because of the different expression domains of both the genes and correlates well according to their spatiotemporal expression pattern in the shoot apex. This motivated me to investigate the triple mutant phenotype of *pin1-5 taa1-1 tar2-1*. Initially, I did not come across *pin1-5 taa1-1, tar2-1* triple mutant plants, however, lines carrying *pin1-5-/- taa1+/- tar2-/-* allelic combination when I followed closely. Among the segregating plants, I found plants lacking apparent SAM, in few cases, a mould of cells accumulated at the tip of SAM, moreover they did not produce true leaves in vegetative phase (Fig.3.13 a, c, d). The root phenotype of triple mutant was similar to mutant lacking auxin signalling such as *monopteros* (*mp* / *arf5* and *bodenlos/iaa12* (*bdl*) (Clark et al. 1993; Gälweiler et al. 1998) (Fig.3.13 b), suggesting that plants lacking biosynthesis and transport are compromised in their postembryonic growth and development. Taken together, my data suggest that SAM derived auxin and acropetal transport of auxin mediated by PIN1 through epidermal cell layer plays a critical role not only in organogenesis but also in SAM patterning.

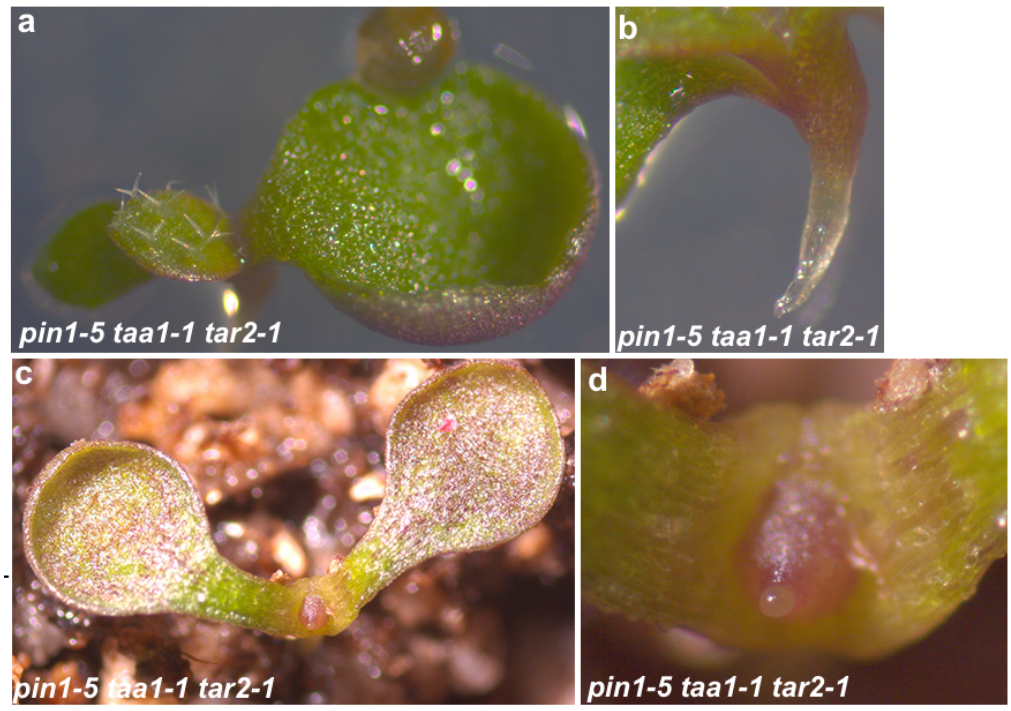

Figure 3.13. Auxin biosynthesis and auxin transport act together for lateral organ formation. Ten days old plant of the triple mutant of *pin1-5-/- taa1-1 -/- tar2-1 -/-* plants, growth is arrested at two cotyledon stage **(a),** and defect in root growth **(b)**, 3-weeks old plant of *pin1-5-/- taa1-/- tar2-1 -/-* shows dome-shaped structure at the tip and lateral organ formation is completely abolished **(c, d).**

3.4.5. Auxin signalling control the transition of stem cell progenitors into differentiating cells in PZ

In the previous section, I have shown that mutant plants lacking auxin transport and biosynthesis do not make lateral organs and show SAM patterning defects. *pin1-5 taa1-1 tar2-1* triple mutant plants lacked both lateral organs and functional SAM, therefore, I decided to investigate whether CZ and RM cells identity is maintained in the affected plants. To characterize this phenotype further, I carried out in-situ hybridization studies on the tissue sections of *taa1 tar2* and *pin1 taa1 tar2* mutant plants. I choose *CLV3* and *WUS* genes to investigate the identity of CZ and RM, respectively, in these plants. A closer examination of *CLV3* and *WUS* expression pattern in *taa1 tar2* and *pin1 taa1* and *tar2* SAM revealed that the *pin1 taa1 tar2* triple mutant plants have an enlarged *CLV3* expression domain compared to

taa1 tar2 double mutant and Col-0 (Fig.3.14 c, f, i). *WUS* expression was detected in Col-0 and *taa1 tar2* plants, but its expression was not detected in the *pin1 taa1 tar2* triple mutant plant SAM (Fig.3.14 b, e, h), suggesting that high expression of *CLV3* in the triple mutant SAM represses *WUS* expression. Although, *CLV3* and *WUS* expression domains were slightly expanded both in *taa1 tar2* double mutant compared to control (Fig.3.14 a, c, e, f). The dramatic increase in the *CLV3* expression suggests that transient stem cells failed to differentiate into PZ cell types. Taken together with the CZ and RM marker gene expression patterns into account, I concluded that auxin signalling is not only vital for organogenesis, but it is also required to organize SAM into distinct functional zones. Stem cells have unique properties, they can maintain their effective number, but at the same time can supply cells for regeneration and new tissues formation. In the absence of differentiation, they accumulate at the tip of SAM, and as *WUS* expression became weaker due to its negative regulation via CLV3-CLV1 signalling cascade. The expansion of CZ in *pin1 taa1 tar2* triple mutant do not proceed beyond a point, suggesting that stem cell differentiation also compromised in the absence of auxin biosynthesis and transport, and thus, stem cells lose their ability to differentiate into distinct cell types.

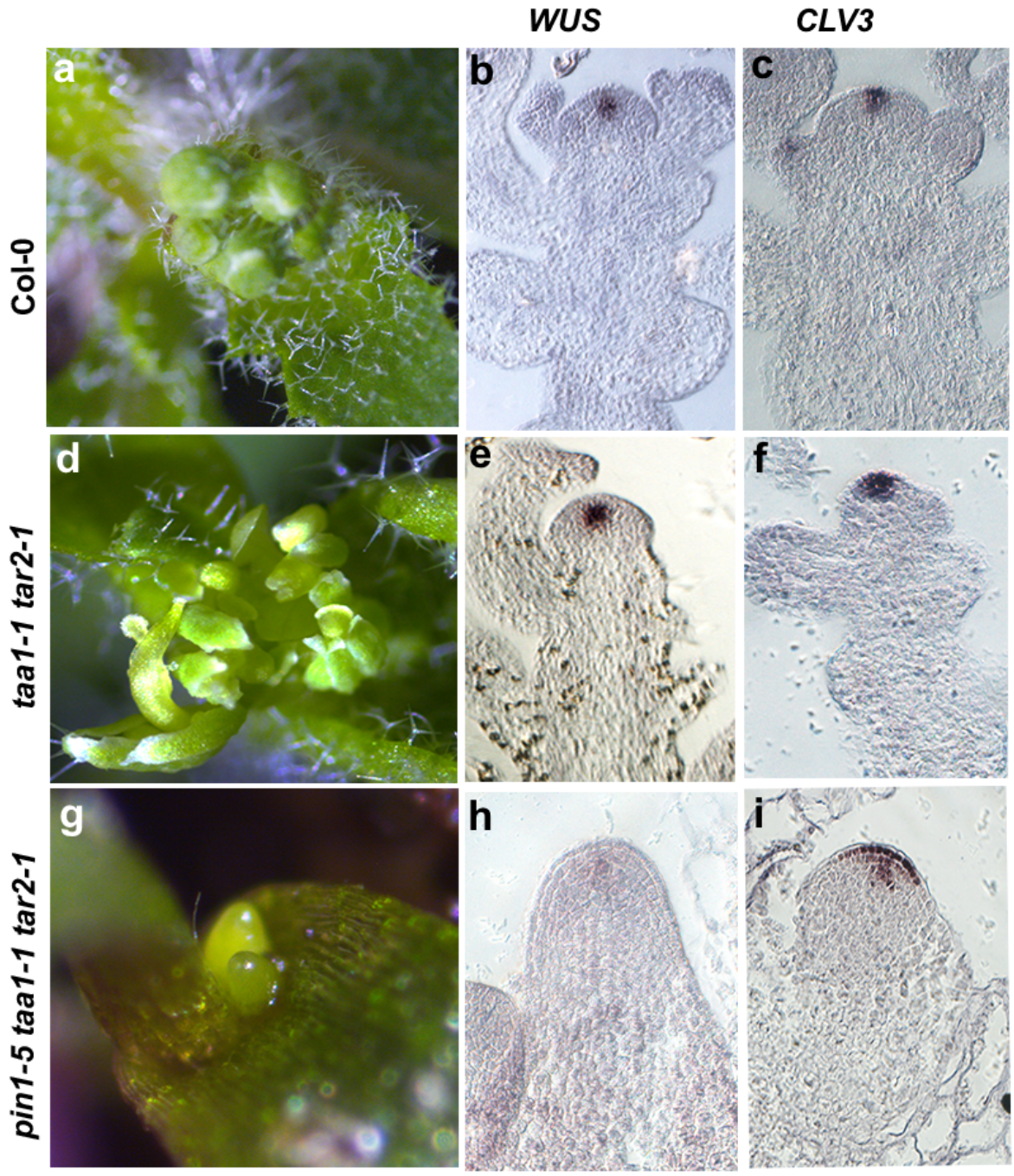

Figure 3.14. Inhibition of auxin biosynthesis and transport fail to maintain the functional SAM zonation.

Representative images of shoot apices of Col-0 plant **(a),** shoot apices of 4-weeks old *taa1-1 tar2-1* double mutant plant showing defects in SAM development **(d),** shoot apex of 3-weeks old *pin1-5 taa1-1 tar2-1* triple mutant plants showing pin-like structure at the tip **(g)**. From left to right representative images of *WUS, CLV3 mRNA* expression in Col-0 **(b, c),** *taa1-1 tar2-1* **(e, f),** and *pin1-5 taa1-1 tar2-1* **(h, i)** respectively by in situ hybridization.

3.4.6. Auxin signalling is required for organ boundary formation and shoot growth

It has been reported that auxin regulates different events related to primordia development. The positioning of the organ is specified by high auxin maxima but whether this would have an impact on organ boundary formation and outgrowth of the primordium. However, the genes involved in primordia patterning were mostly studied in the context of adaxial and abaxial patterning events. Since auxin is perceived both by canonical and non-canonical pathways. Hence it can regulate different aspects of plant growth in a context-dependent manner. Arabidopsis genome encodes 23 ARFs and 29 Aux/IAAs (Remington et al. 2004). Aux/IAAs act as repressors. In the presence of auxin, Aux/IAAs become unstable and allows auxin dependent regulation of gene expression via ARFs. (Tiwari, Wang, and Guilfoyle 2001).

Auxin regulates different aspects of primordium development by regulating the Aux/IAAs-ARF modules in different contexts. Some of these modules are best characterized in detail in lateral root development. For example, *LATERAL ORGAN BOUNDARIES DOMAINs (LBD)* (also known as *ASL* for *ASYMMETRIC LEAVES2-LIKE*) genes are regulated by ARF7/19-IAA14 module, linking the auxin signalling with activation of organ boundary genes (Okushima et al. 2007). In the shoot, the *LBD gene (ASYMMETRIC LEAVES2) AS2* prevent the expression of *SHOOTMERISTEMLESS* (*STM*) in the emerging organ primordium, and thus, allow the differentiation of lateral organ primordium. In order to investigate how auxin affects the organ patterning events in PZ. First, I analyzed the expression of *ARFs* by qRT-PCR in the *taa1-1 tar2-1*. RNA was isolated from 28 days Col-0 and *taa1-1 tar2-1* double mutant shoot apices. cDNA was synthesized from both the samples and used for qRT-PCR assays. The qRT-PCR data revealed that in *taa1 tar2* double mutant, *ARF3, ARF4,* and *ARF5* were consistently downregulated compared to Col-0 plants (Fig.3.15). *ARF5* is known to play an important role in flower development by directly activating the expression of *LEAFY* (Wu et al. 2015; Yamaguchi et al. 2013). Apart from *ARF5, ARF3* and *ARF4* are also highly

expressed in primordia founder cells (Vernoux et al. 2011). Recent studies have shown that *ARF3* and *ARF4* are directly involved in suppression of *STM*, while *ARF5* acts indirectly through the activation of *FIL* and represses the expression of *STM* to promote the organogenesis (Chung et al. 2019).

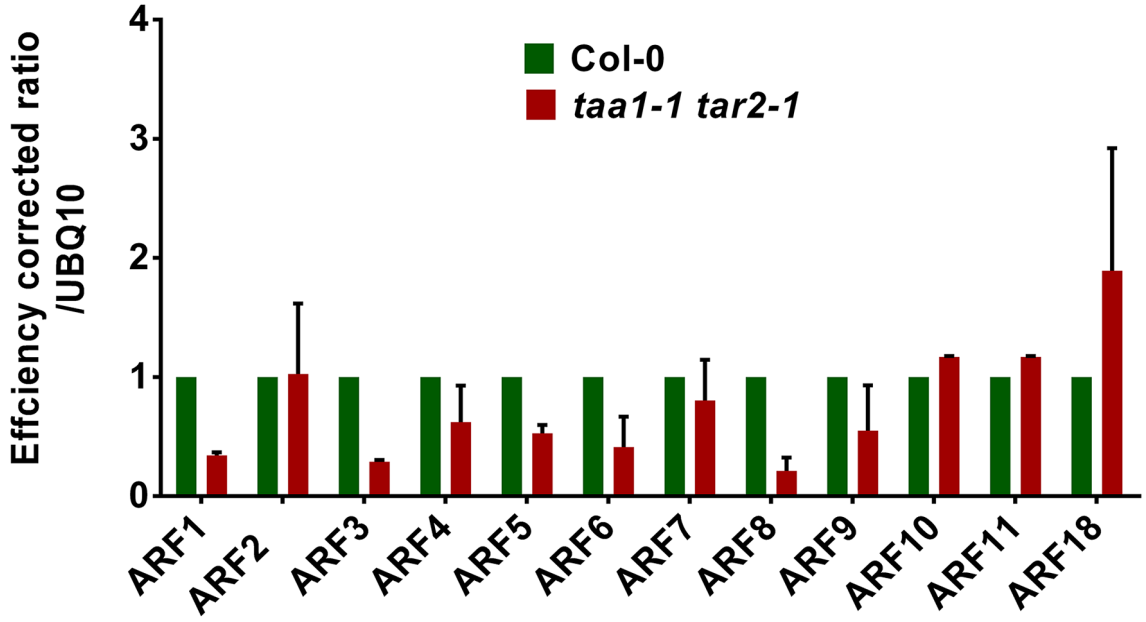

Figure 3.15. The expression of Auxin responsive factors (*ARFs*) get perturbed in auxin biosynthesis mutant.
qRT PCR results of activation and repression of *ARFs* in Col-0 and *taa1-1 tar2-1* double mutant plants. Data shown are the mean of two biological replicates.

I carried out the in-situ hybridization studies on selected *ARFs* (*ARF3 ARF4* and *ARF5*) in the shoot apices of *taa1 tar2* double mutant and *pin1 taa1 tar2* triple mutant plants. In *taa1 tar2* double mutant plants, the overall expression pattern of *ARF3, ARF4* and *ARF5* were maintained, but their expression levels have gone down significantly compared control Col-0 plants (Fig.3.16 a-c, d-f). Interestingly, in the *pin1 taa1 tar2* triple mutant plants expression of *ARF3, ARF4* and *ARF5* were abrogated completely (Fig.3.16 g-i). Taken together these results suggest that *taa1 tar2* mediated auxin biosynthesis, and *pin1* mediated polar transport are

required for the expression of *ARF3, ARF4,* and *ARF5* at the flank of the meristem to determine the fate of primordia founder cells, hence to promote the organogenesis.

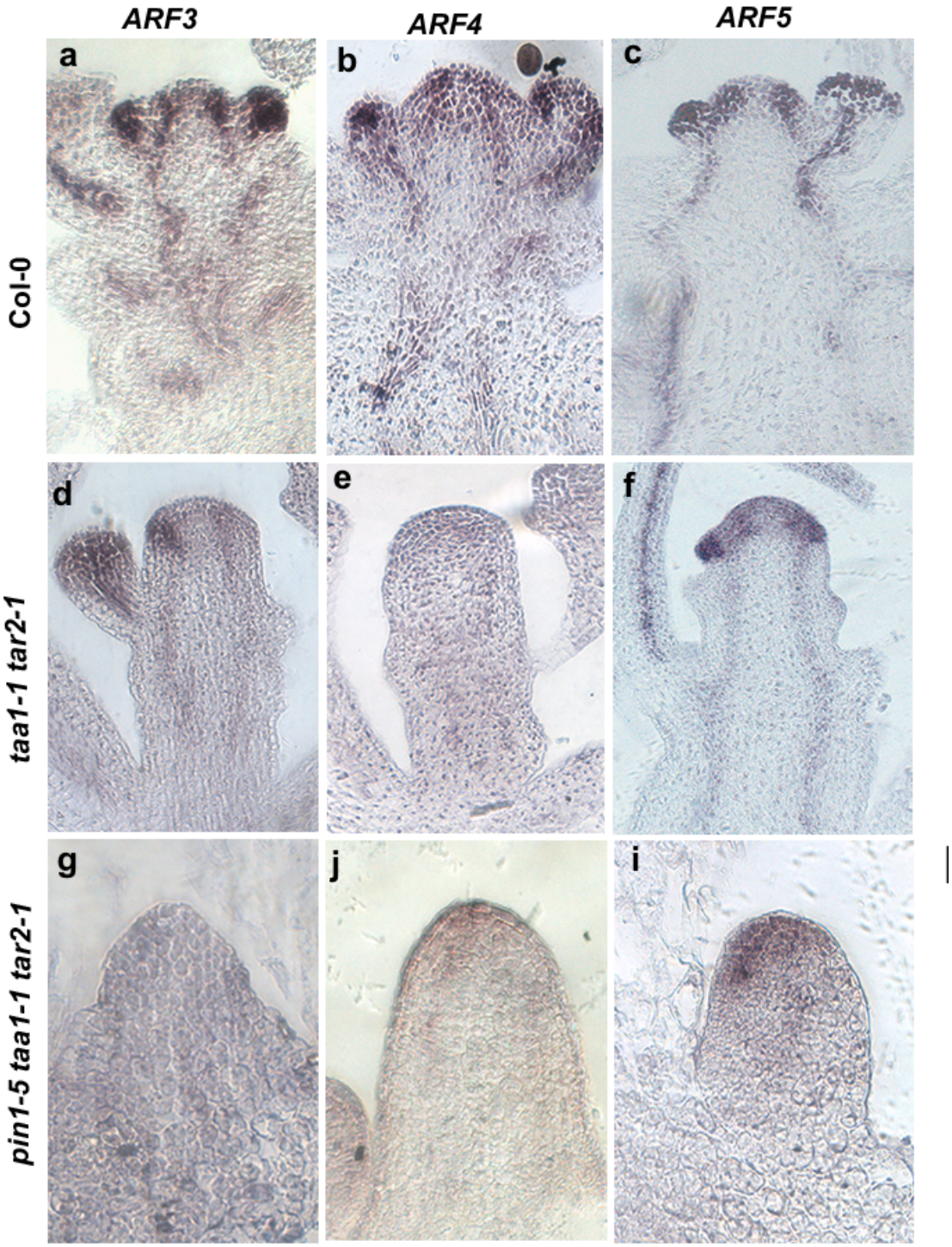

Figure 3.16. Auxin biosynthesis and transport both are essential for maintaining Auxin signalling in the shoot apex.
Representative images of mRNA expression *of ARF3, ARF4* and *ARF5* respectively, in Col-0 **(a-c)**, *taa1-1 tar2-1* **(d-f),** and *pin1-5 taa1-1 tar2-1* **(g-i)** by in-situ hybridisation.

Since *pin1 taa1 tar2* triple mutant plants have significantly reduced auxin levels in the system; therefore, stem cells completely failed to differentiate into PZ cell types. Organ boundaries were not demarcated in the *taa1 tar2* double and *pin1 taa1 tar2* triple mutant. Previous studies show *CUP SHAPED COTYLEDON (CUC1)* and (*CUC2)* are expressed in the boundary region of emerging floral and leaf primordia (Takada et al. 2001). The double mutant plant lacking *CUC1* and *CUC2* also show termination in the embryonic SAM and fused lateral organs (Mitsuhiro Aida et al. 1997; Takada et al. 2001). To understand whether the expression of organ boundary genes was compromised in the plants lacking auxin biosynthesis and transport. I investigated the expression pattern of *CUC1* gene in *taa1 tar2* double and *pin1 taa1 tar2* triple mutant by in-situ hybridization studies. CUC1 is a NAC domain protein. In situ hybridization studies on the shoot apices of *taa1 tar2* and *pin1 taa1 tar2* mutant plants revealed that expression of *CUC1* was depended on the auxin levels in the SAM. In the *taa1 tar2* double mutant plants expression of *CUC1* did not alter; however, its expression was not associated with an organ (Fig.3.17 a, b). Interestingly, in the *pin1-5 taa1-1 tar2-1* triple mutant, expression of *CUC1* was abolished completely in comparison to WT control (Fig.3.17 a, c), suggesting that organ formation requires auxin maxima generated through local auxin biosynthesis and transport. *CUC1* is clearly associated with organ boundaries and primordium formation in the SAM (Fig.3.17 a). Mutant plants lacking auxin biosynthesis and transport fail to form lateral organs and their patterning; hence they do not show organ growth indicating the role of auxin in organ boundary separation, lateral organ formation and proper SAM patterning.

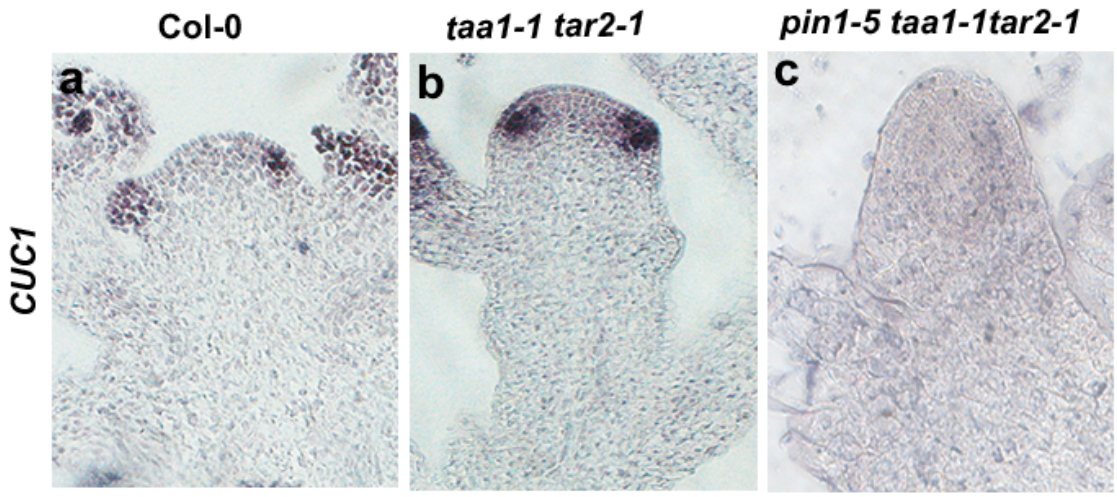

Figure 3. 17.Auxin biosynthesis and transport both are required for organ boundary separation
Representative images of mRNA expression of *CUC1*, in Col-0 **(a),** *taa1-1 tar2-1* **(b),** and *pin1-5 taa1-1 tar2-1* **(c)**.

3.5. Discussion

The phytohormone auxin is known to play a versatile role in different aspects of plant growth and development. In the SAM, auxin maxima lead to recruitment of PZ cells into organ primordia. Once a group of cells recruited to become founder cells, they form the primordia which outgrow from the SAM. Both the processes of organ formation and outgrowth are influenced by active auxin pool. I explored how *TAA1* and *TAR2* mediated auxin biosynthesis contributes the active auxin pool to the meristematic cells. Interestingly, spatiotemporal expression of *TAA1* and *TAR2* is complementary to each other. *TAR2* is expressed in the cells of PZ in adult SAM, follows the same expression pattern in the flower meristems, and in the globular and heart stage of the embryo, while *TAA1* is expressed in the L1 layer throughout the development. Both the genes are functionally redundant. Single mutant plants do not show phenotype, but the plant growth and development is severely compromised in *taa1 tar2* double mutant. Auxin can act like a morphogen where depending upon the dose developmental outcome such as cell-fate specification, division or differentiation can be achieved in different context rapidly. For the formation of lateral organ, auxin threshold need to be maintained in

the shoot apex. Here, I show that DII-Venus protein is stable in *taa1 tar2* double mutant plants So that, a low auxin zone established in SAM, thus plants lacking auxin biosynthesis show less auxin signalling, and as result plants show defects in lateral organ formation and patterning. Previous studies suggest that plants having a mutation in auxin transport protein PIN1, have defects in lateral organ formation and are completely sterile. In consideration with previous studies, my work also shows that mutants defective in auxin biosynthesis, show defects in lateral organ formation and patterning. The fact is that the triple mutant of *pin1 taa1 tar2* show a unique phenotype neither *pin1* nor *taa1* and *tar2-1* show that phenotype. In Arabidopsis, primordia founder cells require a critical threshold of auxin generated through local auxin biosynthesis and transport to differentiate into organs and carving out the boundaries from the SAM.

Stem cells in plants have the unique property that they can divide and differentiate into a specific tissue or cell type, and at the same time, they can self-renew themselves. Since the triple mutant *pin1-5 taa1- tar2-1* plants have more number of stem cells accumulated at the tip of meristems and less auxin signalling in these plants suggest that in the absences of auxin they failed to differentiate. This can very well define the triple mutant phenotype of *pin1 taa1 tar2* where, plant growth and development is arrested at the two cotyledon stage, plants failed to make lateral organs and a functional SAM with zonation.

Chapter 4

WUSCHEL negatively regulates auxin biosynthesis in stem cell niche

4.1. Introduction

In the course of evolution, plants got separated from animals ~ 1.5 billion years ago. Despite that stem cell systems, both in plants and animals, share functional similarities. Stem cells are housed in specialized microenvironments called niches, which send short-range signals from the organizer to maintain the fate of stem cells. Stem cells serve as an important precursor for the generation of new cell types, which form various tissues and organs. In angiosperm, stem cells are pluripotent in nature and are responsible for the growth and development of shoot and root meristems as well as the organs that derive from them. In adult mammals, stem cells are either multipotent or adult in nature, and are required in the postembryonic phase mainly for tissue repair and growth. However, in plant system stem cells are required for rest of the life of a plant to form new organs and mainly postembryonic growth, and are embedded in the meristematic tissue. In essence, plants and animals stem cells are; i) undifferentiated in nature, ii) able to differentiate into the specific cell and tissue types, iii) and has the ability to self-renew. Although at the genetic level so far RETINOBLASTOMA-RELATED (RBR) protein is known to play a role in the differentiation of stem cells both in plants and animals and thus, share the common function to maintain the stem cells (Kohno et al. 2016).

Stem cells in both plants and animal reside in the local microenvironment called niche. Stem cell niches are essential for stem cell self-renewal and maintenance. In the fruit fly *Drosophila,* studies identified the niche cells both for male and female germlines. In *Drosophila* male testis, a stromal niche cell holds germline stem cells (GSC) tightly via two adherens junctions, whereas in the female, the follicle cell stem cell (FSC) resides in an epidermal niche (de Cuevas and Matunis 2011). The FSC is anchored with a basement membrane and cap cells, which together acts as an organizer but they are surrounded by FSC daughter cell, escort cells and germline cyst cell without apparent contact (de Cuevas and Matunis 2011; Sahai-Hernandez, Castanieto, and Nystul 2012). From male niche, Unpaired (Upd) and Dpp are secreted as a

short-range signal (from hub cell or organizer) towards the GSC (de Cuevas and Matunis 2011 Affolter and Basler 2007). In the GSC, Upd and Dpp activate JAK-STAT and BMP signalling pathways and thereby maintain the GSC in undifferentiated state by repressing Bag of Marble (Bam) expression (Affolter and Basler 2007; Kawase et al. 2004; Shivdasani and Ingham 2003; Song et al. 2004). Similarly, localized expression of Upd from the terminal filament, escort stem cell and cap cells activate Bone morphogenetic protein (BMP) ligand, Hedgehog (Hh) and Wingless (Wg) expression in the ovarian niche to maintain the fate of FSCs (de Cuevas and Matunis 2011; Sahai-Hernandez et al. 2012).

Similar to the invertebrate system, stem cell niches in plants also send short-range signals for the maintenance of stem cells. Though, plants have different sets of molecules to regulate and maintain the pluripotency of stem cells. Genetic studies have revealed that the homeodomain transcription factor (TF) *SHOOTMERISTEMLESS* (*STM*) is required for stem cell proliferation. *STM* loss of function mutant displays premature termination of SAM (Barton and Poethig 1993; Long et al. 1996). In situ hybridization and promoter-reporter studies revealed that *STM* is expressed all over the shoot apex except at the sites of young incipient primordia, suggesting that differentiation of stem cells into organ primordium is antagonized by STM (Heisler et al. 2005; Jurkuta et al. 2009; Landrein et al. 2015). Interestingly, STM activates the expression of *ISOPENTENYL TRANSFERASES* (*IPT7*) genes. IPTs are involved in cytokinin (CK) biosynthesis, where they catalyze the first step of CK biosynthesis (Yanai et al. 2005). Despite showing termination of the shoot apex in the seedling stage, *STM* did not appear to be an important candidate gene for stem cell fate promotion and maintenance in Arabidopsis. Because its expression was broad, and it starts expressing in late heart or early torpedo stage embryo when the stem cells are already acquired their fate (Long and Barton 1998). Another homeodomain TF was identified based on the shoot termination phenotype by Thomas Laux and co-workers in 1996, and it was named *WUSCHEL* (*WUS*). *WUS* mRNA

expression studies on tissue sections of early embryo, seedling and inflorescence meristem revealed that its expression starts at 16-cells globular stage embryo, and persist throughout the postembryonic development in narrow domain below stem cells. Thus, the *WUS* expressing cells act as an organizer centre (OC) or niche and sends the signals to the overlying stem cells to maintain their fate (Laux et al. 1996; K. F. X. Mayer et al. 1998). Later studies have shown that WUS protein could move from OC through plasmodesmata to the overlying cells of the central zone (CZ) (Daum et al. 2014; Yadav, et al. 2011). In the cells of CZ, WUS directly binds to the-cis regulatory elements of *CLAVATA3* and activates its expression (Yadav, et al. 2011). WUS not only acts as an activator of *CLV3,* but it also represses several differentiation promoting TFs (Yadav et al. 2013). Thus, a single TF can act as an activator and repressor in a dose-dependent manner. WUS interacts with different affinities with a group of cis-elements in the *CLV3* promoter, and constitute a so-called cis-regulatory module. According to this model, lower concentration of WUS acts as an activator, and at the higher level, it acts as a repressor (Perales et al. 2016; Rodriguez et al. 2016). Loss of WUS activity leads to termination of meristem while *clv3* mutant has enlarged meristems, and enhanced WUS activity (Clark et al. 1995; Laux et al. 1996). WUS–CLV feedback system forms a self-correcting mechanism for maintaining a constant number of stem cells and SAM size (Schoof, Lenhard, Haecker, Klaus F.X. Mayer, et al. 2000).

To understand the role of WUS in regulating cell division pattern in meristem, previous studies have shown that transient knocked down of *WUS* leads to ectopic differentiation of stem cell daughters with a concomitant increase in DR5 responses in the PZ of SAM (Yadav et al. 2010). In the presence of WUS, stem cell daughters did not show differentiation, whereas in the absence of WUS, they will lose their fate.

This observation led us to hypothesize that auxin signalling somehow counteracts the dosages of WUS, and thus, a niche not only promote stem cell fate but also regulate the timely transition of stem cell daughters into differentiating cells.

In Chapter-3, I showed that *TAR2* mainly expressed in the PZ cell types where incipient organ primordia would emerge. A combination of biosynthesis and transport mediated by *TAA1/TAR2* and *PIN1* is required to achieve robustness in organ patterning. However, meristem patterning defects were apparent when *pin1 tar2* double mutant was combined with *taa1*, suggesting that auxin signalling not only important for organogenesis but it is also required for proper patterning of SAM into CZ, PZ and RM. In order to understand the role of WUS in stem cell differentiation, and how does it integrate both stem cell fate promotion and differentiation functions. I analyzed the gene expression data published by (Yadav et al. 2013). In this study, WUS protein was translationally fused with glucocorticoid receptor (GR) and expressed under 35S cauliflower mosaic virus promoter(35S CaMV), a ubiquitous promoter recognized by the transcriptional machinery in every plant cell. Plants carrying *35S::WUS-GR* transgene were treated with DEXAMETHASONE (DEX) and MOCK as well as with DEX/CYCLOHEXIMIDE (CYC) AND CYC alone, respectively. From the gene expression analysis, the authors concluded that *WUS* predominately acts as a repressor and key TFs involved in differentiation are repressed. However, this study also pointed out that genes involved in auxin biosynthesis and signalling are also perturbed by WUS. Therefore, I re-analyzed this data and found that not only key TFs but auxin biosynthesis, transport and signalling genes are also repressed by WUS. I validated the regulation of auxin biosynthesis genes by WUS in this chapter, and my finding suggests that WUS mediated regulation of auxin biosynthesis is critical for maintaining the stem cells fate and timely transition of stem cell daughters in the PZ of SAM.

4.2. Results

4.2.1. WUS represses auxin biosynthesis gene *TAR2* in the stem cell niche

In order to decouple the WUS mediated regulation of auxin responses and how it influences the differentiation of stem cell daughters in PZ. First, I analyzed the gene expression data published by (Yadav *et al.*, 2013). Analysis of WUS responsive transcriptome revealed that genes involved in auxin biosynthesis pathway, such as *ANTHRANILATE SYNTHASE ALPHA SUBUNIT (ASA1), TRYPTOPHAN SYNTHASE ALPHA1TSA1 AND TRYPTOPHAN AMINOTRANSFERASE RELATED2 (TAR2)* are downregulated.

To further validate the microarray data, I did qRT-PCR and tested *ASA1, TSA1* and *TAR2* expression in response to WUS induction. For this, *35S::WUS-GR* plants were grown in the plant growth chamber for 4-weeks and their inflorescence meristems were treated either with 10µm Dexamethasone (DEX) or kept as MOCK. MOCK plants were treated with 1% ethanol. To find out whether the selected genes are direct targets of WUS. In parallel, *35S::WUS-GR* plants were treated with 10µm DEX+10µm cycloheximide (CYC), and CYC alone was used as a control. CYC inhibits protein synthesis, and thus, secondary effects originating from WUS induction can be avoided. Shoot apices were collected 4 h after treatment for RNA isolation. cDNA was synthesized from an equal amount of RNA. The qRT-PCR experiment revealed that the expression of *ASA1, TSA1* and *TAR2* genes in the DEX treated plant was down-regulated. A consistent downregulation was not observed for *ASA1* and *TSA1* genes across the four biological replicates; however, for *TAR2,* I found consistent downregulation in DEX and DEX+CYC treated plants when compared to control, indicating that only *TAR2* is a potential target of WUS (Fig.4.1 a).

TRYPTOPHAN AMIOTRASNFERASE OF ARABIDOPSIS (TAA1), a founding member of this family also expressed in the shoot apex epidermis, although, I did not see any change in its expression in the microarray data. Since genetics work carried out in this thesis has shown that

TAA1 and *TAR2* both are required for shoot patterning. In order to understand whether *TAA1* is also regulated by WUS in SAM. I checked the expression of *TAA1* by qRT-PCR by treating *35S::WUS-GR* plants with 10µm DEX, control plants were treated with 1% ethanol. Similarly, *35S::WUS-GR* lines were subjected to DEX+CYC and CYC alone treatments. I found an increase in the *TAA1* transcript levels in DEX and DEX+CYC treated plants compared to MOCK and CYC alone plants (Fig.4.1, b). Four independent biological replicates were performed for both the experiments. *TAR2* was consistently downregulated across all the replicates; however, *TAA1* upregulation was not consistent.

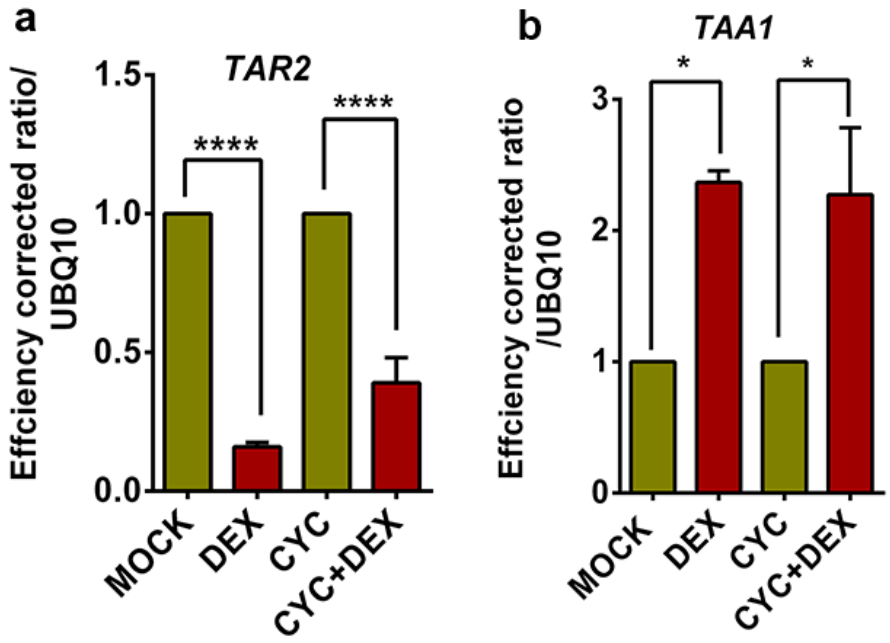

Figure 4.1. WUS represses *TAR2* in the SAM.
Graph shows qRT–PCR results of *TAR2* downregulation **(a),** and upregulation of *TAA1* **(b)** 4-weeks old *35S::WUS-GR* plants treated for 4 h with DEX (10µm) compared to control (MOCK, 1% ethanol); and DEX (10µm)+CYC (10µm) and CYC (10µm) alone. Error bars represent SEM. Asterisk marks represent statistically significant difference ($p < 0.005$).

It was not clear from the qRT-PCR results whether *TAA1* is regulated by WUS or not. I investigated the spatiotemporal regulation of *TAA1* and *TAR2* by in-situ hybridization assays. Shoot apices of 4-weeks old *35S::WUS-GR* plants were treated with 1% ethanol as MOCK and

10µm DEX for 24 h. Shoot apices from the control and treated plants were collected and fixed for *in-situ* hybridisation assays. Since *CLV3* has been shown a direct target of WUS by multiple approaches including live-imaging experiment. *35S::WUS-GR* plants carrying *pCLV3::mGFP-ER* reporter when treated with 10µm DEX a dramatic increase in the *CLV3* expression was observed (Yadav et al. 2010). In line with the previous observations, I did the in-situ hybridization for *CLV3, TAA1* and *TAR2* on the tissue sections of *35S::WUS-GR* shoot apices after fixing them post DEX and MOCK treatment. Antisense probe of *CLV3, TAA1* and *TAR2* was used. Analysis of in-situ images revealed expansion of *CLV3* domain in *35S::WUS-GR* plants treated with DEX compared to control (Fig 4.2 a, d). I did not see any change in *TAA1* expression in the epidermal cell layer in DEX treated plants compared to control (Fig.4.2 b, e), while there was a complete abrogation in the expression of *TAR2* in DEX treated shoot apices compared to MOCK (Fig.4.2 c, f). Taken together, the qRT-PCR and in-situ data, I concluded that spatiotemporal expression of *TAA1* is not regulated by WUS, whereas WUS negatively regulates *TAR2* expression in the shoot apex.

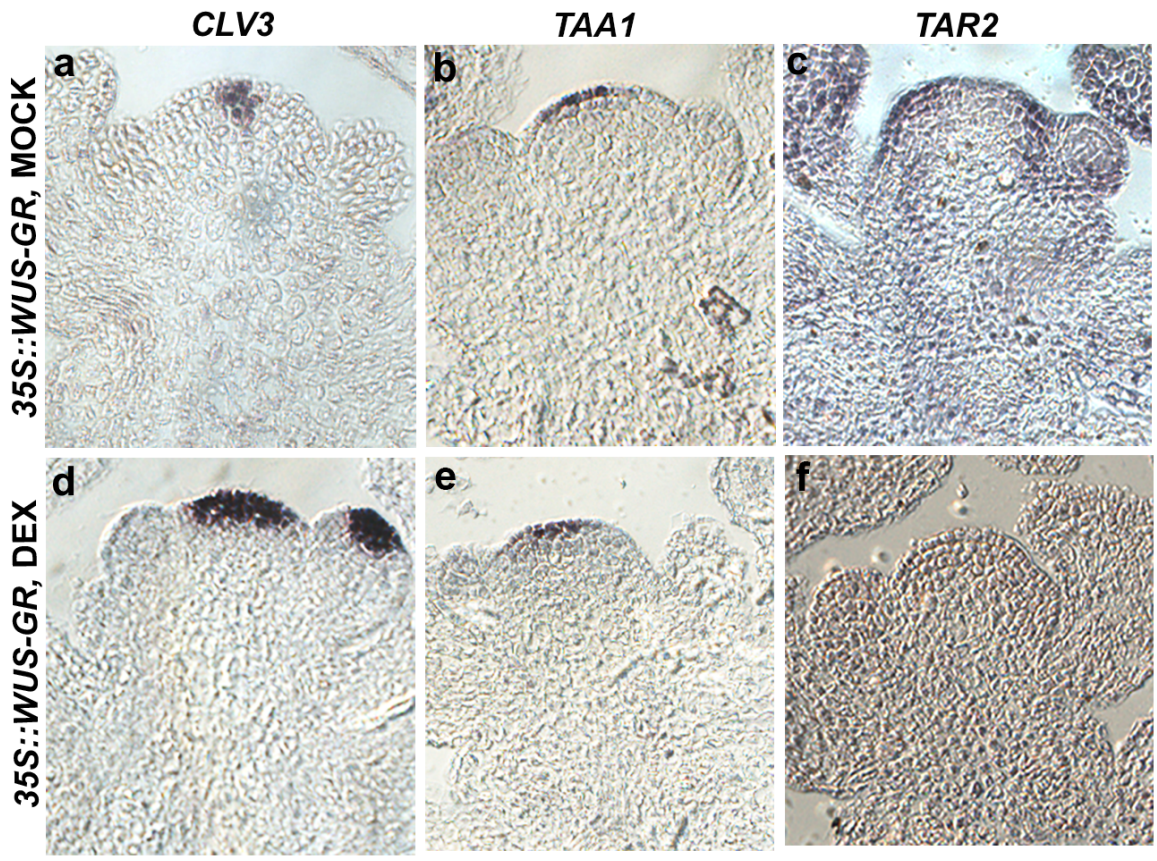

Figure 4.2. WUS represses *TAR2* expression in SAM.
In-situ images show expression of *CLV3, TAA1* and *TAR2* using antisense probe in *35S::WUS-GR* shoot apices treated with Mock (1% ethanol) (**a-c**) and, Dex (**d-f**) for 24 h.

4.2.2. *TAR2* is a direct target of WUS

Previously, I have shown that *TAR2* and *WUS* are the part of two complementary expression domains within the shoot. *TAR2* is highly expressed in the PZ and is negatively regulated by WUS in the cells of OC. How does WUS regulate *TAR2* expression in the OC? To get the molecular evidence for this regulation, I looked the literature and found that WUS binds to cis-regulatory elements containing TAAT core (Yadav, Perales, Gruel, Girke, et al. 2011; Yadav et al. 2013). First, I performed an *in-silico* analysis to search for the TAAT core containing WUS binding sites in *TAR2* promoter. I found two putative WUS binding sites in the *TAR2* promoter present at -897 and -2094 positions upstream of TSS. I designated -897 binding site (BS1) and -2094 binding site (BS2). Further, to test whether BS1 and BS2 are bonafide WUS

binding sites. I carried out electrophoretic mobility shift assay (EMSA). For this, I synthesized double-strand DNA using oligos spanning the BS1 and BS2 region of *TAR2* promoter (Fig.4.3 a) and then incubated with WUS protein *in vitro*. I found that the WUS protein-DNA complex containing BS1 and BS2 cis-regulatory elements showed a shift in the gel, suggesting that WUS interacts with BS1 and BS2 cis-regulatory elements (Fig.4.3 b). In parallel, mutations were introduced in the BS1 and BS2 cis-regulatory elements core to replace TAAT sequence with TGGT (Fig.4.3 a). When WUS protein-DNA complex containing the mutated BS1 or BS2 was run on the gel, I did not find a shift in the gel, suggesting that WUS interacts with BS1 and BS2 cis-regulatory elements via TAAT core in the *TAR2* promoter (Fig.4.3 b).

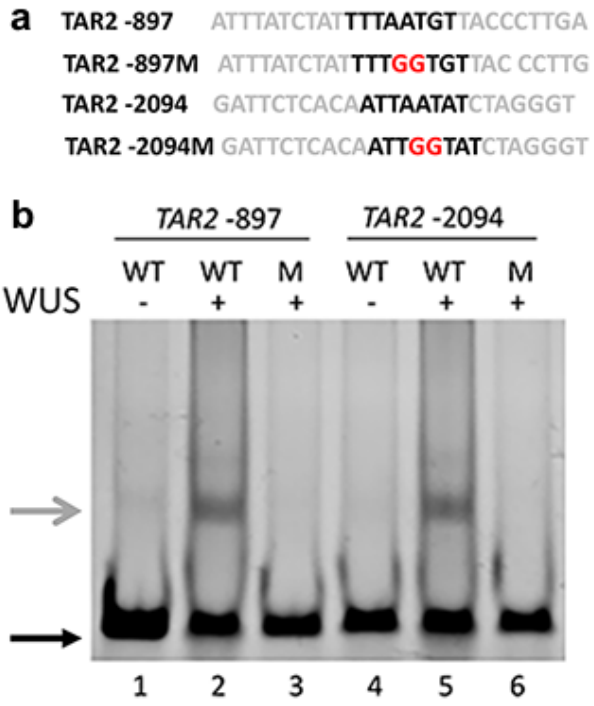

Figure 4. 3.WUS represses *TAR2* in the SAM.
The sequences of WT and mutant form of oligonucleotides **(a).** EMSA results show *TAR2* promoter cis-regulatory elements bound with WUS protein **(b)**. Lane 1 shows oligonucleotide having -897 (BS1) without WUS protein, Lane 2 shows oligonucleotide having -897 (BS1) with WUS protein, Lane 3 shows mutated -897 (BS1) with WUS protein and Lane 4 shows oligonucleotide having -2094 (BS2) without WUS protein, Lane 5 shows oligonucleotide having -2094 (BS2) with WUS protein, Lane 6 shows mutated -2094 (BS2) with WUS protein. Black arrow indicates free probes and grey arrow indicates probe bound to WUS protein **(b).**

4.2.3. *TAR2* expression is dynamic in SAM and inhibited by WUS in the emerging flower meristem

Previous in-situ studies have shown that *WUS* mRNA appears first in the stage-1 flower primordia, and remains there, although, expression of *CLV3* is still not visible in these primordia (K. F. X. Mayer et al. 1998). In order to find out whether *TAR2* expression is regulated in emerging flower primordia by WUS. I made a transcriptional reporter of *WUS.* For this, in *pWUS::SUB-myc-WUS* cassette, *SUB-myc* was replaced with *mCHERRY-NLS*. *pWUS::mCHERRY-NLS* lines were selected on kanamycin, and a homozygous line was crossed with *pTAR2::H2B-YFP* reporter line. In F2, I analyzed the expression of *TAR2*, *WUS* and *CLV3* in the SAM and emerging flower primordia. In the SAM supporting with previous studies, *WUS* and *CLV3* were expressed in CZ and OC, respectively, and *TAR2* expression was completely absent from the cells of CZ, where *pCLV3::mGFP-ER* reporter was active, and *TAR2* showed the high expression in the cells of PZ (Fig.4.4 a). Interestingly, when I analyzed flower meristems more closely, the *TAR2* expression was found all over the floral buttress and in the emerging organ primordia from P1 to P3, whereas in stage-1 flower (P4), it gets restricted towards the periphery of primordium when *pWUS::mCHERRY* appeared (Fig.4.4 b). In later stages, *TAR2* expression pushed on the flanks of the floral meristem as *WUS* expands from the centre towards the periphery and as the *WUS* expression became stronger in flowers. *TAR2* expression was confined towards the PZ (Fig.4.4 b). In parallel, when I looked at the WUS protein for which, I have used *pWUS::eGFP-WUS* line. This construct *pWUS::EGFP-WUS* was previously used to study the WUS protein movement (Yadav, Perales, Gruel, Yadav, et al. 2011). A close examination of shoot apices carrying *pWUS::eGFP-WUS* revealed that the presence of WUS protein in the centre of the flower primordium, Taken together these results suggest that functional WUS is able to repress *TAR2.* Perhaps this is the first example in the

stem cell niche, where a repressed target gene does not show its expression in the presence of an upstream regulator.

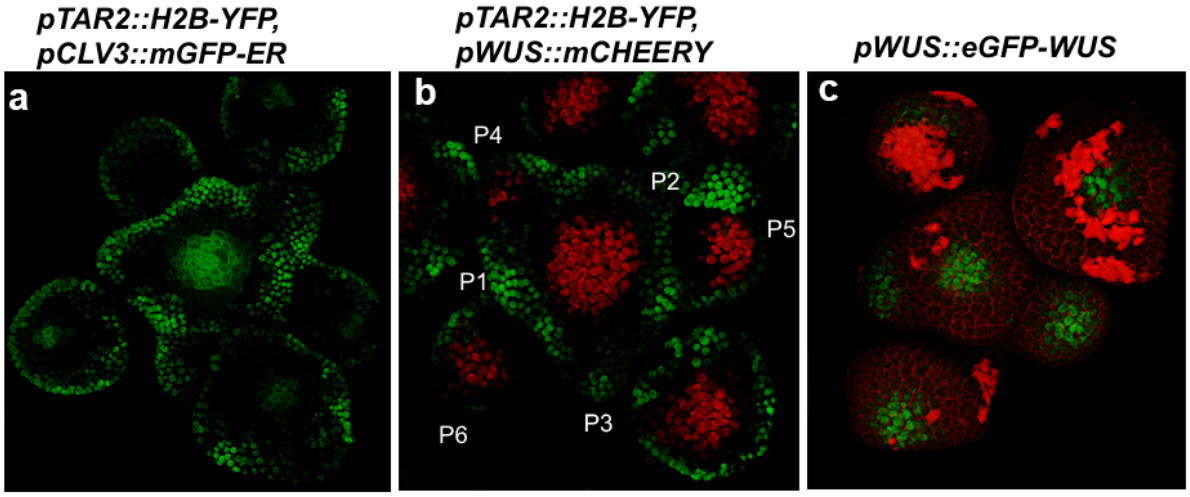

Figure 4.4. *TAR2, CLV3 and WUS* are expressed in complementary domains of SAM.
Three- dimensional (3D) reconstructed top views of shoot apex carrying *pTAR2::H2B-YFP* (green), *pCLV3::mGFP-ER* (green) reporters **(a).** Note: *pTAR2::H2B-YFP* is nuclear localized at the PZ and, *pCLV3::mGFP-ER* is endoplasmic reticulum (ER) localized in the centre of the meristem. Confocal images showing double transgenic of *pTAR2::H2B-YFP* (green) at the PZ and *pWUS::mCHERRY* in the cells of OC (red) **(b).** Representative confocal image of *pWUS::eGFP-WUS* (green), cell outlines are stained with PI (red) **(c).**

4.2.4. WUS loss of function results in *TAR2* mis-expression in SAM

To, further investigate WUS mediated *TAR2* repression in the SAM. I investigated *TAR2* expression pattern in *WUS* loss of function background. Since in *wus-1* (a strong allele of WUS loss of function) mutant the shoot meristem and floral meristem terminate at the two cotyledon stage, so, it was very difficult to spot the *pTAR2::H2B-YFP* expression in the terminated shoot apex. To overcome this technical issue, I used a hypomorphic *wus-7* allele. *wus-7* was identified in an EMS screen by Thomas Laux group, and they showed *wus-7* mutant has a missense mutation in the DNA binding domain, makes WUS protein to a limited extent functional in its ability to exert regulation of target genes. Therefore, *wus-7* plants make partially functional

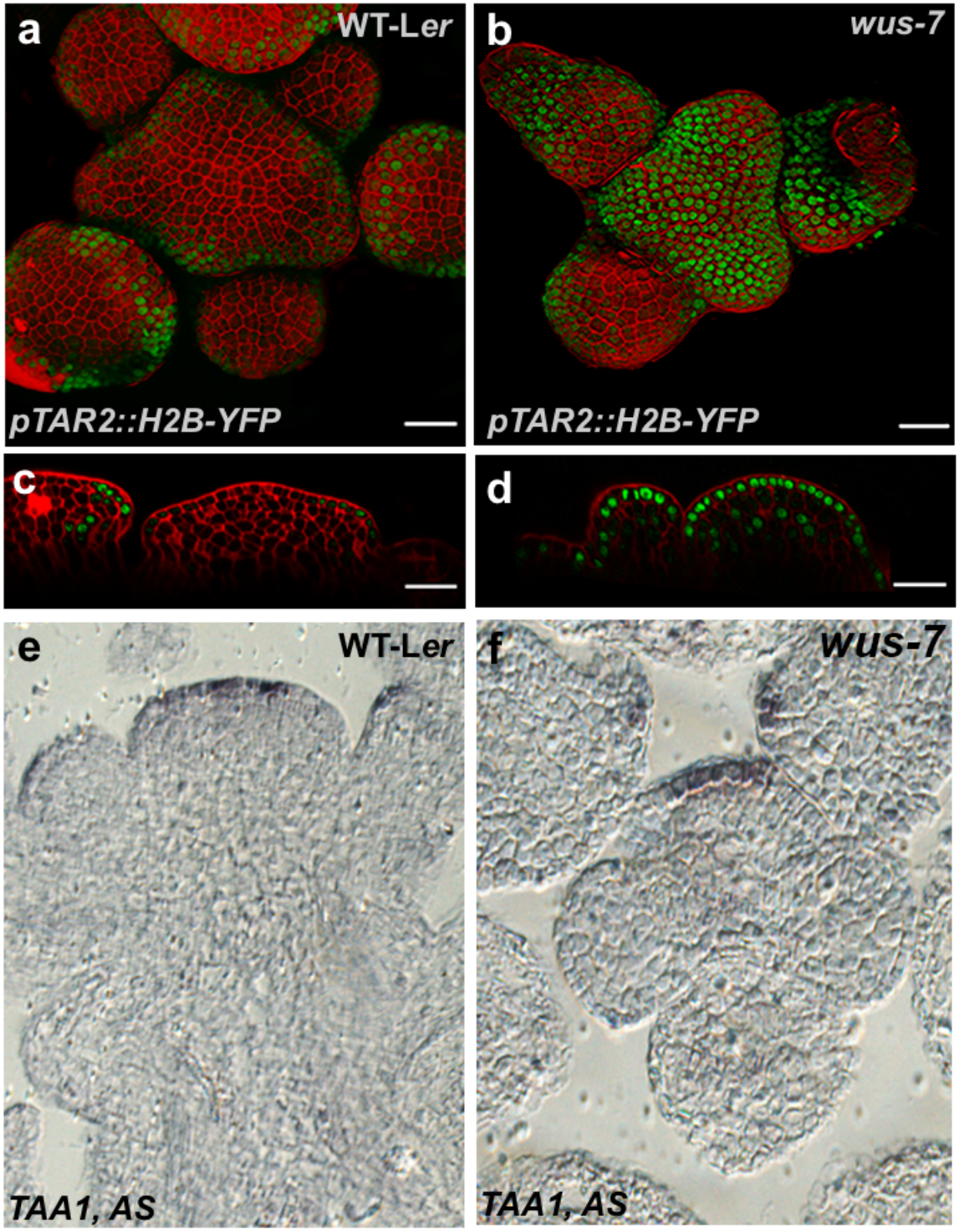

Figure 4.5. *WUS* regulates *TAR2* expression in SAM.
3D reconstructed confocal images show *pTAR2::H2B-YFP* expression in WT-L*er* top view **(a),** and in *wus-7* mutant **(b),** side views of the same images are shown in **(c),** and **(d)** respectively. Cell outlines are stained with PI. Representative in-situ images of *TAA1* mRNA expression in the epidermal cell layer of 4- weeks old WT-L*er* **(a)**, and *wus-7* mutant SAM **(b)** respectively. Scale bars: 20µm.

SAM and also produce more flowers, with few floral organs (Graf et al. 2010; Laux et al. 1996). In lab condition, I also observed *wus-7* plants make more number of flowers, without carpels, and were completely sterile. In order to understand WUS mediate *TAR2* regulation in *planta*. I made a cross between *wus-7*+/- and *pTAR2::H2B-YFP* reporter line originally generated in WT-L*er*. F1 plants were grown, and seeds were collected. Progeny of four independent plants of F1 were screened in the F2 generation. In F2, *wus-7*-/- plants expressing *pTAR2::H2B-YFP* were identified based on the flower phenotype and analyzed for *TAR2* expression by confocal microscopy. Parallelly the segregating WT-L*er* looking plants were also checked for *pTAR2::H2B-YFP* expression. In WT-L*er* looking plants, *pTAR2::H2B-YFP* expression was restricted to PZ (Fig.4.5 a, c), however, in the *wus-7*-/-, its expression expanded dramatically towards the CZ and RM cell types (Fig.4.5 b, d). Although, *pTAR2::H2B-YFP* reporter showed mis-expression in *wus-7* all over the SAM (Fig.4.5 b, d)). In the epidermal cell layer, its expression was uniform whereas in the inner cell layers its expression was sporadic, suggesting that in *wus-7* the protein might be able to repress *TAR2* in the inner cell layer due to higher dosages of WUS in these cells (Fig.4.5 b, d). In parallel, to validate further that *TAA1* is not regulated by WUS. I explored the mRNA expression pattern of *TAA1* by in situ hybridization in *wus-7* mutant and found that its expression pattern did not deviate from the epidermal cell layer (Fig.4.5 e, f). Here, my findings clearly suggest that WUS negatively regulates *TAR2* in the CZ and RM cell types, but *TAA1* expression is not controlled by it.

4.2.5. WUS prevents *TAR2* expression in stem cell daughters

In order to investigate the functional significance of BS1 and BS2 cis-regulatory elements on the regulation of *TAR2* by WUS. I deleted the BS1 and BS2 cis-regulatory elements from *TAR2* promoter. To do this, I generated three deletion promoter-reporter constructs for *TAR2,* in the first construct *pTAR2*(m1)::*H2B-YFP,* I deleted BS1(-897), in the second construct In *pTAR2*(m2)*::H2B-YFP* BS2(-2094) was deleted and in the third construct *pTAR2*(WUSΔ)*::TAR2* both the binding sites were deleted simultaneously. All three constructs were dipped in the WT-L*er*. For each construct, several independent lines were isolated to study the regulation of *TAR2.* Interestingly, the reporter having mutation in BS1 *pTAR2*(m1)::*H2B-YFP* showed mis-expression towards the stem cell daughters in the PZ of SAM compared to *pTAR2::H2B-YFP* (Fig.4.6 b, d). In BS2, I did not notice a discernible change in the expression of *TAR2* (Fig.4.6e,g). The double deletion construct *pTAR2*(ΔWUS)*::H2B-YFP* was also investigated, and it showed mis-expression towards the centre of the meristem, however, the pattern of *TAR2* expression in the *pTAR2*(ΔWUS)*::H2B-YFP* plants were more broader and uniform in comparison to *pTAR2::H2B-YFP* WT reporter (Fig.4.6 a, c, f, h). A comparison was made between the *pTAR2::H2B-YFP* WT reporter and *pTAR2*(ΔWUS)*::H2B-YFP* reporter for the cells expressing and those not expressing the reporter in PZ and towards the centre of the meristem. I observed an increase in the number of H2B-YFP positive cells in *pTAR2*(ΔWUS)*::H2B-YFP* plants compared to control *pTAR2::H2B-YFP* WT reporter (Fig.4.6 i), suggesting that the cumulative impact of BS1 and BS2 on the spatiotemporal regulation of *TAR2* was significant. Taken together, my data show that deletion of WUS binding cis-regulatory elements in the promoter of *TAR2* leads to the mis-expression of *TAR2* towards the centre of the meristem. This data clearly indicates that WUS binding via BS1 and BS2 is essential for WUS mediated *TAR2* repression in the CZ and OC.

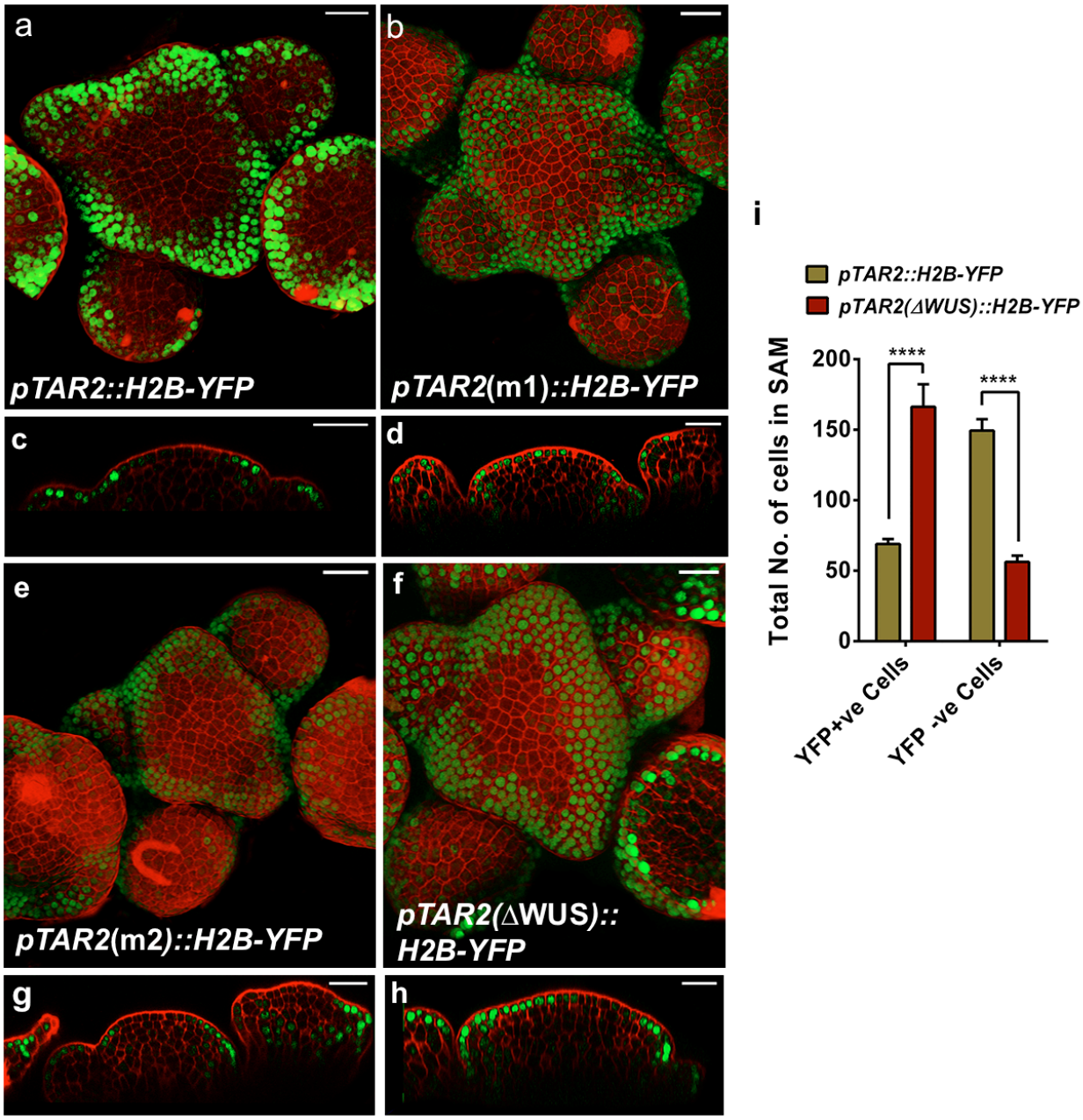

Figure 4.6. Deletion of WUS binding sites in the *TAR2* promoter leads to expansion of *TAR2* expression towards the centre of the meristem.

3D reconstructed top views of SAM of 4-weeks old WT-L*er* plants expressing *pTAR2::H2B-YFP* (green) **(a),** *pTAR2*(m1)*::H2B-YFP* (green) **(b)**, *pTAR2*(m2)*::H2B-YFP* (green) **(e),** and *pTAR2*(ΔWUS)*::H2B-YFP* (green) **(f)**. Side views of **(a), (b), (e)** and **(f)** are shown in **(c), (d), (g)** and **(h)** respectively. Cell outlines are stained with PI (red). Note: The expression of *pTAR2*(m1)*::H2B-YFP* and *pTAR2*(ΔWUS)*::H2B-YFP* reporter show broad expression in comparison to control. Graph **(i)** shows quantification of YFP+ve cells in *pTAR2::H2B-YFP* (n=10) and *pTAR2*(ΔWUS)*::H2B-YFP* (n=10). Error bars represent SEM. Asterisk marks represent statistically significant difference ($p < 0.005$). Scale bars: 20µm.

4.2.6. High dosage of WUS results in a decrease in *TAR2* transcription in PZ

In Arabidopsis, several studies suggest that WUS-CLV3 autoregulatory negative feedback loop is required to maintain a balance between stem cells proliferation and SAM size maintenance. WUS, a master regulator of stem cell fate promotion, activates *CLV3* in the CZ, and CLV3 is secreted as a small ligand in the SAM where it binds to CLV1 receptor. CLV3-CLV1 initiates the signalling, which restricts *WUS* expression in the niche cells (Brand et al. 2000; Schoof et al. 2000; Yadav, et al. 2011). For instance, *wus-1* do not produce true leaves and show the premature termination of SAM (Laux et al. 1996). The *clv3-2* alleles show stronger phenotype than *clv3-1,* and show an enlarged SAM due to over-proliferation of stem cells (Clark et al. 1995). The *clv3-2* mutant also has an elevated level of WUS in affected SAM. Here the questions arise; Are the cells expressing the elevated level of WUS in *clv3-2* mutant show expression of *TAR2*? How does *TAR2* expression respond to high dosages of WUS in the SAM? To answer these questions and to study the impact of elevated level of WUS on *TAR2* repression in the *clv3-2* mutant. I crossed the *clv3-2* mutant with *pTAR2::H2B-YFP* reporter line, and made reporter homozygous in the *clv3-2* genetic background following the F2 and F3 generations. I also obtained *pCLV3::H2B-YFP* and *pWUS::eGFP-WUS* reporter lines in the *clv3-2* mutant background from Dr Venu Reddy's lab (University of California Riverside). I did confocal imaging of plants expressing *pTAR2::H2B-YFP, pWUS::eGFP-WUS,* and *pCLV3::H2B-YFP* transgenes in the *clv3-2* mutant. Since the expression of *TAR2* was not visible due to overwhelming accumulation of stem cells in the main shoot, I focused on the emerging axillary inflorescences. Analysis of confocal images revealed very weak expression of *pTAR2::H2B-YFP* reporter at the flanks of the meristem in the *clv3-2* mutant and a complete absence of *TAR2* expression in the overproliferated stem cells, where *pCLV3::H2B-YFP* reporter was active (Fig.4.7 a, b, d, e). Similarly, niche cells and stem cells, which were

expressing eGFP-WUS protein was clearly devoid of *pTAR2::H2B-YFP* expression (Fig.4.7 c, f).

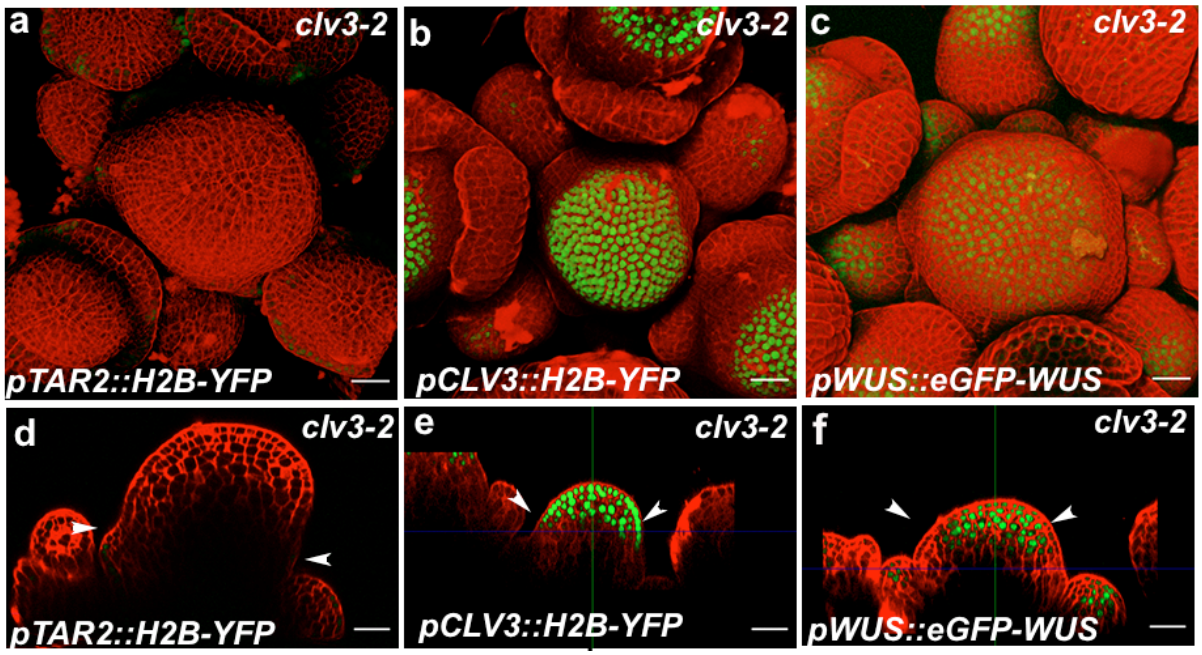

Figure 4. 7. *TAR2, WUS* and *CLV3* expression in the *clv3-2* mutant.
3D reconstructed confocal images show the expression of *pTAR2::H2B-YFP* (green) in the *clv3-2* axillary meristems (AM) top view **(a),** and side view **(d),** arrowheads indicate the restriction of *pTAR2* activity in the PZ **(d).** *pCLV3::H2B-YFP* (green) in the *clv3-2* mutant top view **(b)** and side view **(e)**, *pWUS::eGFP-WUS* (green) in *clv3-2* top view **(c),** and side view **(f).** Arrowheads indicate expression and localization of WUS in stem cells region. Cell outlines are stained with PI (red). Scale bars: 20µm

To further validate this data, I performed in-situ hybridization experiments using *TAR2* antisense and sense probe for control on WT-L*er* and *clv3-2* mutant shoot apices parallelly. A closer examination of in-situ images revealed that *TAR2* signal was present at the PZ in WT-L*er* shoot apices (Fig.4.8 a); however, *clv3-2* mutant plants were lacking expression of *TAR2* in the SAM (Fig.4.8 c). Moreover, very weak *TAR2* expression was spotted in the floral meristem (Fig.4.8 c), although I did not find any signal in the sense probe in WT-L*er* and *clv3-2* mutant (Fig.4.8 b, d). Taken together *pTAR2::H2B-YFP* reporter analysis and *TAR2* mRNA expression pattern in *clv3-2* provides another line of evidence that WUS represses *TAR2* in the stem cell niche to maintain a disparate distribution of auxin in CZ and PZ cell types.

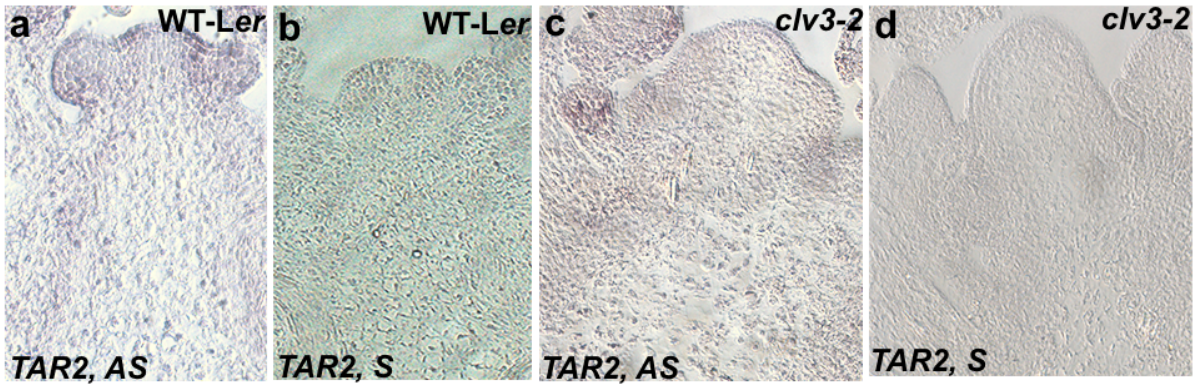

Figure 4.8. *TAR2* is repressed in the *clv3-2* mutant.
Representative in-situ images are showing the mRNA expression of *TAR2* using antisense and sense probe in WT-L*er* **(a, b)** and in the *clv3-2* mutant **(c, d),** respectively.

4.2.7. High dosages of WUS modulates auxin levels in the SAM

WUS mRNA is expressed in the cells of OC, and protein can move from the OC to CZ (Laux et al. 1996; Yadav, Perales, Gruel, Yadav, et al. 2011). In *clv3-2* high concentration of WUS results in decreased expression of *TAR2* at PZ of SAM. Here, I asked a question, how does higher dosage of WUS influences auxin input sensor and auxin level in the SAM? In order to find out this, I made a cross between *clv3-2* mutant and *R2D2*. R2D2 is a ratiometric reporter fused to domain II of AUX/IAA28 (DII), and expressed under *pRPS5A (pRPS5A::DII-n3×Venus* and *RPS5A-mDII-ntdTomato*) (Liao et al. 2015). Homozygous lines for *R2D2* reporter in the *clv3-2* were identified by following successive generation of segregating plants until F3. Since in this reporter, Domain-II of AUX/IAA fused with Venus is sensitive to auxin-mediated degradation. Wherever in the tissue high auxin availability is ensured, protein attached to DII will be degraded by auxin signalling and no signal will be detected, however when auxin availability is compromised DII-Venus will remain intact, and Venus fluorescence will be detected within the cells. Since this question is also important from the point of the relative contribution of *TAA1* and *TAR2* mediated auxin biosynthesis in SAM. In chapter 3, I have shown in the absence of auxin biosynthesis genes *TAA1* and *TAR2*, SAMs of *taa1-1 tar2-*

1 double mutant plants show more stable DII-Venus expression, indicating that auxin availability is less in these tissue in the absence of auxin biosynthesis. In consideration with this observation, in *clv3-2*, I found *TAR2* is weakly expressed. Since *clv3-2* mutant has high dosages of WUS, so, *TAR2* repression by WUS has increased in the *clv3-2* mutant. Here this question arises, does the *clv3-2* have less auxin availability in the shoot apex. In order to answer this question, I have analyzed the axillary meristems of *clv3-2* mutant with R2D2 reporter. Confocal Images of WT Col-0 and *clv3-2* plants carrying R2D2 reporter were captured with the same confocal settings, such as laser power, gain, pinhole etc in Leica SP8 confocal microscope. R2D2 expression pattern in *clv3-2* SAM was strikingly different from WT Col-0, DII-Venus expression was expanded throughout the CZ in the *clv3-2* mutant except in few cells where WUS is not present (Fig.4.9 a, b). In contrast to WT, DII-Venus is stable in the stem cell region of stage 3 and 4 floral primordia in the *clv3-2*, indicating that higher dosages of WUS perturbed the auxin threshold ratios between the CZ and PZ cells types and as a result, CZ boundary has also got shifted towards the flanks of the meristem and PZ has got reduced substantially. This finding is significant because there is a low auxin level and signalling environment in stem cell niche region compared to PZ in SAM, but it is only evident in the *clv3-2* mutant. Most of the auxin signalling detection system designed based on input and output sensors are not sensitive enough to read the disparate distribution of auxin signalling in the SAM except the boundary region. Taken together, I show that auxin level is perturbed by WUS in SAM in a dose-dependent manner. The higher concentration of WUS leads to reduce the amount of auxin levels in the SAM, and thus, reduction in auxin signalling despite having functional transport.

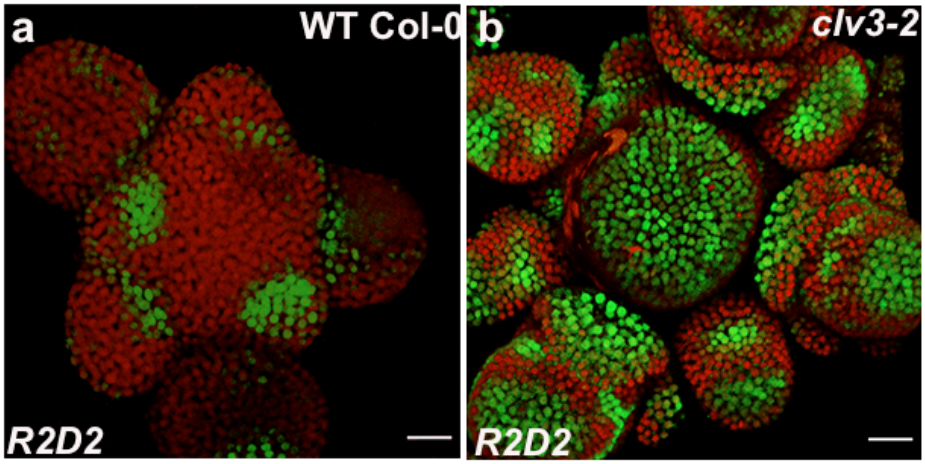

Figure 4.9. Auxin level (input) in the *clv3-2* mutant.
3D reconstructed top views of SAMs expressing R2D2 reporter in WT Col-0 **(a)** and *clv3-2* mutant **(b).** Scale bars: 20µm

4.2.8. Mis-expression of *TAR2* reduces SAM size and plant growth

At molecular level negative regulation of *TAR2* is critical to maintain low auxin level in stem cells niche. Data presented in the previous section showed deletion of WUS binding sites in *TAR2* promoter results in the mis-expression of *TAR2* reporter in the stem cell daughters, which are recruited into organ primordia at the flanks of the meristem, now start showing the expression of the reporter gene. The next question comes here; Is it going to affect the relative size of SAM or relative ratios of CZ and PZ cell numbers because the increased availability of auxin will bring the differentiation program closer to the daughters of stem cells. To investigate these possibilities, I made two constructs. One with WT promoter *pTAR2::TAR2*, and another where both the WUS bindings sites (-897, -2094) were deleted *pTAR2*(ΔWUS*)::TAR2*, these constructs were introduced in WT-L*er* background. Details of cloning and selection of transgenic lines are described in Chapter 2. Lines were made homozygous for the *pTAR2::TAR2* and *pTAR2*(ΔWUS)*::TAR2* transgenes, respectively, by following parent until T3 generation. Thirty days old SAMs, carrying *pTAR2::TAR2* and *pTAR2*(ΔWUS)*::TAR2,* were stained with PI and imaged using confocal microscopy to see the impact of deletion of

WUS binding sites on the shoot apex. Confocal images from *pTAR2::TAR2* and *pTAR2*(ΔWUS)*::TAR2* SAMs were analyzed using Morphograph X software. This analysis revealed that the size of the SAM is reduced in plants expressing *pTAR2*(ΔWUS)*::TAR2* in comparison *pTAR2::TAR2* (Fig.4.10 a, e). I identified close to ~70% plant lines for *pTAR2(*ΔWUS)*::TAR2* in which the growth of the plastochron was slower compared to their WT counterpart (*pTAR2::TAR2*) (Fig.4.10 i, j).

Again, to see the consequences of WUS binding site deletion on the stem cells domain. I used the *pCLV3::mGFP-ER* reporter line, which was already available in the lab. I have made two more constructs *pTAR2::TAR2* and *pTAR2*(ΔWUS)*::TAR2*, in *pMDC32* vector backbone (details of cloning is given in chapter 2). The same construct *pTAR2::TAR2* was used to rescue the double mutant phenotype of *taa-1 tar2-1* in chapter 3. Both the construct *pTAR2::TAR2* and *pTAR2*(ΔWUS)*::TAR2* were dipped in *pCLV3::mGFP-ER* reporter. Twenty-one independent lines were selected on hygromycin for each construct and, confocal images were captured using Leica SP8 confocal microscope. *CLV3* positive cells were counted in the L1 layer using FIJI software for both *pTAR2::TAR2* and *pTAR2*(ΔWUS)*::TAR2* constructs. A closer examination of confocal images and quantification of data revealed a significant decrease in the number of *CLV3* positive cells in the *pTAR2(ΔWUS)::TAR2* SAMs compared to *pTAR2::TAR2* shoot apices (Fig.4.10 c, d, g, h, l).

Thus, the plants carrying *pTAR2*(ΔWUS)*::TAR2* showed reduced plastochron growth, SAM size and less number of stem cells in comparison to the plants carrying *pTAR2::TAR2* transgene. Next, I asked; Are the *pTAR2*(ΔWUS*)::TAR2* plants showing phenotypes due to *TAR2* mis-expression in the centre of the meristem? To confirm this, plants carrying *pTAR2::TAR2* and *pTAR2(*ΔWUS)*::TAR2* were fixed for in-situ hybridization assays, and

TAR2 expression was determined by applying *TAR2* antisense probe in the cross-sections of *pTAR2::TAR2* and *pTAR2(*ΔWUS*)::TAR2* shoot apices.

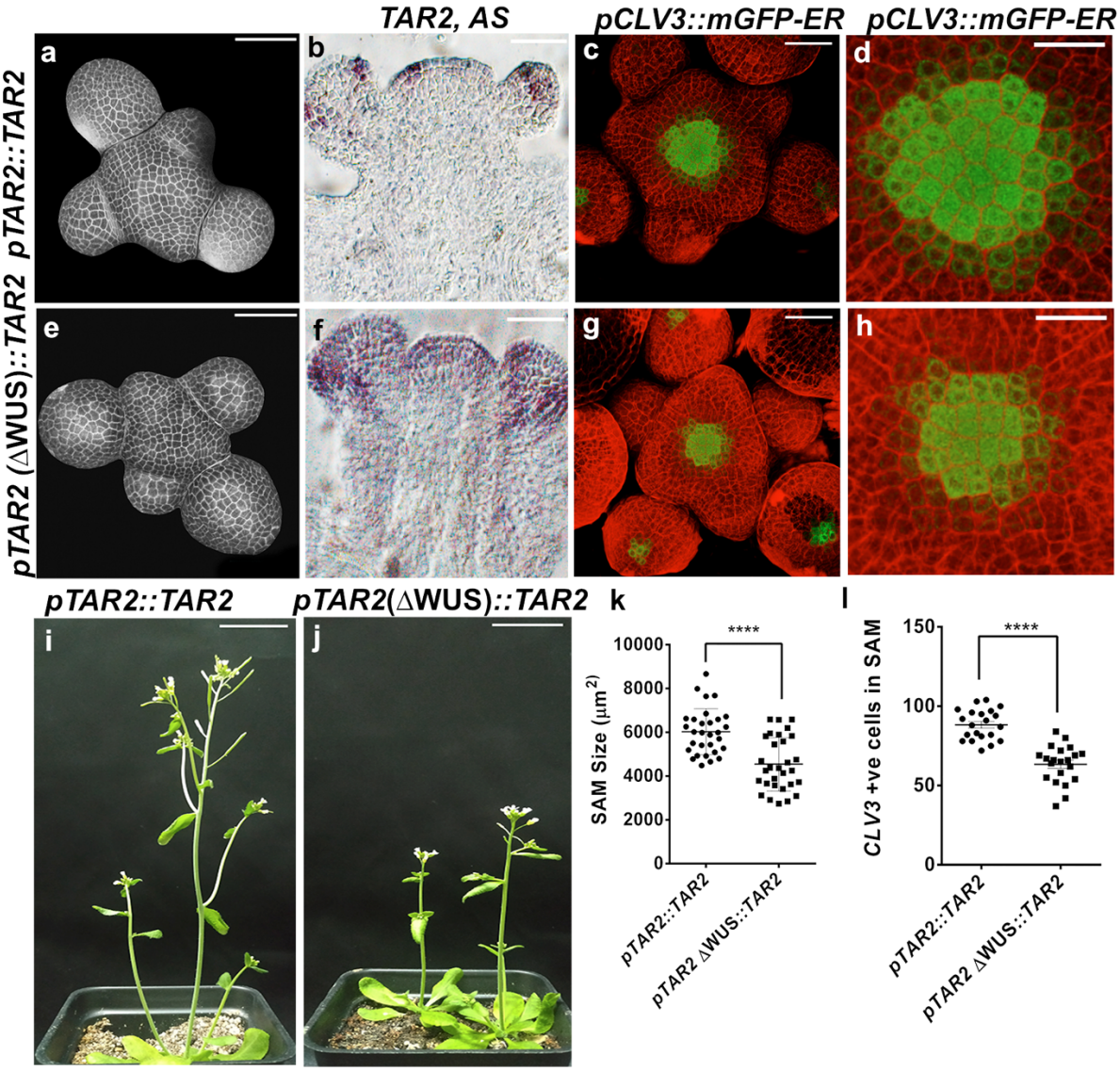

Figure 4.10. WUS binding sites in *TAR2* promoter are essential for SAM size and plant growth. 3D images of 4-weeks old shoot apices of plants carrying *pTAR2::TAR2* **(a),** and *pTAR2*(ΔWUS*)::TAR2* **(e).** Representative images of *in-situs* are showing longitudinal sections of shoot apices applied with *TAR2* antisense probe in *pTAR2::TAR2* line **(b),** and *pTAR2*(ΔWUS)*::TAR2* **(f),** transgenic lines. Similarly *pTAR2::TAR2* **(c, d),** and *pTAR2*(ΔWUS)*::TAR2* **(g, h)** constructs in *pCLV3::mGFP-ER* reporter background. Representative images of 4-weeks old Arabidopsis adult plants having *pTAR2::TAR2* **(i),** and *pTAR2*(ΔWUS)*::TAR2* **(j)** constructs were grown parallelly. Note; Plants carrying *pTAR2*(ΔWUS)*::TAR2* show slower growth compared to *pTAR2::TAR2*. Dot plot **(h)** represents SAM size measurement in *pTAR2::TAR2* (n=30) and *pTAR2*(ΔWUS)*::TAR2* (n=30) lines. Dot plot **(i),** represents the quantification of *CLV3* positive cells in *pTAR2::TAR2* (n=21) and *pTAR2*(ΔWUS)*::TAR2* (n=21). Statistical test: Student t-test. Asterisk marks represent a statistically significant difference ($p < 0.005$). Scale bars:50µm.

Here, in the cross-sections also SAM size found to be reduced in *pTAR2(*ΔWUS*)::TAR2* as compare to *pTAR2::TAR2* plants Fig.4.10 (b, f), parallelly analysis of *in-situ* images also revealed *TAR2* expression pattern similar to WT-L*er* in *pTAR2::TAR2* shoot apices, however, in *pTAR2(*ΔWUS*)::TAR2* shoot apices, I observed broader expression of *TAR2* towards the centre of the meristem (Fig.4.10 b, f). Taken together these results suggest that WUS mediated *TAR2* repression is required to maintain a minimum threshold of auxin in stem cells niche to maintain the stem cells fate and SAM size, hence to maintain the plant growth and development.

4.2.9. Ectopic expression of *TAR2* is detrimental for stem cells

Based on the *TAR2* mis-expression, I hypothesized that higher levels of auxin in CZ would be detrimental for stem cell fate maintenance. In the stem cell niche, higher CK levels promote WUS expression, but it is not clear whether high auxin would be detrimental for stem cell fate. In the stem cells niche, a dynamic regulation between WUS and auxin is critical for maintaining the stem cells fate and for their timely transition into the transit amplifying cells and later on for differentiation. It has been described in chapter 3 of this thesis, auxin biosynthesis gene *TAR2* is highly expressed in the PZ, but it is completely absent from the centre of the meristem. In the centre of meristem WUS mediated repression of *TAR2* keeping its level of expression low. However, at the PZ where cells are undergoing for differentiation, *TAR2* is highly expressed. *TAR2* mediated auxin biosynthesis and PIN1 mediated auxin transport together promotes progenitor cell differentiation.

Next, I asked; how do the stem cells will respond to high auxin? In order to test this hypothesis, I over-expressed *TAR2* under three heterologous promoters in WT-L*er* Arabidopsis. In the first experiment, I choose *35S* promoter and isolated (n=21) T1 lines. In the T1 generation, none of the *35S::TAR2* plants showed phenotype. However, in the T2 generation, when the

same lines were put again on the MS plates, 11/21 lines showed premature termination of the shoot apex

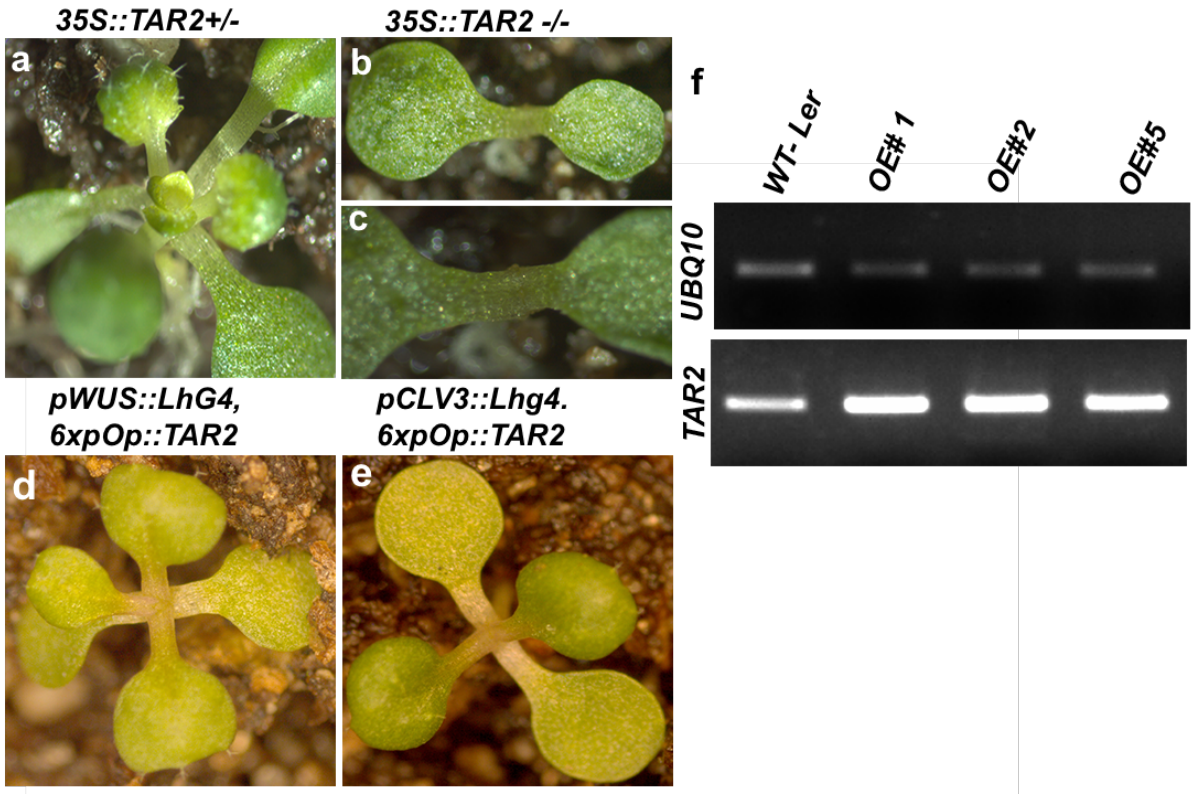

Figure 4.11.Ectopic expression of *TAR2* leads to termination of SAM
Twelve days old *35S::TAR2* +/- plants **(a)**, when the same plants were put in T2, they show termination of SAM **(b, c)**. Ectopic overexpression of *TAR2* in *CLV3* and *WUS* domain **(d, e)**. Semiquantitative RT-PCR experiment showing elevated levels of *TAR2* mRNA in three independent *35S::TAR2* lines in WT-L*er* **(f)**. *UBQ10* has been used as an internal control.

(Fig.4.11 a-c). Semiquantitative RT-PCR experiments revealed that lines having elevated expression levels of *TAR2* transcript were clearly terminated shoot apex (Fig. 4.11 f). This data also suggests that beyond a threshold, auxin levels in SAM can trigger termination of the shoot. To understand the role of auxin more discretely in the stem cell niche, I used the two-component system for the remaining two experiments. For this, I used previously characterized *pCLV3::LhG4* and *pWUS::LhG4* driver lines. *TAR2* was cloned behind *6xpOP* promoter to make as operator lines. *pCLV3::LhG4* and *pWUS::LhG4* driver lines were transformed with *6xpOP::TAR2* construct, and several independent T1 lines were selected on gentamycin. T1

plants carrying *pCLV3::LhG4 x 6xpOP::TAR2* made 3-4 true leaves before shoot termination (n=48) (Fig 4.11 d). In contrast, T1 plants carrying *pWUS::LhG4 x 6xpOP::TAR2* made only two true leaves (n=40) (Fig.4.11 e). Taken together, these results suggest overexpression of *TAR2* in both stem cells and niche cells is detrimental for stem cell fate promotion and their maintenance. Interestingly, *pWUS* is activated prior to *pCLV3* in embryogenesis, and this might have resulted in the later delayed termination of the shoot, suggesting that shoot stem cell niches are highly sensitive to high auxin levels and it directly influences their functioning.

4.3. Discussion

Previous studies have shown that WUS acts as a bifunctional transcription factor (Ikeda, Mitsuda and Ohme-Takagi, 2009). It contains the N-terminal DNA binding domain, which is also known as homeodomain, and a C-terminal domain. The C-terminal domain of WUS can be divided into three distinct motifs, (i) an acidic motif, (ii) an EAR motif and (iii) a WUS-BOX (Kieffer et al. 2006). EAR motif is known to function as a repressive motif, and it is conserved in plants (Ohta et al. 2001). WUS binds to the promoters of several differentiation promoting transcription factors like *KANADI1* (*KAN1*), *KANADI2* (*KAN2*), *ASYMMETRIC LEAVES2* (*AS2*), *YABBY3* (*YAB3*) and represses their expression (Yadav et al. 2013). It also interacts directly with the promoter of *CLV3* and activates its transcription (Yadav, Perales, Gruel, Girke, et al. 2011). On the other hand, WUS also binds with the cis-regulatory elements present in the second intron of *AGAMOUS* (*AG*) and activates *AG* transcription in the floral meristem (Lohmann et al. 2001). The common feature among the best characterized cis-regulatory elements of WUS is the presence of a TAAT core. It has been shown perturbation in the TAAT core leads to complete abrogation in WUS binding to the cis-regulatory elements (Lohmann et al. 2001; Yadav et al. 2013; Yadav, Perales, Gruel, Girke, et al. 2011). In the present study, I have identified *TAR2* as a new target of WUS. *TAR2* is involved in auxin biosynthesis, and expressed in the cells of the PZ and have the expression pattern

complementary to *WUS*. Since *WUS* is expressed in cells of OC and *TAR2* is in the cells of PZ. *TAR2* expression is completely devoid from OC and CZ cells.

The phytohormone auxin is known to play a versatile role in different aspects of plant growth and development. In the SAM, auxin maxima lead to recruitment of PZ cells into organ primordia. Once a group of the cells recruited to become founder cells, they form the primordia which outgrow from the SAM. Both the processes of organ formation and outgrowth are influenced by active auxin pool. Despite having genetic evidence based on the WUS-CLV feedback loop, which takes care of stem cell homeostasis and SAM size in plants, very little is known how stem cells enter into differentiation pathways. We lack the knowledge of how precisely stem cells self-renewal and differentiation is regulated. This work provides insight and a mechanism by which stem cells activity is maintained in the CZ and about the niche cells maintenance. Auxin levels in CZ and niche cells are precisely gated by WUS to prevent premature differentiation of stem cell daughters into organs. In the centre of the meristem and niche cells, repression of *TAR2* by WUS is essential to maintain stem cell fate. I show this repression by qRT-PCR and *in-situs* in 35S::*WUS-GR* after DEX induction

Next, *TAR2* was found a direct target of WUS, EMSA results show the direct interaction of WUS protein with BS1 and BS2 in *TAR2* promoter. Even during the specification of stem cells in the flower meristem *TAR2* appears first, later on as WUS expression gets activated. *TAR2* gets depleted from those cells and restricts its activity towards the PZ in flower meristem. Here, again I show the repression is critical and regulated that in *wus-7* mutant because of mutation in DNA binding domain, the direct binding of WUS with *TAR2* got abrogated and resulted in *TAR2* expression all over the shoot apex, and a similar pattern was also observed in the flower primordia. This data provides the one more strong line of evidence to prove WUS mediated *TAR2* repression is essential to maintain *TAR2* expression and auxin biosynthesis at the PZ. Deletion in binding sites results in misexpression *TAR2* reporter in the CZ and deletion of WUS

binding also have an impact on shoot size, stem cells number and plant growth and development. In conclusion, besides *WUS-CLV3* autoregulatory feedback loop, regulation of auxin biosynthesis and auxin responses by *WUS* could be one more mechanism, by which stem cells can maintain their fate and number in the shoot apex.

Chapter 5
Bibliography

Adamowski, Maciek and Jiři Friml. 2015. "PIN-Dependent Auxin Transport: Action, Regulation, and Evolution." Plant Cell 27(1):20–32.

Affolter, Markus and Konrad Basler. 2007. "The Decapentaplegic Morphogen Gradient: From Pattern Formation to Growth Regulation." *Nature Reviews Genetics* 8(9):663–74.

Aguilar-Gurrieri, Carmen, Amédé Larabi, Vinesh Vinayachandran, Nisha A. Patel, Kuangyu Yen, Rohit Reja, Ima-O Ebong, Guy Schoehn, Carol V Robinson, B. Franklin Pugh, and Daniel Panne. 2016. "Structural Evidence for Nap1-dependent H2A–H2B Deposition and Nucleosome Assembly." *The EMBO Journal* 35(13):1465–82.

Aida, M, T. Ishida, H. Fukaki, H. Fujisawa, and M. Tasaka. 1997. "Genes Involved in Organ Separation in Arabidopsis: An Analysis of the Cup-Shaped Cotyledon Mutant." *The Plant Cell* 9(6):841–57.

Aida, Mitsuhiro, Tetsuya Ishida, Hidehiro Fukaki, Hisao Fujisawa, and Masao Tasaka. 1997. "<1997_The Plant Cell …_Genes Lnvolved in Organ Separation in Arabidopsis An Analysis of the Cup-Shaped Cotyledon Mutant_Aida, Ishida, Fukaki.Pdf>." 9(June):841–57.

Bajguz, Andrzej and Alicja Piotrowska. 2009. "Conjugates of Auxin and Cytokinin." *Phytochemistry* 70(8):957–69.

Barlier, Isabelle, Mariusz Kowalczyk, Alan Marchant, Karin Ljung, Rishikesh Bhalerao, Malcolm Bennett, Goeran Sandberg, and Catherine Bellini. 2000. "The SUR2 Gene of Arabidopsis Thaliana Encodes the Cytochrome P450 CYP83B1, a Modulator of Auxin Homeostasis." *Proceedings of the National Academy of Sciences of the United States of America* 97(26):14819–24.

Barrero, José María, Rebeca González-Bayón, Juan Carlos Del Pozo, María Rosa Ponce, and José Luis Micol. 2007. "INCURVATA2 Encodes the Catalytic Subunit of DNA Polymerase α and Interacts with Genes Involved in Chromatin-Mediated Cellular Memory in Arabidopsis Thaliana." *Plant Cell* 19(9):2822–38.

Barton, M. K. and R. S. Poethig. 1993. "Formation of the Shoot Apical Meristem in Arabidopsis Thaliana: An Analysis of Development in the Wild Type and in the Shoot Meristemless Mutant." *Development* 119(3):823–31.

Bartrina, Isabel, Elisabeth Otto, Miroslav Strnad, Tomáš Werner, and Thomas Schmülling. 2011. "Cytokinin Regulates the Activity of Reproductive Meristems, Flower Organ Size, Ovule Formation, and Thus Seed Yield in Arabidopsis Thaliana." *Plant Cell* 23(1):69–80.

Benková, Eva, Marta Michniewicz, Michael Sauer, Thomas Teichmann, Daniela Seifertová, Gerd Jürgens, and Jiří Friml. 2003. "Local, Efflux-Dependent Auxin Gradients as a Common Module for Plant Organ Formation." *Cell* 115(5):591–602.

Benning, C. 1986. "Evidence Supporting a Model of Voltage-Dependent Uptake of Auxin into Cucurbita Vesicles." *Planta* 169(2):228–37.

Bhatia, Neha, Behruz Bozorg, André Larsson, Carolyn Ohno, Henrik Jönsson, and Marcus G. Heisler. 2016. "Auxin Acts through MONOPTEROS to Regulate Plant Cell Polarity and Pattern Phyllotaxis." *Current Biology*.

Bhatia, Neha, Behruz Bozorg, Carolyn Ohno, Marcus G. Heisler, Carolyn Ohno, and Henrik Jo. 2016. "Auxin Acts through MONOPTEROS to Regulate Plant Cell Polarity and Pattern Phyllotaxis Report Auxin Acts through MONOPTEROS to Regulate Plant Cell Polarity and Pattern Phyllotaxis." 3202–8.

Billou, Ikram, Jian Xu, Marjolein Wildwater, Viola Willemsen, Ivan Paponov, Jiří Frimi, Renze Heldstra, Mitsuhiro Aida, Klaus Palme, and Ben Scheres. 2005. "The PIN Auxin Efflux Facilitator Network Controls Growth and Patterning in Arabidopsis Roots." *Nature* 433(7021):39–44.

Blakeslee, Joshua J., Anindita Bandyopadhyay, Ran Lee Ok, Jozef Mravec, Boosaree Titapiwatanakun, Michael Sauer, Srinivas N. Makam, Yan Cheng, Rodolphe Bouchard, Jiří Adamec, Markus Geisler, Akitomo Nagashima, Tatsuya Sakai, Enrico Martinoia, Jiří Friml, Wendy Ann Peer, and Angus S. Murphy. 2007. "Interactions among PIN-FORMED and P-Glycoprotein Auxin Transporters in Arabidopsis." *Plant Cell* 19(1):131–47.

Bleckmann, Andrea, Stefanie Weidtkamp-peters, Claus A. M. Seidel, and A. B. Genetik. 2010. "Stem Cell Signaling in Arabidopsis Requires CRN to Localize CLV2 to the Plasma Membrane 1 [W][OA]." 152(January):166–76.

Boer, D. Roeland, Alejandra Freire-Rios, Willy A. M. Van Den Berg, Terrens Saaki, Iain W. Manfield, Stefan Kepinski, Irene López-Vidrieo, Jose Manuel Franco-Zorrilla, Sacco C. De Vries, Roberto Solano, Dolf Weijers, and Miquel Coll. 2014. "Structural Basis for DNA Binding Specificity by the Auxin-Dependent ARF Transcription Factors." *Cell* 156(3):577–89.

Brand, U, J. C. Fletcher, M. Hobe, E. M. Meyerowitz, and R. Simon. 2000. "Dependence of Stem Cell Fate in Arabidopsis on a Feedback Loop Regulated by CLV3 Activity." *Science (New York, N.Y.)* 289(5479):617–19.

Brand, Ulrike, Jennifer C. Fletcher, Martin Hobe, Elliot M. Meyerowitz, and Rüdiger Simon.

2000. “Dependence of Stem Cell Fate in Arabidopsis on a Feedback Loop Regulated by CLV3 Activity.” *Science* 289(5479):617–19.

Brand, Ulrike, Margit Grünewald, Martin Hobe, and Rüdiger Simon. 2002. “Regulation of CLV3 Expression by Two Homeobox Genes in Arabidopsis.” *Plant Physiology* 129(2):565–75.

Brumos, Javier, Linda M. Robles, Jeonga Yun, Thien C. Vu, Savannah Jackson, Jose M. Alonso, and Anna N. Stepanova. 2018. “Local Auxin Biosynthesis Is a Key Regulator of Plant Development.” *Developmental Cell* 47(3):306-318.e5.

Carles, Cristel C. and Jennifer C. Fletcher. 2003. “Shoot Apical Meristem Maintenance: The Art of a Dynamic Balance.” *Trends in Plant Science* 8(8):394–401.

Chen, Qingguo, Xinhua Dai, Henrique De-Paoli, Youfa Cheng, Yumiko Takebayashi, Hiroyuki Kasahara, Yuji Kamiya, and Yunde Zhao. 2014. “Auxin Overproduction in Shoots Cannot Rescue Auxin Deficiencies in Arabidopsis Roots.” *Plant and Cell Physiology* 55(6):1072–79.

Cheng, Y., X. Dai, and Y. Zhao. 2007. “Auxin Synthesized by the YUCCA Flavin Monooxygenases Is Essential for Embryogenesis and Leaf Formation in Arabidopsis.” *The Plant Cell Online* 19(8):2430–39.

Cheng, Youfa, Xinhua Dai, and Yunde Zhao. 2006. “Auxin Biosynthesis by the YUCCA Flavin Monooxygenases Controls the Formation of Floral Organs and Vascular Tissues in Arabidopsis.” *Genes and Development* 20(13):1790–99.

Cheng, Youfa, Xinhua Dai, and Yunde Zhao. 2007. “Auxin Synthesized by the YUCCA Flavin Monooxygenases Is Essential for Embryogenesis and Leaf Formation in Arabidopsis.” *Plant Cell* 19(8):2430–39.

Chung, Yuhee, Yang Zhu, Miin Feng Wu, Sara Simonini, Andre Kuhn, Alma Armenta-Medina, Run Jin, Lars Østergaard, C. Stewart Gillmor, and Doris Wagner. 2019. “Auxin Response Factors Promote Organogenesis by Chromatin-Mediated Repression of the Pluripotency Gene SHOOTMERISTEMLESS.” *Nature Communications* 10(1).

Clark, S. E., M. P. Running, and E. M. Meyerowitz. 1995. “CLAVATA3 Is a Specific Regulator of Shoot and Floral Meristem Development Affecting the Same Processes as CLAVATA1.” *Development* 121(7):2057–67.

Clark, Steven E., Mark P. Running, and Elliot M. Meyerowitz. 1993. “CLAVATA1 , a Regulator of Meristem and Flower Development in Arabidopsis.” 418:397–418.

Clark, Steven E., Robert W. Williams, and Elliot M. Meyerowitz. 1997. “The CLAVATA1 Gene Encodes a Putative Receptor Kinase That Controls Shoot and Floral Meristem Size in Arabidopsis.” 89:575–85.

Clough, Steven J. and Andrew F. Bent. 1998. “Floral Dip: A Simplified Method for Agrobacterium-Mediated Transformation of Arabidopsis Thaliana.” *Plant Journal* 16(6):735–43.

Cock, J. Mark and Sheila Mccormick. 2001. “A Large Family of Genes That Share Homology with CLAVATA3.”

Cohen, J. D. and R. S. Bandurski. 1982. “Chemistry and Physiology of the Bound Auxins.” *Annual Review of Plant Physiology* 33(1):403–30.

Cole, Melanie, John Chandler, Dolf Weijers, Bianca Jacobs, Petra Comelli, and Wolfgang Werr. 2009. “DORNRÖSCHEN Is a Direct Target of the Auxin Response Factor MONOPTEROS in the Arabidopsis Embryo.” *Development* 136(10):1643–51.

Comai, Luca and Tsune Kosuge. 2009. “Cloning and Characterization of IaaM , a Virulence Determinant of Pseudomonas Savastanoi Nlasmid Spended TpH Fsrm Eume.” 149(1):40–46.

de Cuevas, Margaret and Erika L. Matunis. 2011. “The Stem Cell Niche: Lessons from the Drosophila Testis.” *Development (Cambridge, England)* 138(14):2861–69.

Cui, Dayong, Jingbo Zhao, Yanjun Jing, Mingzhu Fan, Jing Liu, Zhicai Wang, Wei Xin, and Yuxin Hu. 2013. “The Arabidopsis IDD14, IDD15, and IDD16 Cooperatively Regulate Lateral Organ Morphogenesis and Gravitropism by Promoting Auxin Biosynthesis and Transport.” *PLoS Genetics* 9(9).

Cui, Yanwei, Chong Hu, Yafen Zhu, Kaili Cheng, Xiaonan Li, Zhuoyun Wei, Li Xue, Fang Lin, Hongyong Shi, Jing Yi, Suiwen Hou, Kai He, Jia Li, and Xiaoping Gou. 2018. “Cik Receptor Kinases Determine Cell Fate Specificatioduring Early Anther Development in Arabidopsis[Open].” *Plant Cell* 30(10):2383–2401.

Daum, Gabor, Anna Medzihradszky, Takuya Suzaki, and Jan U Lohmann. 2014. “A Mechanistic Framework for Noncell Autonomous Stem Cell Induction in Arabidopsis.” 2014(19).

Daum, Gabor, Anna Medzihradszky, Takuya Suzaki, and Jan U. Lohmann. 2014. “A Mechanistic Framework for Noncell Autonomous Stem Cell Induction in Arabidopsis.” *Proceedings of the National Academy of Sciences of the United States of America* 111(40):14619–24.

Delbarre, Alain, Philippe Muller, Viviane Imhoff, and Jean Guern. 1996. "Comparison of Mechanisms Controlling Uptake and Accumulation of 2,4-Dichlorophenoxy Acetic Acid, Naphthalene-1-Acetic Acid, and Indole-3-Acetic Acid in Suspension-Cultured Tobacco Cells." *Planta* 198(4):532–41.

Deyhle, Florian, Ananda Kumar Sarkar, Elise J. Tucker, and Thomas Laux. 2007. "WUSCHEL Regulates Cell Differentiation during Anther Development." 302:154–59.

DeYoung, Brody J., Kristen L. Bickle, Katherine J. Schrage, Paul Muskett, Kanu Patel, and Steven E. Clark. 2006. "The CLAVATA1-Related BAM1, BAM2 and BAM3 Receptor Kinase-like Proteins Are Required for Meristem Function in Arabidopsis." *Plant Journal* 45(1):1–16.

Deyoung, Brody J., Kristen L. Bickle, Katherine J. Schrage, Paul Muskett, Kanu Patel, Steven E. Clark, Ann Arbor, John Innes Centre, Stress Biology, and John Innes Centre. 2006. "The CLAVATA1-Related BAM1 , BAM2 and BAM3 Receptor Kinase-like Proteins Are Required for Meristem Function in Arabidopsis." 3:1–16.

Dharmasiri, Nihal, Sunethra Dharmasiri, and Mark Estelle. 2005. "The F-Box Protein TIR1 Is an Auxin Receptor." *Nature* 435(7041):441–45.

Dharmasiri, Nihal, Sunethra Dharmasiri, Dolf Weijers, Esther Lechner, Masashi Yamada, Lawrence Hobbie, Jasmin S. Ehrismann, Gerd Jürgens, and Mark Estelle. 2005. "Plant Development Is Regulated by a Family of Auxin Receptor F Box Proteins." *Developmental Cell* 9(1):109–19.

Ditengou, Franck Anicet, Dulceneia Gomes, Hugues Nziengui, Philip Kochersperger, Hanna Lasok, Violante Medeiros, Ivan A. Paponov, Szilvia Krisztina Nagy, Tímea Virág Nádai, Tamás Mészáros, Beáta Barnabás, Beata Izabela Ditengou, Katja Rapp, Linlin Qi, Xugang Li, Claude Becker, Chuanyou Li, Róbert Dóczi, and Klaus Palme. 2018. "Characterization of Auxin Transporter PIN6 Plasma Membrane Targeting Reveals a Function for PIN6 in Plant Bolting." *New Phytologist* 217(4):1610–24.

Elliott, R. C., A. S. Betzner, E. Huttner, M. P. Oakes, W. Q. Tucker, D. Gerentes, P. Perez, and D. R. Smyth. 1996. "AINTEGUMENTA, an APETALA2-like Gene of Arabidopsis with Pleiotropic Roles in Ovule Development and Floral Organ Growth." *The Plant Cell* 8(2):155 LP – 168.

Fàbregas, Norma, Pau Formosa-Jordan, Ana Confraria, Riccardo Siligato, Jose M. Alonso, Ranjan Swarup, Malcolm J. Bennett, Ari Pekka Mähönen, Ana I. Caño-Delgado, and Marta Ibañes. 2015. "Auxin Influx Carriers Control Vascular Patterning and Xylem Differentiation in Arabidopsis Thaliana." *PLoS Genetics* 11(4):1005296.

Ferreira, Fernando J. and Joseph J. Kieber. 2005. "Cytokinin Signaling." *Current Opinion in*

Plant Biology 8(5):518–25.

Fletcher, Jennifer C., Ulrike Brand, Mark P. Running, Rüdiger Simon, and Elliot M. Meyerowitz. 1999. "Signaling of Cell Fate Decisions by <Em>CLAVATA3</Em> in <Em>Arabidopsis</Em> Shoot Meristems." *Science* 283(5409):1911 LP – 1914.

Gallavotti, Andrea, Solmaz Barazesh, Simon Malcomber, Darren Hall, David Jackson, Robert J. Schmidt, and Paula McSteen. 2008. "Sparse Inflorescence1 Encodes a Monocot-Specific YUCCA-like Gene Required for Vegetative and Reproductive Development in Maize." *Proceedings of the National Academy of Sciences of the United States of America* 105(39):15196–201.

Gallois, Jean Luc, Fabiana R. Nora, Yukiko Mizukami, and Robert Sablowski. 2004. "WUSCHEL Induces Shoot Stem Cell Activity and Developmental Plasticity in the Root Meristem." *Genes and Development* 18(4):375–80.

Gälweiler, Leo, Changhui Guan, Andreas Müller, Ellen Wisman, Kurt Mendgen, Alexander Yephremov, and Klaus Palme. 1998. "Regulation of Polar Auxin Transport by AtPIN1 in Arabidopsis Vascular Tissue." *Science* 282(5397):2226–30.

Ganguly, Anindya, Minho Park, Mahipal Singh Kesawat, and Hyung Taeg Cho. 2014. "Functional Analysis of the Hydrophilic Loop in Intracellular Trafficking of Arabidopsis PIN-FORMED Proteins." *Plant Cell* 26(4):1570–85.

Garay-Arroyo, Adriana, Enrique Ortiz-Moreno, María De La Paz Sánchez, Angus S. Murphy, Berenice García-Ponce, Nayelli Marsch-Martínez, Stefan De Folter, Adriana Corvera-Poiré, Fabiola Jaimes-Miranda, Mario A. Pacheco-Escobedo, Joseph G. Dubrovsky, Soraya Pelaz, and Elena R. Álvarez-Buylla. 2013. "The MADS Transcription Factor XAL2/AGL14 Modulates Auxin Transport during Arabidopsis Root Development by Regulating PIN Expression." *EMBO Journal* 32(21):2884–95.

Geisler, Markus and Angus S. Murphy. 2006. "The ABC of Auxin Transport: The Role of p-Glycoproteins in Plant Development." *FEBS Letters* 580(4):1094–1102.

van Gelderen, Kasper, Chiakai Kang, Richard Paalman, Diederik Keuskamp, Scott Hayes, and Ronald Pierik. 2018. "Far-Red Light Detection in the Shoot Regulates Lateral Root Development through the HY5 Transcription Factor." *Plant Cell* 30(1):101–16.

Gordon, Sean P., Vijay S. Chickarmane, Carolyn Ohno, and Elliot M. Meyerowitz. 2009. "Multiple Feedback Loops through Cytokinin Signaling Control Stem Cell Number within the Arabidopsis Shoot Meristem." *Proceedings of the National Academy of Sciences of the United States of America* 106(38):16529–34.

Graf, Philipp, Alicja Dolzblasz, Tobias Würschum, Michael Lenhard, Ulrike Pfreundt, and Thomas Laux. 2010. "MGOUN1 Encodes an Arabidopsis Type IB DNA Topoisomerase Required in Stem Cell Regulation and to Maintain Developmentally Regulated Gene Silencing." *Plant Cell* 22(3):716–28.

Gruel, Jérémy, Benoit Landrein, Paul Tarr, Christoph Schuster, Yassin Refahi, Arun Sampathkumar, Olivier Hamant, Elliot M. Meyerowitz, and Henrik Jönsson. 2016. "An Epidermis-Driven Mechanism Positions and Scales Stem Cell Niches in Plants." *Science Advances* 2(1):22–24.

Guilfoyle, Tom J. and Gretchen Hagen. 2012. "Getting a Grasp on Domain III/IV Responsible for Auxin Response Factor–IAA Protein Interactions." *Plant Science* 190:82–88.

Guo, Yongfeng, Linqu Han, Matthew Hymes, Robert Denver, and Steven E. Clark. 2011. "NIH Public Access." 63(6):734–47.

Haga, Ken and Tatsuya Sakai. 2012. "PIN Auxin Efflux Carriers Are Necessary for Pulse-Induced but Not Continuous Light-Induced Phototropism in Arabidopsis." *Plant Physiology* 160(2):763–76.

Hagen, Gretchen and Tom Guilfoyle. 2002. "Auxin-Responsive Gene Expression: Genes, Promoters and Regulatory Factors." *Plant Molecular Biology* 49(3–4):373–85.

Han, Pei, Qing Li, and Yu-xian Zhu. 2008. "Mutation of Arabidopsis BARD1 Causes Meristem Defects by Failing to Confine WUSCHEL Expression to The." 20(June):1482–93.

He, Wenrong, Javier Brumos, Hongjiang Li, Yusi Ji, Meng Ke, Xinqi Gong, Qinglong Zeng, Wenyang Li, Xinyan Zhang, Fengying An, Xing Wen, Pengpeng Li, Jinfang Chu, Xiaohong Sun, Cunyu Yan, Nieng Yan, De Yu Xie, Natasha Raikhel, Zhenbiao Yang, Anna N. Stepanova, Jose M. Alonso, and Hongwei Guo. 2011. "A Small-Molecule Screen Identifies L-Kynurenine as a Competitive Inhibitor of TAA1/TAR Activity in Ethylene-Directed Auxin Biosynthesis and Root Growth in Arabidopsis." *Plant Cell* 23(11):3944–60.

Heisler, Marcus G., Carolyn Ohno, Pradeep Das, Patrick Sieber, Gonehal V. Reddy, Jeff A. Long, and Elliot M. Meyerowitz. 2005. "Patterns of Auxin Transport and Gene Expression during Primordium Development Revealed by Live Imaging of the Arabidopsis Inflorescence Meristem." *Current Biology* 15(21):1899–1911.

Heologis, A. Thanasios T. 1997. "Protein – Protein Interactions among the Aux TAA Proteins." 94(October):11786–91.

Heyl, Alexander and Thomas Schmülling. 2003. "Cytokinin Signal Perception and Transduction." *Current Opinion in Plant Biology* 6(5):480–88.

Hibara, Ken-ichiro, Md Rezaul Karim, Shinobu Takada, Ken-ichiro Taoka, Masahiko Furutani, Mitsuhiro Aida, and Masao Tasaka. 2006. "Arabidopsis CUP-SHAPED COTYLEDON3 Regulates Postembryonic Shoot Meristem and Organ Boundary Formation." *The Plant Cell* 18(11):2946–57.

Hofmann, Nancy R. 2011. "YUC and TAA1/TAR Proteins Function in the Same Pathway for Auxin Biosynthesis." *Plant Cell* 23(11):3869.

Hossain, Md Sanower and Zannat Urbi. 2016. "Effect of Naphthalene Acetic Acid on the Adventitious Rooting in Shoot Cuttings of Andrographis Paniculata (Burm.f.) Wall. Ex Nees: An Important Therapeutical Herb." *International Journal of Agronomy* 2016.

Hu, Chong, Yafen Zhu, Yanwei Cui, Kaili Cheng, Wan Liang, Zhuoyun Wei, Mingsong Zhu, Hongju Yin, Li Zeng, Ya Xiao, Minghui Lv, Jing Yi, Suiwen Hou, Kai He, Jia Li, and Xiaoping Gou. 2018. "A Group of Receptor Kinases Are Essential for CLAVATA Signalling to Maintain Stem Cell Homeostasis." *Nature Plants* 4(4):205–11.

Ikeda, Miho, Nobutaka Mitsuda, and Masaru Ohme-Takagi. 2009. "Arabidopsis Wuschel Is a Bifunctional Transcription Factor That Acts as a Repressor in Stem Cell Regulation and as an Activator in Floral Patterning." *Plant Cell* 21(11):3493–3505.

Jeong, Sangho, Amy E. Trotochaud, and Steven E. Clark. 1999. "The Arabidopsis CLAVATA2 Gene Encodes a Receptor-like Protein Required for the Stability of the CLAVATA1 Receptor-like Kinase." 11(October):1925–33.

Jönsson, Henrik, Marcus G. Heisler, Olivier Hamant, Pawel Krupinski, Magalie Uyttewaal, Carolyn Ohno, Jan Traas, and Elliot M. Meyerowitz. 2010. "Alignment between PIN1 Polarity and Microtubule Orientation in the Shoot Apical Meristem Reveals a Tight Coupling between Morphogenesis and Auxin Transport." *PLoS Biology* 8(10).

Jurkuta, Rebecca Joy, Nicholas J. Kaplinsky, Jennifer E. Spindel, and M. Kathryn Barton. 2009. "Partitioning the Apical Domain of the Arabidopsis Embryo Requires the BOBBER1 NudC Domain Protein." *Plant Cell* 21(7):1957–71.

Kakimoto, T. 2001. "Identification of Plant Cytokinin Biosynthetic Enzymes as Dimethylallyl Diphosphate:ATP/ADP Isopentenyltransferases." *Plant and Cell Physiology* 42(7):677–85.

Kakimoto, Tatsuo. 2003. "Perception and Signal Transduction of Cytokinins." *Annual Review of Plant Biology* 54:605–27.

Kang, Kiyoon, Young Soon Kim, Sangkyu Park, and Kyoungwhan Back. 2009. "Senescence-Induced Serotonin Biosynthesis and Its Role in Delaying Senescence in Rice Leaves."

Plant Physiology 150(3):1380–93.

Katano, Mana, Kazuki Takahashi, Tomonari Hirano, Yusuke Kazama, Tomoko Abe, Hirokazu Tsukaya, and Ali Ferjani. 2016. "Suppressor Screen and Phenotype Analyses Revealed an Emerging Role of the Monofunctional Peroxisomal Enoyl-CoA Hydratase 2 in Compensated Cell Enlargement." *Frontiers in Plant Science* 7(FEB2016):1–11.

Kawase, Eihachiro, Marco D. Wong, Bee C. Ding, and Ting Xie. 2004. "Gbb/Bmp Signaling Is Essential for Maintaining Germline Stem Cells and for Repressing Bam Transcription in the Drosophila Testis." *Development* 131(6):1365–75.

Kaya, Hidetaka, Kei-ichi Shibahara, Ken-ichiro Taoka, Masaki Iwabuchi, Bruce Stillman, and Takashi Araki. 2001. "FASCIATA Genes for Chromatin Assembly Factor-1 in Arabidopsis Maintain the Cellular Organization of Apical Meristems." 104:131–42.

Kepinski, Stefan and Ottoline Leyser. 2005. "The Arabidopsis F-Box Protein TIR1 Is an Auxin Receptor." *Nature* 435(7041):446–51.

Kerstetter, Randall A., Debbie Laudencia-chingcuanco, Laurie G. Smith, and Sarah Hake. 1997. "Loss-of-Function Mutations in the Maize Homeobox Gene , Knotted1 , Are Defective in Shoot Meristem Maintenance." 3054:3045–54.

Kieber, Joseph J. and G. Eric Schaller. 2018. "Cytokinin Signaling in Plant Development." *Development (Cambridge, England)* 145(4):1–7.

Kieffer, Martin, Yaniv Stern, Holly Cook, Elena Clerici, Christoph Maulbetsch, Thomas Laux, and Brendan Davies. 2006. "Analysis of the Transcription Factor WUSCHEL and Its Functional Homologue in Antirrhinum Reveals a Potential Mechanism for Their Roles in Meristem Maintenance." *Plant Cell* 18(3):560–73.

Kim, Jungmook, Klaus Harter, and Athanasios Theologis. 1997. "Protein-Protein Interactions among the Aux/IAA Proteins." *Proceedings of the National Academy of Sciences of the United States of America* 94(22):11786–91.

Kinoshita, Atsuko, Shigeyuki Betsuyaku, Yuriko Osakabe, Shinji Mizuno, Shingo Nagawa, Yvonne Stahl, Rüdiger Simon, Kazuko Yamaguchi-Shinozaki, Hiroo Fukuda, and Shinichiro Sawa. 2010. "RPK2 Is an Essential Receptor-like Kinase That Transmits the CLV3 Signal in Arabidopsis (Development 137, (3911-3920))." *Development* 137(24):4327.

Kohno, Susumu, Shunsuke Kitajima, Nobunari Sasaki, and Chiaki Takahashi. 2016. "Retinoblastoma Tumor Suppressor Functions Shared by Stem Cell and Cancer Cell Strategies." *World Journal of Stem Cells* 8(4):170–84.

De Koning, Leanne, Armelle Corpet, James E. Haber, and Geneviève Almouzni. 2007. "Histone Chaperones: An Escort Network Regulating Histone Traffic." *Nature Structural and Molecular Biology* 14(11):997–1007.

Konishi, Mineko, Tyler J. Donner, Enrico Scarpella, and Shuichi Yanagisawa. 2015. "MONOPTEROS Directly Activates the Auxin-Inducible Promoter of the Dof5.8 Transcription Factor Gene in Arabidopsis Thaliana Leaf Provascular Cells." *Journal of Experimental Botany* 66(1):283–91.

Křeček, Pavel, Petr Skůpa, Jiří Libus, Satoshi Naramoto, Ricardo Tejos, Jiří Friml, and Eva Zažímalová. 2009. "The PIN-FORMED (PIN) Protein Family of Auxin Transporters." *Genome Biology* 10(12):1–11.

Kurakawa, Takashi, Nanae Ueda, Masahiko Maekawa, Kaoru Kobayashi, Mikiko Kojima, Yasuo Nagato, Hitoshi Sakakibara, and Junko Kyozuka. 2007. "Direct Control of Shoot Meristem Activity by a Cytokinin-Activating Enzyme." *Nature* 445(7128):652–55.

Kuroha, Takeshi, Hiroki Tokunaga, Mikiko Kojima, Nanae Ueda, Takashi Ishida, Shingo Nagawa, Hiroo Fukuda, Keiko Sugimoto, and Hitoshi Sakakibara. 2009. "Functional Analyses of LONELY GUY Cytokinin-Activating Enzymes Reveal the Importance of the Direct Activation Pathway in Arabidopsis." *Plant Cell* 21(10):3152–69.

Kwon, Chang Seob, Changbin Chen, and Doris Wagner. 2005. "WUSCHEL Is a Primary Target for Transcriptional Regulation by SPLAYED in Dynamic Control of Stem Cell Fate in Arabidopsis." *Genes & Development* 19(8):992–1003.

Landrein, Benoît, Annamaria Kiss, Massimiliano Sassi, Aurélie Chauvet, Pradeep Das, Millan Cortizo, Patrick Laufs, Seiji Takeda, Mitsuhiro Aida, Jan Traas, Teva Vernoux, Arezki Boudaoud, and Olivier Hamant. 2015. "Mechanical Stress Contributes to the Expression of the STM Homeobox Gene in Arabidopsis Shoot Meristems." *ELife* 4:e07811.

Laux, Thomas, Klaus F. X. Mayer, Jürgen Berger, and Gerd Jürgens. 1996. "The WUSCHEL Gene Is Required for Shoot and Floral Meristem Integrity in Arabidopsis." *Development* 122(1):87–96.

Leibfried, Andrea, Jennifer P. C. To, Wolfgang Busch, Sandra Stehling, Andreas Kehle, Monika Demar, Joseph J. Kieber, and Jan U. Lohmann. 2005. "WUSCHEL Controls Meristem Function by Direct Regulation of Cytokinin-Inducible Response Regulators." *Nature* 438(7071):1172–75.

Lenhard, Michael, Gerd Jürgens, and Thomas Laux. 2002. "The WUSCHEL and SHOOTMERISTEMLESS Genes Fulfil Complementary Roles in Arabidopsis Shoot Meristem Regulation." *Development* 129(13):3195–3206.

Lenhard, Michael and Thomas Laux. 1999. “Shoot Meristem Formation and Maintenance.” *Current Opinion in Plant Biology* 2(1):44–50.

Li, Si Bei, Zong Zhou Xie, Chun Gen Hu, and Jin Zhi Zhang. 2016. “A Review of Auxin Response Factors (ARFs) in Plants.” *Frontiers in Plant Science* 7(FEB2016):1–7.

Liao, Che-Yang, Wouter Smet, Geraldine Brunoud, Saiko Yoshida, Teva Vernoux, and Dolf Weijers. 2015. “Reporters for Sensitive and Quantitative Measurement of Auxin Response.” *Nature Methods* 12(3):207–10.

Lieber, Diana, Jorge Lora, Sandra Schrempp, Michael Lenhard, Thomas Laux, and Albert-ludwigs-university Freiburg. 2011. “Article Arabidopsis WIH1 and WIH2 Genes Act in the Transition from Somatic to Reproductive Cell Fate.” *Current Biology* 21(12):1009–17.

Ljung, Karin. 2013. “Auxin Metabolism and Homeostasis during Plant Development.” 950:943–50.

Lohmann, Jan U., Ray L. Hong, Martin Hobe, Maximilian A. Busch, François Parcy, Rüdiger Simon, and Detlef Weigel. 2001. “A Molecular Link between Stem Cell Regulation and Floral Patterning in Arabidopsis.” *Cell* 105(6):793–803.

Long, Jeff A. and M. Kathryn Barton. 1998. “The Development of Apical Embryonic Pattern in Arabidopsis.” *Development* 125(16):3027–35.

Long, Jeff A., Erich I. Moan, June I. Medford, and M. Kathryn Barton. 1996. “A Member of the KNOTTED Class of Homeodomain Proteins Encoded by the STM Gene of Arabidopsis.” *Nature* 379(6560):66–69.

Long, Jeff A., Carolyn Ohno, Zachery R. Smith, and Elliot M. Meyerowitz. 2006. “TOPLESS Regulates Apical Embryonic Fate in Arabidopsis.” *Science* 312(5779):1520–23.

Lottspeich, Friedrich, Wolfgang Steglich, and Regine Kahmann. 1996. “Two Potential Indole-3-Acetaldehyde Dehydrogenases in the Phytopathogenic Fungus Ustilago Maydis.” 656:648–56.

Ludwig-Müller, Jutta. 2011. “Auxin Conjugates: Their Role for Plant Development and in the Evolution of Land Plants.” *Journal of Experimental Botany* 62(6):1757–73.

Mano, Yoshihiro and Keiichirou Nemoto. 2012. “The Pathway of Auxin Biosynthesis in Plants.” *Journal of Experimental Botany* 63(8):2853–72.

Marin, Elena, Virginie Jouannet, Aurélie Herz, Annemarie S. Lokerse, Dolf Weijers, Herve

Vaucheret, Laurent Nussaume, Martin D. Crespi, and Alexis Maizel. 2010. “Mir390, Arabidopsis TAS3 TasiRNAs, and Their AUXIN RESPONSE FACTOR Targets Define an Autoregulatory Network Quantitatively Regulating Lateral Root Growth.” *Plant Cell* 22(4):1104–17.

Mayer, K. F., H. Schoof, a Haecker, M. Lenhard, G. Jürgens, and T. Laux. 1998. “Role of WUSCHEL in Regulating Stem Cell Fate in the Arabidopsis Shoot Meristem.” *Cell* 95(6):805–15.

Mayer, Klaus F. X., Heiko Schoof, Achim Haecker, Michael Lenhard, Gerd J??rgens, and Thomas Laux. 1998. “Role of WUSCHEL in Regulating Stem Cell Fate in the Arabidopsis Shoot Meristem.” *Cell* 95(6):805–15.

Meng, Wen Jing, Zhi Juan Cheng, Ya Lin Sang, Miao Miao Zhang, Xiao Fei Rong, Zhi Wei Wang, Ying Ying Tang, and Xian Sheng Zhang. 2017. “Type-B ARABIDOPSIS RESPONSE REGULATORs Specify the Shoot Stem Cell Niche by Dual Regulation of WUSCHEL.” *Plant Cell* 29(6):1357–72.

Meyerowitz, EM. 1997. “Genetic Control of Cell Division Patterns in Developing Plants.” *Cell* 88:299–308.

Mikkelsen, Michael Dalgaard, Peter Naur, and Barbara Ann Halkier. 2004. “Arabidopsis Mutants in the C-S Lyase of Glucosinolate Biosynthesis Establish a Critical Role for Indole-3-Acetaldoxime in Auxin Homeostasis.” *Plant Journal* 37(5):770–77.

Morgan, Kristin E., Thomas I. Zarembinski, Athanasios Theologis, and Steffen Abel. 1999. “Biochemical Characterization of Recombinant Polypeptides Corresponding to the Predicted Bαα Fold in Aux/IAA Proteins.” *FEBS Letters* 454(3):283–87.

Mravec, Jozef, Petr Skůpa, Aurélien Bailly, Klára Hoyerová, Pavel Křeček, Agnieszka Bielach, Jan Petrášek, Jing Zhang, Vassilena Gaykova, York Dieter Stierhof, Petre I. Dobrev, Kateřina Schwarzerová, Jakub Rolčík, Daniela Seifertová, Christian Luschnig, Eva Benková, Eva Zažímalová, Markus Geisler, and Jiří Friml. 2009. “Subcellular Homeostasis of Phytohormone Auxin Is Mediated by the ER-Localized PIN5 Transporter.” *Nature* 459(7250):1136–40.

Mu, Ralf and Andrea Bleckmann. 2008. “The Receptor Kinase CORYNE of Arabidopsis Transmits the Stem Cell – Limiting Signal CLAVATA3 Independently of CLAVATA1.” 20(April):934–46.

Müller, Andreas, Changhui Guan, Leo Gälweiler, Petra Tänzler, Peter Huijser, Alan Marchant, Geraint Parry, Malcolm Bennett, Ellen Wisman, and Klaus Palme. 1998. “AtPIN2 Defines a Locus of Arabidopsis for Root Gravitropism Control.” *EMBO Journal* 17(23):6903–11.

Murray, James A. H., Angharad Jones, Christophe Godin, and Jan Traas. 2012. "Systems Analysis of Shoot Apical Meristem Growth and Development: Integrating Hormonal and Mechanical Signaling." *Plant Cell* 24(10):3907–19.

Murray, M. G. and W. F. Thompson. 1980. "Nucleic Acids Research." 8(19):4321–25.

Mutte, Sumanth K., Hirotaka Kato, Carl Rothfels, Michael Melkonian, Gane Ka Shu Wong, and Dolf Weijers. 2018. "Origin and Evolution of the Nuclear Auxin Response System." *ELife* 7:1–25.

Nemoto, Keiichirou, Masamitsu Hara, Masashi Suzuki, Hikaru Seki, Toshiya Muranaka, and Yoshihiro Mano. 2009. "The NtAMI1 Gene Functions in Cell Division of Tobacco BY-2 Cells in the Presence of Indole-3-Acetamide." *FEBS Letters* 583(2):487–92.

Nimchuk, Zachary L., Yun Zhou, Paul T. Tarr, Brenda A. Peterson, and Elliot M. Meyerowitz. 2015. "Plant Stem Cell Maintenance by Transcriptional Cross-Regulation of Related Receptor Kinases." *Development (Cambridge)* 142(6):1043–49.

Noda, Yukiko, Motoyuki Kohjima, Tomoko Izaki, Kazuhisa Ota, Sosuke Yoshinaga, Fuyuhiko Inagaki, Takashi Ito, and Hideki Sumimoto. 2003. "Molecular Recognition in Dimerization between PB1 Domains." *Journal of Biological Chemistry* 278(44):43516–24.

Normanly, Jennifer. 2010. "Approaching Cellular and Molecular Resolution of Auxin Biosynthesis and Metabolism." *Cold Spring Harbor Perspectives in Biology* 2(1):1–17.

Normanly, Jennifer, Jerry D. Cohent, and Gerald R. Fink. 1993. "Arabidopsis Thaliana Auxotrophs Reveal a Tryptophan-Independent Biosynthetic Pathway for Indole-3-Acetic Acid." 90(November):10355–59.

Normanly, Jennifer, Paula Grisafi, Gerald R. Fink, and Bonnie Bartel. 1997. "Arabidopsis Mutants Resistant to the Auxin Effects of Indole-3-Acetonitrile Are Defective in the Nitrilase Encoded by the NIT1 Gene." *Plant Cell* 9(10):1781–90.

Ogawa, Mari, Hidefumi Shinohara, Youji Sakagami, and Yoshikatsu Matsubayash. 2008. "Arabidopsis CLV3 Peptide Directly Binds CLV1 Ectodomain." *Science*.

Ohta, M., K. Matsui, K. Hiratsu, H. Shinshi, and M. Ohme-Takagi. 2001. "Repression Domains of Class II ERF Transcriptional Repressors Share an Essential Motif for Active Repression." *Plant Cell* 13(8):1959–68.

Ohyama, Kentaro, Hidefumi Shinohara, and Mari Ogawa-ohnishi. 2009. "A Glycopeptide Regulating Stem Cell Fate in Arabidopsis Thaliana." 5(8):578–80.

Okada, Kiyotaka, Junichi Ueda, Masako K. Komaki, Callum J. Bell, and Yoshiro Shimura. 1991. “Requirement of the Auxin Polar Transport System in Early Stages of Arabidopsis Floral Bud Formation.” *Plant Cell* 3(7):677–84.

Okushima, Yoko, Hidehiro Fukaki, Makoto Onoda, Athanasios Theologis, and Masao Tasaka. 2007. “ARF7 and ARF19 Regulate Lateral Root Formation via Direct Activation of LBD/ASL Genes in Arabidopsis.” *Plant Cell* 19(1):118–30.

Paponov, Ivan A, Martina Paponov, William Teale, Margit Menges, Sohini Chakrabortee, James A. H. Murray, and Klaus Palme. 2008. “Comprehensive Transcriptome Analysis of Auxin Responses in Arabidopsis.” *Molecular Plant* 1(2):321–37.

Paponov, Ivan A., Martina Paponov, William Teale, Margit Menges, Sohini Chakrabortee, James A. H. Murray, and Klaus Palme. 2008. “Comprehensive Transcriptome Analysis of Auxin Responses in Arabidopsis.” *Molecular Plant* 1(2):321–37.

Park, Woong June, Verena Kriechbaumer, Axel Müller, Markus Piotrowski, Robert B. Meeley, Alfons Gierl, and Erich Glawischnig. 2003. “The Nitrilase ZmNIT2 Converts Indole-3-Acetonitrile to Indole-3-Acetic Acid.” *Plant Physiology* 133(2):794–802.

Pekker, Irena, John Paul Alvarez, and Yuval Eshed. 2005. “Auxin Response Factors Mediate Arabidopsis Organ Asymmetry via Modulation of KANADI Activity.” *Plant Cell* 17(11):2899–2910.

Perales, Mariano, Kevin Rodriguez, Stephen Snipes, Ram Kishor Yadav, Mercedes Diaz-Mendoza, and G. Venugopala Reddy. 2016. “Threshold-Dependent Transcriptional Discrimination Underlies Stem Cell Homeostasis.” *Proceedings of the National Academy of Sciences* 113(41):E6298–6306.

Péret, Benjamin, Kamal Swarup, Alison Ferguson, Malvika Seth, Yaodong Yang, Stijn Dhondt, Nicholas James, Ilda Casimiro, Paula Perry, Adnan Syed, Haibing Yang, Jesica Reemmer, Edward Venison, Caroline Howells, Miguel A. Perez-Amador, Jeonga Yun, Jose Alonso, Gerrit T. S. Beemster, Laurent Laplaze, Angus Murphy, Malcolm J. Bennett, Erik Nielsen, and Ranjan Swarup. 2012. “AUX/LAX Genes Encode a Family of Auxin Influx Transporters That Perform Distinct Functions during Arabidopsis Development.” *Plant Cell* 24(7):2874–85.

Perrot-Rechenmann, Catherine. 2010. “Cellular Responses to Auxin: Division versus Expansion.” *Cold Spring Harbor Perspectives in Biology* 2(5):1–16.

Phillips, Kimberly A., Andrea L. Skirpan, Xing Liu, Ashley Christensen, Thomas L. Slewinski, Christopher Hudson, Solmaz Barazesh, Jerry D. Cohen, Simon Malcomber, and Paula McSteen. 2011. “Vanishing Tassel2 Encodes a Grass-Specific Tryptophan

Aminotransferase Required for Vegetative and Reproductive Development in Maize." *Plant Cell* 23(2):550–66.

Pollmann, Stephan, Daniel Neu, Thomas Lehmann, Oliver Berkowitz, Tina Schäfer, and Elmar W. Weiler. 2006. "Subcellular Localization and Tissue Specific Expression of Amidase 1 from Arabidopsis Thaliana." *Planta* 224(6):1241–53.

Quittenden, Laura J., Noel W. Davies, Jason A. Smith, Peter P. Molesworth, Nathan D. Tivendale, and John J. Ross. 2009. "Auxin Biosynthesis in Pea: Characterization of the Tryptamine Pathway." *Plant Physiology* 151(3):1130–38.

Rahman, Abidur, Maho Takahashi, Kyohei Shibasaki, Shuang Wu, Takehito Inaba, Seiji Tsurumi, and Tobias I. Baskin. 2010. "Gravitropism of Arabidopsis Thaliana Roots Requires the Polarization of PIN2 toward the Root Tip in Meristematic Cortical Cells." *Plant Cell* 22(6):1762–76.

Rakusová, Hana, Mohamad Abbas, Huibin Han, Siyuan Song, Hélène S. Robert, and Jiří Friml. 2016. "Termination of Shoot Gravitropic Responses by Auxin Feedback on PIN3 Polarity." *Current Biology* 26(22):3026–32.

Ramos, J. A., N. Zenser, O. Leyser, and J. Callis. 2001. "Rapid Degradation of Auxin/Indoleacetic Acid Proteins Requires Conserved Amino Acids of Domain II and Is Proteasome Dependent." *Plant Cell* 13(10):2349–60.

Reddy, G. Venugopala, Marcus G. Heisler, David W. Ehrhardt, and Elliot M. Meyerowitz. 2004. "Real-Time Lineage Analysis Reveals Oriented Cell Divisions Associated with Morphogenesis at the Shoot Apex of Arabidopsis Thaliana." *Development* 131(17):4225–37.

Reinhardt, Didier, Therese Mandel, and Cris Kuhlemeier. 2000a. "Auxin Regulates the Initiation and Radial Position of Plant Lateral Organs." *Plant Cell* 12(4):507–18.

Reinhardt, Didier, Therese Mandel, and Cris Kuhlemeier. 2000b. "Reinhardt." 12(April):1–12.

Reinhardt, Didier, Eva-Rachele Pesce, Pia Stieger, Therese Mandel, Kurt Baltensperger, Malcolm Bennett, Jan Traas, Jirí Friml, and Cris Kuhlemeier. 2003a. "Regulation of Phyllotaxis by Polar Auxin Transport." *Nature* 426(6964):255–60.

Reinhardt, Didier, Eva-Rachele Pesce, Pia Stieger, Therese Mandel, Kurt Baltensperger, Malcolm Bennett, Jan Traas, Jirí Friml, and Cris Kuhlemeier. 2003b. "Regulation of Phyllotaxis by Polar Auxin Transport." *Nature* 426(6964):255–60.

Remington, David L., Todd J. Vision, Thomas J. Guilfoyle, and Jason W. Reed. 2004.

"Contrasting Modes of Diversification in the Aux/IAA and ARF Gene Families." *Plant Physiology* 135(3):1738–52.

Reuille, Pierre Barbier De, Daniel Kierzkowski, George W. Bassel, Thierry Sch, Gerardo Tauriello, Namrata Bajpai, Alain Weber, Annamaria Kiss, Agata Burian, Hugo Hofhuis, Aleksandra Sapala, Marcin Lipowczan, Maria B. Heimlicher, Sarah Robinson, Emmanuelle M. Bayer, Konrad Basler, Petros Koumoutsakos, Adrienne H. K. Roeder, Tinri Aegerter-wilmsen, Naomi Nakayama, Miltos Tsiantis, Angela Hay, Dorota Kwiatkowska, Ioannis Xenarios, Cris Kuhlemeier, Richard S. Smith, Ecole Normale, and De Lyon. 2015. "MorphoGraphX : A Platform for Quantifying Morphogenesis in 4D." 1–20.

Rodriguez, Kevin, Mariano Perales, Stephen Snipes, Ram Kishor Yadav, Mercedes Diaz-Mendoza, and G. Venugopala Reddy. 2016. "DNA-Dependent Homodimerization, Sub-Cellular Partitioning, and Protein Destabilization Control WUSCHEL Levels and Spatial Patterning." *Proceedings of the National Academy of Sciences* 113(41):E6307–15.

Rojo, Enrique, Vijay K. Sharma, Valentina Kovaleva, Natasha V. Raikhel, and Jennifer C. Fletcher. 2002. "CLV3 Is Localized to the Extracellular Space, Where It Activates the Arabidopsis CLAVATA Stem Cell Signaling Pathway." *Plant Cell* 14(5):969–77.

Roosjen, Mark, Sébastien Paque, and Dolf Weijers. 2018. "Auxin Response Factors: Output Control in Auxin Biology." *Journal of Experimental Botany* 69(2):179–88.

Ruiz Rosquete, Michel, Elke Barbez, and Jürgen Kleine-Vehn. 2012. "Cellular Auxin Homeostasis: Gatekeeping Is Housekeeping." *Molecular Plant* 5(4):772–86.

Ry, S. U. M. M. A. 2008. "Indole-3-Acetic Acid (IAA) Biosynthesis in the Smut Fungus Ustilago Maydis and Its Relevance for Increased IAA Levels in Infected Tissue." 9:339–55.

Sahai-Hernandez, Pankaj, Angela Castanieto, and Todd G. Nystul. 2012. "Drosophila Models of Epithelial Stem Cells and Their Niches." *Wiley Interdisciplinary Reviews. Developmental Biology* 1(3):447–57.

Santelia, Diana, Vincent Vincenzetti, Elisa Azzarello, Lucien Bovet, Yoichiro Fukao, Petra Düchtig, Stefano Mancuso, Enrico Martinoia, and Markus Geisler. 2005. "MDR-like ABC Transporter AtPGP4 Is Involved in Auxin-Mediated Lateral Root and Root Hair Development." *FEBS Letters* 579(24):5399–5406.

Sardar, Puspendu and Frank Kempken. 2018. "Characterization of Indole-3-Pyruvic Acid Pathway-Mediated Biosynthesis of Auxin in Neurospora Crassa." 1–22.

Schoof, Heiko, Michael Lenhard, Achim Haecker, Klaus F X Mayer, Gerd Ju, Thomas Laux, Molekularbiologie Der Pflanzen, Auf Der Morgenstelle, Gerd Jürgens, and Thomas Laux. 2000. "The Stem Cell Population of Arabidopsis Shoot Meristems in Maintained by a Regulatory Loop between the CLAVATA and WUSCHEL Genes." *Cell* 100(6):635–44.

Schoof, Heiko, Michael Lenhard, Achim Haecker, Klaus F.X. Mayer, Gerd Jürgens, and Thomas Laux. 2000. "The Stem Cell Population of Arabidopsis Shoot Meristems Is Maintained by a Regulatory Loop between the CLAVATA and WUSCHEL Genes." *Cell* 100(6):635–44.

Shivdasani, Anish A. and Philip W. Ingham. 2003. "Regulation of Stem Cell Maintenance and Transit Amplifying Cell Proliferation by TGF-β Signaling in Drosophila Spermatogenesis." *Current Biology* 13(23):2065–72.

Sidler, Michael, Paul Hassa, Sameez Hasan, Christoph Ringli, and Robert Dudler. 1998. "Involvement of an ABC Transporter in a Developmental Pathway Regulating Hypocotyl Cell Elongation in the Light." *Plant Cell* 10(10):1623–36.

Šimášková, Mária, José Antonio O'Brien, Mamoona Khan, Giel Van Noorden, Krisztina Ötvös, Anne Vieten, Inge De Clercq, Johanna Maria Adriana Van Haperen, Candela Cuesta, Klára Hoyerová, Steffen Vanneste, Peter Marhavý, Krzysztof Wabnik, Frank Van Breusegem, Moritz Nowack, Angus Murphy, Jia Friml, Dolf Weijers, Tom Beeckman, and Eva Benková. 2015. "Cytokinin Response Factors Regulate PIN-FORMED Auxin Transporters." *Nature Communications* 6.

Simon, Sibu, Petr Skůpa, Tom Viaene, Marta Zwiewka, Ricardo Tejos, Petr Klíma, Mária Čarná, Jakub Rolčík, Riet De Rycke, Ignacio Moreno, Petre I. Dobrev, Ariel Orellana, Eva Zažímalová, and Jiří Friml. 2016. "PIN6 Auxin Transporter at Endoplasmic Reticulum and Plasma Membrane Mediates Auxin Homeostasis and Organogenesis in Arabidopsis." *New Phytologist* 211(1):65–74.

Simonini, Sara, Stefano Bencivenga, Martin Trick, and Lars Østergaard. 2017. "Auxin-Induced Modulation of ETTIN Activity Orchestrates Gene Expression in Arabidopsis." *Plant Cell* 29(8):1864–82.

Sinha, N. R., R. E. Williams, and S. Hake. 1993. "Overexpression of the Maize Homeo Box Gene, KNOTTED-1, Causes a Switch from Determinate to Indeterminate Cell Fates." *Genes and Development* 7(5):787–95.

Song, Xiaoqing, Marco D. Wong, Eihachiro Kawase, Rongwen Xi, Bee C. Ding, John J. McCarthy, and Ting Xie. 2004. "Bmp Signals from Niche Cells Directly Repress Transcription of a Differentiation-Promoting Gene, Bag of Marbles, in Germline Stem Cells in the Drosophila Ovary." *Development* 131(6):1353–64.

Sparks, Erin E., Colleen Drapek, Allison Gaudinier, Song Li, Mitra Ansariola, Ning Shen, Jessica H. Hennacy, Jingyuan Zhang, Gina Turco, Jalean J. Petricka, Jessica Foret, Alexander J. Hartemink, Raluca Gordân, Molly Megraw, Siobhan M. Brady, and Philip N. Benfey. 2016. "Establishment of Expression in the SHORTROOT-SCARECROW Transcriptional Cascade through Opposing Activities of Both Activators and Repressors." *Developmental Cell* 39(5):585–96.

Spinelli, Silvana V., Ana Paula Martin, Ivana L. Viola, Daniel H. Gonzalez, and Javier F. Palatnik. 2011. "A Mechanistic Link between STM and CUC1 during Arabidopsis Development." *Plant Physiology* 156(4):1894–1904.

Steeves, Taylor A. and Sussex, Ian M. 1989. *Pattern in Plant Development*. Second Edi. New York: Cambridge University Press.

Stepanova, Anna N., Joyce Robertson-Hoyt, Jeonga Yun, Larissa M. Benavente, De Yu Xie, Karel Dole??al, Alexandra Schlereth, Gerd J??rgens, and Jose M. Alonso. 2008. "TAA1-Mediated Auxin Biosynthesis Is Essential for Hormone Crosstalk and Plant Development." *Cell* 133(1):177–91.

Stoma, Szymon, Mikael Lucas, Jérôme Chopard, Marianne Schaedel, Jan Traas, and Christophe Godin. 2008. "Flux-Based Transport Enhancement as a Plausible Unifying Mechanism for Auxin Transport in Meristem Development." *PLoS Computational Biology* 4(10).

Strader, Lucia C. and Bonnie Bartel. 2011. "Transport and Metabolism of the Endogenous Auxin Precursor Indole-3-Butyric Acid." *Molecular Plant* 4(3):477–86.

Strader, Lucia C., Angela Hendrickson Culler, Jerry D. Cohen, and Bonnie Bartel. 2010. "Conversion of Endogenous Indole-3-Butyric Acid to Indole-3-Acetic Acid Drives Cell Expansion in Arabidopsis Seedlings." *Plant Physiology* 153(4):1577–86.

Sugawara, Satoko, Shojiro Hishiyama, Yusuke Jikumaru, Atsushi Hanada, Takeshi Nishimura, Tomokazu Koshiba, Yunde Zhao, Yuji Kamiya, and Hiroyuki Kasahara. 2009. "Biochemical Analyses of Indole-3-Acetaldoximedependent Auxin Biosynthesis in Arabidopsis." *Proceedings of the National Academy of Sciences of the United States of America* 106(13):5430–35.

Swarup, Kamal, Eva Benková, Ranjan Swarup, Ilda Casimiro, Benjamin Péret, Yaodong Yang, Geraint Parry, Erik Nielsen, Ive De Smet, Steffen Vanneste, Mitch P. Levesque, David Carrier, Nicholas James, Vanessa Calvo, Karin Ljung, Eric Kramer, Rebecca Roberts, Neil Graham, Sylvestre Marillonnet, Kanu Patel, Jonathan D. G. Jones, Christopher G. Taylor, Daniel P. Schachtman, Sean May, Goran Sandberg, Philip Benfey, Jiri Friml, Ian Kerr, Tom Beeckman, Laurent Laplaze, and Malcolm J. Bennett. 2008. "The Auxin Influx

Carrier LAX3 Promotes Lateral Root Emergence." *Nature Cell Biology* 10(8):946–54.

Swarup, Ranjan, Eric M. Kramer, Paula Perry, Kirsten Knox, H. M. Ottolin. Leyser, Jim Haseloff, Gerrit T. S. Beemster, Rishikesh Bhalerao, and Malcolm J. Bennett. 2005. "Root Gravitropism Requires Lateral Root Cap and Epidermal Cells for Transport and Response to a Mobile Auxin Signal." *Nature Cell Biology* 7(11):1057–65.

Swarup, Ranjan, Ranjan Swarup, Alan Marchant, Alan Marchant, Karin Ljung, Karin Ljung, Goran Sandberg, Goran Sandberg, Klaus Palme, Klaus Palme, Malcolm Bennett, and Malcolm Bennett. 2001. "Root Apex." *Genes & Development* 2648–53.

Szemenyei, Heidi, Mike Hannon, and Jeff A. Long. 2008. "TOPLESS Mediates Auxin-Dependent Transcriptional Repression during Arabidopsis Embryogenesis." *Science* 319(5868):1384–86.

Takada, S., K. I. Hibara, T. Ishida, and M. Tasaka. 2001. "The CUP-SHAPED COTYLEDON1 Gene of Arabidopsis Regulates Shoot Apical Meristem Formation." *Development* 128(7):1127–35.

Takei, Kentaro, Hitoshi Sakakibara, and Tatsuo Sugiyama. 2001. "Identification of Genes Encoding Adenylate Isopentenyltransferase, a Cytokinin Biosynthesis Enzyme, in Arabidopsis Thaliana." *Journal of Biological Chemistry* 276(28):26405–10.

Tan, Xu, Luz Irina A. Calderon-Villalobos, Michal Sharon, Changxue Zheng, Carol V. Robinson, Mark Estelle, and Ning Zheng. 2007. "Mechanism of Auxin Perception by the TIR1 Ubiquitin Ligase." *Nature* 446(7136):640–45.

Tanaka, H., P. Dhonukshe, P. B. Brewer, and J. Friml. 2006. "Spatiotemporal Asymmetric Auxin Distribution: A Means to Coordinate Plant Development." *Cellular and Molecular Life Sciences* 63(23):2738–54.

Tao, Yi, Jean-luc Ferrer, Karin Ljung, Florence Pojer, Fangxin Hong, Jeff A. Long, Lin Li, Javier E. Moreno, Marianne E. Bowman, Lauren J. Ivans, Youfa Cheng, Jason Lim, Yunde Zhao, Joseph P. Noel, Joanne Chory, and Carlos L. Ballare. 2008. "Rapid Synthesis of Auxin via a New Tryptophan-Dependent Pathway Is Required for Shade Avoidance in Plants." 164–76.

Terasaka, Kazuyoshi, Joshua J. Blakeslee, Boosaree Titapiwatanakun, Wendy A. Peer, Anindita Bandyopadhyay, Srinivas N. Makam, Ok Ran Lee, Elizabeth L. Richards, Angus S. Murphy, Fumihiko Sato, and Kazufumi Yazaki. 2005. "PGP4, an ATP Binding Cassette P-Glycoprotein, Catalyzes Auxin Transport in Arabidopsis Thaliana Roots." *Plant Cell* 17(11):2922–39.

Tivendale, Nathan D., John J. Ross, and Jerry D. Cohen. 2014. “The Shifting Paradigms of Auxin Biosynthesis.” *Trends in Plant Science* 19(1):44–51.

Tiwari, Shiv B., Gretchen Hagen, and Tom J. Guilfoyle. 2004. “Aux/IAA Proteins Contain a Potent Transcriptional Repression Domain.” *Plant Cell* 16(2):533–43.

Tiwari, Shiv B., Xiao-jun Wang, and Tom J. Guilfoyle. 2001. “AUX / IAA Proteins Are Active Repressors , and Their Stability and Activity Are Modulated by Auxin Author (s): Shiv B . Tiwari , Xiao-Jun Wang , Gretchen Hagen and Tom J . Guilfoyle Published by : American Society of Plant Biologists (ASPB) Stable URL.” *The Plant Cell* 13(12):2809–22.

Tripathi, Amit K., Khushwant Singh, Ashwani Pareek, and Sneh L. Singla-Pareek. 2015. “Histone Chaperones in Arabidopsis and Rice: Genome-Wide Identification, Phylogeny, Architecture and Transcriptional Regulation.” *BMC Plant Biology* 15(1):1–25.

Tsavkelova, E. A., S. Yu Klimova, T. A. Cherdyntseva, and A. I. Netrusov. 2006. “Microbial Producers of Plant Growth Stimulators and Their Practical Use : A Review.” 42(2):117–26.

Tzin, Vered and Gad Galili. 2010. “The Biosynthetic Pathways for Shikimate and Aromatic Amino Acids in Arabidopsis Thaliana.” (i).

Ueno, Makoto, Hitoshi Shibata, Junichi Kihara, Yuichi Honda, and Sakae Arase. 2003. “Increased Tryptophan Decarboxylase and Monoamine Oxidase Activities Induce Sekiguchi Lesion Formation in Rice Infected with Magnaporthe Grisea.” *Plant Journal* 36(2):215–28.

Ulmasov, T, J. Murfett, G. Hagen, and T. J. Guilfoyle. 1997. “Aux/IAA Proteins Repress Expression of Reporter Genes Containing Natural and Highly Active Synthetic Auxin Response Elements.” *The Plant Cell* 9(11):1963 LP – 1971.

Ulmasov, Tim, Gretchen Hagen, and Tom J. Guilfoyle. 1999a. “Activation and Repression of Transcription by Auxin-Response Factors.” *Proceedings of the National Academy of Sciences of the United States of America* 96(10):5844–49.

Ulmasov, Tim, Gretchen Hagen, and Tom J. Guilfoyle. 1999b. “Dimerization and DNA Binding of Auxin Response Factors.” *Plant Journal* 19(3):309–19.

Ulmasov, Tim, Jane Murfett, Gretchen Hagen, and Tom J. Guilfoyle. 1997. “Aux/IAA Proteins Repress Expression of Reporter Genes Containing Natural and Highly Active Synthetic Auxin Response Elements.” *The Plant Cell* 9(11):1963.

Uzunova, Veselina V., Mussa Quareshy, Charo I. Del Genio, and Richard M. Napier. 2016. "Tomographic Docking Suggests the Mechanism of Auxin Receptor TIR1 Selectivity." *Open Biology* 6(10).

Vandenbussche, Filip, Jan Petrášek, Petra Žádníková, Klára Hoyerová, Bedřich Pešek, Vered Raz, Ranjan Swarup, Malcolm Bennett, Eva Zažímolavá, Eva Benkova, and Dominique Van Der Straeten. 2010. "The Auxin Influx Carriers AUX1 and LAX3 Are Involved in Auxin-Ethylene Interactions during Apical Hook Development in Arabidopsis Thaliana Seedlings." *Development* 137(4):597–606.

Vernoux, T., J. Kronenberger, O. Grandjean, P. Laufs, and J. Traas. 2000. "PIN-FORMED 1 Regulates Cell Fate at the Periphery of the Shoot Apical Meristem." *Development (Cambridge, England)* 127(23):5157–65.

Vernoux, Teva, Géraldine Brunoud, Etienne Farcot, Valérie Morin, Hilde Van Den Daele, Jonathan Legrand, Marina Oliva, Pradeep Das, Antoine Larrieu, Darren Wells, Yann Guédon, Lynne Armitage, Franck Picard, Soazig Guyomarc'H, Coralie Cellier, Geraint Parry, Rachil Koumproglou, John H. Doonan, Mark Estelle, Christophe Godin, Stefan Kepinski, Malcolm Bennett, Lieven De Veylder, and Jan Traas. 2011. "The Auxin Signalling Network Translates Dynamic Input into Robust Patterning at the Shoot Apex." *Molecular Systems Biology* 7(508).

Vroemen, Casper W., Andreas P. Mordhorst, Cathy Albrecht, Mark A. C. J. Kwaaitaal, and Sacco C. de Vries. 2003. "The CUP-SHAPED COTYLEDON3 Gene Is Required for Boundary and Shoot Meristem Formation in Arabidopsis." *The Plant Cell* 15(7):1563–77.

Wang, Jin, Caihuan Tian, Cui Zhang, Bihai Shi, Xiuwei Cao, Tian Qi Zhang, Zhong Zhao, Jia Wei Wang, and Yuling Jiao. 2017. "Cytokinin Signaling Activates WUSCHEL Expression during Axillary Meristem Initiation." *Plant Cell* 29(6):1373–87.

Wang, Zhi, Fengying Chen, Xiaoying Li, Hong Cao, Meng Ding, Cun Zhang, Jinghong Zuo, Chaonan Xu, Jimei Xu, Xin Deng, Yong Xiang, Wim J. J. Soppe, and Yongxiu Liu. 2016. "Arabidopsis Seed Germination Speed Is Controlled by SNL Histone Deacetylase-Binding Factor-Mediated Regulation of AUX1." *Nature Communications* 7:1–14.

Weijers, Dolf and Doris Wagner. 2016. "Transcriptional Responses to the Auxin Hormone." *Annual Review of Plant Biology* 67(1):539–74.

Werner, T., I. Köllmer, I. Bartrina, K. Holst, and T. Schmülling. 2006. "New Insights into the Biology of Cytokinin Degradation." *Plant Biol (Stuttg)* 8(03):371–81.

Willige, Björn C. and Joanne Chory. 2015. "A Current Perspective on the Role of AGCVIII

Kinases in PIN-Mediated Apical Hook Development." *Frontiers in Plant Science* 6(OCTOBER):1–7.

Winkler, Martin, Michael Niemeyer, Antje Hellmuth, Philipp Janitza, Gideon Christ, Sophia L. Samodelov, Verona Wilde, Petra Majovsky, Marco Trujillo, Matias D. Zurbriggen, Wolfgang Hoehenwarter, Marcel Quint, and Luz Irina A. Calderó. Villalobos. 2017. "Variation in Auxin Sensing Guides AUX/IAA Transcriptional Repressor Ubiquitylation and Destruction." *Nature Communications* 8.

Wu, Miin Feng, Nobutoshi Yamaguchi, Jun Xiao, Bastiaan Bargmann, Mark Estelle, Yi Sang, and Doris Wagner. 2015. "Auxin-Regulated Chromatin Switch Directs Acquisition of Flower Primordium Founder Fate." *ELife* 4(OCTOBER2015):1–20.

Yadav, Ram Kishor, Mariano Perales, Jérémy Gruel, Thomas Girke, Henrik Jönsson, and G. Venugopala Reddy. 2011. "WUSCHEL Protein Movement Mediates Stem Cell Homeostasis in the Arabidopsis Shoot Apex." *Genes and Development* 25(19):2025–30.

Yadav, Ram Kishor, Mariano Perales, Jérémy Gruel, Carolyn Ohno, Marcus Heisler, Thomas Girke, Henrik Jönsson, and G. Venugopala Reddy. 2013. "Plant Stem Cell Maintenance Involves Direct Transcriptional Repression of Differentiation Program." *Molecular Systems Biology* 9(654).

Yadav, Ram Kishor, Mariano Perales, Jérémy Gruel, Ram Kishor Yadav, and Mariano Perales. 2011. "WUSCHEL Protein Movement Mediates Stem Cell Homeostasis in the Arabidopsis Shoot Apex Service WUSCHEL Protein Movement Mediates Stem Cell Homeostasis in the Arabidopsis Shoot Apex." 2025–30.

Yadav, Ram Kishor RK R. K., Mariano Perales, Jérémy Gruel, Carolyn Ohno, Marcus Heisler, Thomas Girke, Henrik Jönsson, G. Venugopala Reddy, G. Venugopala Reddy, Carolyn Ohno, Marcus Heisler, Thomas Girke, Henrik Jönsson, G. Venugopala Reddy, and G. Venugopala Reddy. 2013. "Plant Stem Cell Maintenance Involves Direct Transcriptional Repression of Differentiation Program." *Molecular Systems Biology* 9(654):654.

Yadav, Ram Kishor, Montreh Tavakkoli, and G. Venugopala Reddy. 2010. "WUSCHEL Mediates Stem Cell Homeostasis by Regulating Stem Cell Number and Patterns of Cell Division and Differentiation of Stem Cell Progenitors." *Development (Cambridge, England)* 137(21):3581–89.

Yamaguchi, Nobutoshi, Miin Feng Wu, Cara M. Winter, Markus C. Berns, Staci Nole-Wilson, Ayako Yamaguchi, George Coupland, Beth A. Krizek, and Doris Wagner. 2013. "A Molecular Framework for Auxin-Mediated Initiation of Flower Primordia." *Developmental Cell* 24(3):271–82.

Yanai, Osnat, Eilon Shani, Karel Dolezal, Petr Tarkowski, Robert Sablowski, Goran Sandberg,

Alon Samach, and Naomi Ori. 2005. “Arabidopsis KNOXI Proteins Activate Cytokinin Biosynthesis.” *Current Biology* 15(17):1566–71.

Yang, Songguang, Chenlong Li, Linmao Zhao, Sujuan Gao, Jingxia Lu, Minglei Zhao, Chia Yang Chen, Xuncheng Liu, Ming Luo, Yuhai Cui, Chengwei Yang, and Keqiang Wu. 2015. “The Arabidopsis SWI2/SNF2 Chromatin Remodeling ATPase BRAHMA Targets Directly to PINs and Is Required for Root Stem Cell Niche Maintenance.” *Plant Cell* 27(6):1670–80.

Yoshida, Nobumasa, Yukihiro Yanai, Lingjing Chen, Yoshihiro Kato, Junzo Hiratsuka, Tatsushi Miwa, Z. Renee Sung, and Shigeru Takahashi. 2001. “EMBRYONIC FLOWER2, a Novel Polycomb Group Protein Homolog, Mediates Shoot Development and Flowering in Arabidopsis.” *The Plant Cell* 13(11):2471.

Žádníkova, Petra, Jan Petrášek, Peter Marhavý, Vered Raz, Filip Vandenbussche, Zhaojun Ding, Kateřina Schwarzerová, Miyo T. Morita, Masao Tasaka, Jan Hejatko, Dominique Van Der Straeten, Jiři Friml, and Eva Benková. 2010. “Role of PIN-Mediated Auxin Efflux in Apical Hook Development of Arabidopsis Thaliana.” *Development* 137(4):607–17.

Zazımalova, Eva. 2015. “Why So Many? −− Auxin Transporters .Pdf.” 1–15.

Zhang, Tian-Qi, Heng Lian, Chuan-Miao Zhou, Lin Xu, Yuling Jiao, and Jia-Wei Wang. 2017. “ A Two-Step Model for de Novo Activation of WUSCHEL during Plant Shoot Regeneration .” *The Plant Cell* 29(5):1073–87.

Zhao, Yunde. 2010. “Auxin Biosynthesis and Its Role in Plant Development.” *Annual Review of Plant Biology* 61(1):49–64.

Zhao, Yunde. 2012. “Auxin Biosynthesis : A Simple Two-Step Pathway Converts Tryptophan to Indole-3-Acetic Acid in Plants.” *Molecular Plant* 5(2):334–38.

Zhao, Yunde, Anna K. Hull, Joseph R. Ecker, Jennifer Normanly, Joanne Chory, and John L. Celenza. 2002. “Trp-Dependent Auxin Biosynthesis In.” *Genes & Development* 3100–3112.

Zhou, Yun, Xing Liu, Eric M. Engstrom, Zachary L. Nimchuk, Jose L. Pruneda-Paz, Paul T. Tarr, An Yan, Steve A. Kay, and Elliot M. Meyerowitz. 2015. “Control of Plant Stem Cell Function by Conserved Interacting Transcriptional Regulators.” *Nature* 517(7534):377–80.

Zhou, Yun, An Yan, Han Han, Ting Li, Yuan Geng, Xing Liu, and Elliot M. Meyerowitz. 2018. “Hairy Meristem with Wuschel Confines Clavata3 Expression to the Outer Apical

Meristem Layers." *Science* 361(6401):502–6.

Zhu, Yan, Aiwu Dong, Denise Meyer, Olivier Pichon, Jean Pierre Renou, Kaiming Cao, and Wen Hui Shen. 2006. "Arabidopsis NRP1 and NRP2 Encode Histone Chaperones and Are Required for Maintaining Postembryonic Root Growth." *Plant Cell* 18(11):2879–92.

Zhu, Yan, Aiwu Dong, and Wen Hui Shen. 2007. "Chromatin Remodeling in Arabidopsis Root Growth." *Plant Signaling and Behavior* 2(3):160–62.

Zimmerman, P. W. and F. Wilcoxon. 1935. "Several Chemical Growth Substances Which Cause Initiation of Roots and Other Responses in Plants." *Contributions from Boyce Thompson Institute* 7:209–29.

Zolman, Bethany K., Naxhiely Martinez, Arthur Millius, A. Raquel Adham, and Bonnie Bartel. 2008. "Identification and Characterization of Arabidopsis Indole-3-Butyric Acid Response Mutants Defective in Novel Peroxisomal Enzymes." *Genetics* 180(1):237–51.

Zolman, Bethany K., Michelle Nyberg, and Bonnie Bartel. 2007. "IBR3, a Novel Peroxisomal Acyl-CoA Dehydrogenase-like Protein Required for Indole-3-Butyric Acid Response." *Plant Molecular Biology* 64(1–2):59–72.

Zürcher, E. and B. Müller. 2016. "Cytokinin Synthesis, Signaling, and Function-Advances and New Insights." Pp. 1–38 in *International Review of Cell and Molecular Biology*. Vol. 324. Elsevier Inc.

Zürcher, Evelyne, Deborah Tavor-Deslex, Dmytro Lituiev, Katalin Enkerli, Paul T. Tarr, and Bruno Müller. 2013. "A Robust and Sensitive Synthetic Sensor to Monitor the Transcriptional Output of the Cytokinin Signaling Network in Planta." *Plant Physiology* 161(3):1066–75.

ANNEXURE: List of the Chemicals

Chemical Name	Company	Catalogue No.
Murashige and Skoog (MS) medium	Sigma -Aldrich	M5519
Bacto-agar	Hi-Media	GR-M026
Sucrose	Sigma -Aldrich	S0389
MES	Sigma -Aldrich	M3671
Sodium hypochlorite	Merck	1.93607.1021
Triton X-100	Sigma -Aldrich	T8787
Tryptone	Hi-Media	RM014
Yeast extract	BD-Biosciences	212750
Sodium chloride (NaCl)	Merck	7710
Trizma (Tris)	Sigma -Aldrich	T6060
Hexadecyltrimethylammonium bromide (CTAB)	Sigma -Aldrich	H6269
β-Mercaptoethanol	Sigma -Aldrich	M3148
Phenol : Chloroform : Isoamyl alcohol	Hi-Media	MB078
Chloroform : Isoamyl alcohol (24:1)	Hi-Media	MB115
Isopropanol	Vetec	V800228
MOPS	EMD Millipore Corp.	475922
Potassium chloride (KCl)	Sigma -Aldrich	P4504
Manganese(II) chloride (MnCl2)	Biochem Life Sciences	BC0331
Glycerol	Vetec	V800196
Potassium acetate (KAc)	Sigma -Aldrich	P1190
Calcium chloride (CaCl2)	Sigma -Aldrich	C1016
Dimethyl sulfoxide(DMSO)	EMD Millipore Corp	317275
Sodium dodecyl sulphate (SDS)	Sigma -Aldrich	L3771
Methanol	Merck	1.07018.2521
Boric Acid	Sigma -Aldrich	B6768
FM4-64FX	Invitrogen	F34653
Propidium Iodide (PI)	Invitrogen	P1304MP
Paraformaldehyde PFA	Sigma -Aldrich	P6148

Diethyl pyro carbonate (DEPC)	Sigma -Aldrich	D5758
Eosin	Hi-Media	S007
Histoclear (Xylene substitute)	Sigma	A5597
paraplast	Medite	
probe on-plus slides	Medite	
Sodium hydroxide (NaOH)	Vetec	V800383
$MgCl_2$	EMD Millipore Corp	442611
Na citrate	Merck	7810
Sodium phosphate dibasic (Na_2HPO4)	Sigma -Aldrich	55136
Sodium phosphate monobasic (NaH_2PO4)	Sigma -Aldrich	20229
Dextran sulphate	Sigma -Aldrich	D8906
t-RNA	Roche	10109495001
Ammonium Acetate (NH4Ac)	Sigma -Aldrich	A1542
Sodium acetate (NaAc)	Sigma -Aldrich	S5636
Triethanolamine Hydrochloride	Sigma -Aldrich	T1502
DIG-UTP	Roche	11277073910
Protector RNase inhibitor	Roche	03335399001
T7-RNA polymerase	Roche	19011723
Ethanol	Merck	1.00983.0511
Formamide	Sigma-Aldrich	F7503
Proteinase K	Sigma-Aldrich	P8044
Glycine	Sigma-Aldrich	G7126
Denhardt's Solution 50x	Sigma-Aldrich	D2532
Blocking reagent	Roche	11096176001
(Bovine serum albumin)BSA	Sigma-Aldrich	A7906
NBT-BCIP	Roche	11681451001
Dexamethasone (DEX)	Sigma-Aldrich	D4902
Cycloheximide CYC	Sigma-Aldrich	C7698
L-Kynuriene	Sigma-Aldrich	
N-1-naphthylphthalamic acid (NPA) (NPA)	Chem-Service	N1250
Silwet L-77	Plant media	30630216-2

Isopropyl-β-D-thiogalactoside (IPTG)	Hi-Media	MB072
Glacial acetic acid	Vetec	V800020
Tween20	Sigma	P1379
EtBR	Sigma	E7637
Skim milk	BD Biosciences	232200
Coomassie brilliant blue	Sigma	B0149
HEPES	Sigma	H3375
Deoxyribonucleic acid from herring sperm	Sigma	D7290
Accuprep Plasmid mini extraction kit	Bioneer	K3030
ReliaPrep™ RNA Miniprep Systems	Promega	Z6111
Accuprep mini gel extraction kit	Bioneer	K3035
iScript cDNA synthesis	Bio-Rad	#170-8891
iTaq Universal SYBR Green Supermix	Bio-Rad	172-5120
pENTER-D-TOPO pENTR™/D-TOPO™ Cloning Kit	Thermofisher Scientific/ Invitrogen	K240020
Gateway™ LR Clonase™ II Enzyme miX	Thermofisher Scientific/Invitrogen	11791020

List of the antibodies used for this study.

Name	Catalogue Number	Company
Anti-6-His antibody produced in rabbit	Sigma	SAB4301134
HRP-conjugated Anti-Rabbit IgG Concentrate	Sigma	RABHRP1
anti-Digoxigenin-AP Fab fragments antibody	11093274910	Roche